Unclassified
SECURITY CLASSIFICATION OF THIS PAGE

REPORT DOCUMENTATION PAGE

88

1a. REPORT SECURITY CLASSIFICATION Unclassified	1b. RESTRICTIVE MARKINGS
2a. SECURITY CLASSIFICATION AUTHORITY UNCLASSIFIED	3. DISTRIBUTION/AVAILABILITY OF REPORT Approved for public release, distribution unlimited
2b. DECLASSIFICATION/DOWNGRADING SCHEDULE	
4. PERFORMING ORGANIZATION REPORT NUMBER(S)	5. MONITORING ORGANIZATION REPORT NUMBER(S) AFOSR-TR- AFOSR-89-0405
6a. NAME OF PERFORMING ORGANIZATION The Pennsylvania State University	6b. OFFICE SYMBOL (If applicable)
6c. ADDRESS (City, State, and ZIP Code) Materials Research Laboratory University Park, PA 16802	7a. NAME OF MONITORING ORGANIZATION Air Force Office of Scientific Research
	7b. ADDRESS (City, State, and ZIP Code) Bolling Air Force Base Washington, DC 20332-6448
8a. NAME OF FUNDING/SPONSORING ORGANIZATION Air Force Office of Scientific Research	8b. OFFICE SYMBOL (If applicable) NA
8c. ADDRESS (City, State, and ZIP Code) Bolling Air Force Base Washington, DC 20332-6448	9. PROCUREMENT INSTRUMENT IDENTIFICATION NUMBER AFOSR-89-0405
	10. SOURCE OF FUNDING NUMBERS PROGRAM ELEMENT NO. 61102F; PROJECT NO. 2302; TASK NO CS; WORK UNIT ACCESSION N

11. TITLE (Include Security Classification)

Advanced Civil Engineering Materials Based on Inorganic Polymers

12. PERSONAL AUTHOR(S)
Paul W. Brown

13a. TYPE OF REPORT	13b. TIME COVERED	14. DATE OF REPORT (Year, Month, Day)	15. PAGE COUNT
Final	FROM 10/1/89 TO 2/28/93	April 29, 1993	155

16. SUPPLEMENTARY NOTATION CONCRETE, ORGANIC POLYMERS

17. COSATI CODES			18. SUBJECT TERMS (Continue on reverse if necessary and identify by block number)
FIELD	GROUP	SUB-GROUP	

19. ABSTRACT (Continue on reverse if necessary and identify by block number)

The present program was undertaken to evaluate cement chemistries more suitable for macrodefect-free cement materials. Therefore, the thrust of this work is oriented to the chemistry of advanced cements. Two strategies are being employed. The first is to modify conventional high alumina and portland cements to develop advanced properties. Such properties in this context include improvement in moisture sensitivity and extension of useful service range to temperatures higher than those tolerated by conventional organic polymers. The second strategy is to evaluate novel chemistries. This has included forming alkali zirconium phosphates at low temperature. This class of materials exhibits zero thermal expansion, is stable to high temperature and therefore may be useful in aerospace applications where dimensional stability is important.

20. DISTRIBUTION/AVAILABILITY OF ABSTRACT	21. ABSTRACT SECURITY CLASSIFICATION
☐ UNCLASSIFIED/UNLIMITED ☒ SAME AS RPT. ☐ DTIC USERS	Unclassified
22a. NAME OF RESPONSIBLE INDIVIDUAL MARTIN LEWIS, MAJ, USAF	22b. TELEPHONE (Include Area Code) 202-767-6963
	22c. OFFICE SYMBOL AFOSR/NA

DD Form 1473, JUN 86 Previous editions are obsolete.

SECURITY CLASSIFICATION OF THIS PAGE
UNCLASSIFIED

COMPLETED PROJECT SUMMARY

ADVANCED CIVIL ENGINEERING MATERIALS BASED ON INORGANIC POLYMERS

PRINCIPAL INVESTIGATOR:
PAUL W. BROWN

INCLUSIVE DATES:
10/1/89-2/28/93

CONTRACT/GRANT NUMBER:
AFOSR-89-0405

SENIOR RESEARCH PERSONNEL:
P.W. Brown
D. Shi

JUNIOR RESEARCH PERSONNEL:
W. Ma,
J. Bothe,
E. Gruczcinski,
J. Dumm,
J. Gulick,
R. Dudenhoefer

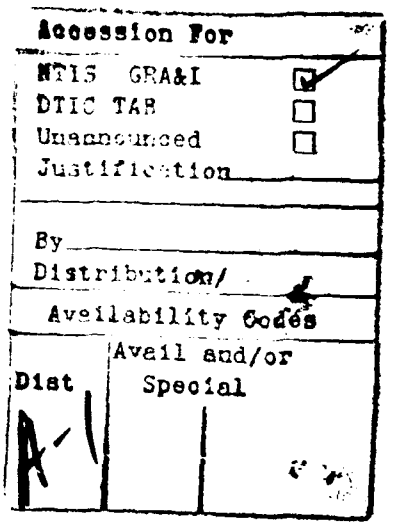

OUTPUTS ACKNOWLEDGING AFOSR

Published

W. Ma and P.W. Brown, "Cement-Inorganic Polymer Composites, Microstructure and Strength Development," 9th Intl. Cong. Chem. Cem. Vol. IV, 424-29, Delhi, (1992).

P.W. Brown, "Phase Equilibria and Cement Hydration," in The Materials Science of Concrete, J.P. Skalny, Ed., Am. Ceram. Soc. (1989).

P.W. Brown, D. Shi, and J.P. Skalny, "Porosity/Permeability Relationships" The Materials Science of Concrete II, J.P. Skalny, Ed., Am. Ceram. Soc. (1991).

J.J. Beaudoin and P.W. Brown, "The Structure of Hardened Cement Paste," Principle Paper 9th Internation Congress on the Chemistry of Cement, Delhi (1992).

Cements Research Progress-1989, P. W. Brown, Ed., American Ceramic Society (1991).

Cements Research Progress-1990, P.W. Brown, Ed., American Ceramic Society (1993).

D. Shi, P.W. Brown and W. Ma, "Lognormal Simulation of the Pore Size Distributions in Cementitious Materials," J. Am. Ceram. Soc. 74, 1861 (1991).

P.W. Brown and D. Shi, "A Model for the Variations in the Aqueous Phase During the Hydration of Tricalcium Silicate," Advances in Cement Research 4, 17-27 (1992).

W.Ma, P.W. Brown, and D. Shi, "Solubility of $Ca(OH)_2$ and $CaSO_4 \cdot 2H_2O$ in the Liquid Phase from Hardened Cement Paste," Cem. Concr. Res. 22, 531-40 (1992).

Y. Fang, D.K. Agrawal, D.M. Roy. R. Roy and P.W. Brown, "Ultrasonically Accelerated Synthesis of Hydroxyapatite," J. Mat. Res. 7, 1-5 (1992).

R. Dudenhoefer, G. Messing, P.W. Brown, J.J. Johnson, Jr., "Synthesis and Characterization of Monomagnesium Phosphate Tetrahydrate," J. Cryst. Growth. 125, 121-26 (1992).

P.W. Brown, "The Kinetics of Tricalcium Aluminate and Tetracalcium Aluminoferrite Hydration in the Presence of Calcium Sulfate," J. Am. Ceram. Soc., accepted.

W. Ma and P.W. Brown, "Cement-Phosphate Composites: Mechanical Behavior and Microstructure of High Alumina Cement Modified by Phosphate-based Reactants, Cem. Concr. Res., accepted

P.W. Brown, J. Gulick, and J. Dumm, "The Ternary Diagram $MgO-H_3PO_4-H_2O$ at 25°C" J. Am. Cer. Soc., accepted

P.W. Brown, J.R. Hellmann and M. Klimkiewicz, "Evolution of Microstructure in Ceramics and Composites," J. Micro.Tech. (invited)

E. Gruszczynski, J.V. Bothe, and P.W. Brown, "Ettringite Formation at Elevated Temperatures," Cem. Concr. Res.

Submitted

W. Ma and P.W. Brown, "Hydration Of Sodium Phosphate-Modified High Alumina Cement," J. Mater. Res.

W. Ma and P.W. Brown, "The Effect of Phosphate Additions on Hydration of Portland Cement," Adv. Cem. Res.

In Progress

P.W. Brown, R. Dudenhoefer, and G. Messing, "Kinetics of Magnesium Phosphate Formation," in prep (for J. Am. Ceram. Soc)

P.W. Brown, "Generic Aspects of Hydration and Microstructural Development," Materials Science of Concrete-IV, J.P. Skalny, Ed, invited.

Advances in the Production and Use of Cements, P.W. Brown, Ed, Engr. Fnd. (1992), in preparation.

Patent Disclosure

Low Temperature Formation of "N-Z-P" Ceramics

Narrative

Background

In the last decade there has been a significant development in technology which uses conventional cement in advanced applications. Generically, such materials are called macrodefect-free cements (MDF cements). MDF cements develop desirable properties, such as the ability to exhibit ductility, abrasion resistance which may be superior to that of metals, and relatively high strengths. For example compressive strengths exceeding 100,000 psi have been achieved.

Conventional MDF cement are composites which are comprised of cement and a water-soluble polymer, such a polyvinyl alcohol. As water is used in cement hydration, polyvalent cations are liberated and these form cross-links with the polymer. Unfortunately MDF cements are unlikely to be useful in civil engineering applications because they are moisture sensitive. When exposed to water or even to high humidity, the polymers unzip with an attendant strength loss and the remaining unreacted cement starts to hydrate causing a loss in dimensional stability. Thus, while MDF cements develop impressive mechanical properties, they suffer significant disadvantages with regard to their stabilities. In addition, because MDF cements employ organic polymers, their use is limited to low temperatures.

Therefore, while MDF cements represent an exciting class of materials, their applications appear to be limited in areas of interest to the Air Force and for companion civilian applications. Such applications might include: rapid runway or highway repair; use of non-metallic, and non-corroding reinforcing materials; low permeability, high strength materials for containment applications (fuel, water, wastes, etc) which could be rapidly fabricated. Our objective was to explore the use of phosphatic materials, which would react with the constituents of liberated during cement hydration. Such reaction results in the formation of chemically and thermally stable compounds, which contribute to strength and stability of ta cement.

Objectives

The present program explored the effects of the use of selected inorganic polymers as alternatives to the use of organic polymers in MDF cements. The program explored the use of classes of cements likely to exhibit greater thermal stabilities than conventional cements. Four classes of cements were investigated in this study:

conventional calcium silicate cements (OPC)
conventional calcium aluminate cements (HAC)
magnesium phosphates cements
alkali zirconium phosphate cements (NZP).

Condensed phosphates were used in place of conventional organic polymers. These were selected because they are inorganic polymers generally analogous to organic polymers, they are water soluble and they will react with polyvalent cations to form low-solubility structures. Finally, they are more thermally stable than organic polymers. The phosphate materials selected for study included four condensed sodium phosphates. In addition two calcium phosphates, which are not polymeric, were used. These were sodium hexametaphosphate $(NaPO_3)_n$, sodium metaphosphate $(NaPO_3)_n \cdot Na_2O$, sodium tripolyphosphate $Na_5P_3O_{10}$, sodium trimetaphosphate $(NaPO_3)_3$, calcium phosphate $CaHPO_4$, and calcium pyrophosphate $Ca_2P_2O_7$.

The objectives of the program were to evaluate the effects of the presence of these phosphatic compounds on the kinetics of cement hydration. If the presence of these materials excessively retarded the reactions of interest, an eventual technological payoff would be unlikely. The effects of these compounds on the compositions and the crystallinities of the product phases were also determined. One factor which can adversely influence the properties of a cement is the slow conversion of the first-formed products to more stable ones. This is well known in the calcium aluminate cements. In some instances solution chemistry analyses were carried out to determine the stabilities of the phases and to help in the establishment of kinetic mechanisms. The microstructures which developed were also explored to determine the spatial relationships among reactants and products. Finally, mechanical property determinations were made. However, the emphasis of the program was to establish the chemistries of these cementing reactions. Processing with exclusive objective of achieving elevated properties was not emphasized.

Primary Experimental Equipment Used

The principal experimental methods employed in this study involved the use of isothermal calorimetry to determine reaction kinetics, X-ray diffraction analyses to determine the crystalline products which formed based on their structures, direct microstructural observation using conventional SEM and environmental SEM, solution chemical analyses to determine the compositions of liquid phases co-existing with solid phases.

Isothermal Calorimetry

Isothermal calorimetric studies were performed to test reactivities of the cements being investigated by determining rates of heat evolution. In isothermal calorimetry, heat evolved during reaction is conducted across thermopiles which surround the calorimetric cell. The heat output is thereby converted to a voltage output which is recorded against time. Applying a known thermoelectric coefficient allows the rate of heat evolution to be determined. In the method used, approximately three grams of water were inoculated into an equivalent mass of reactant powders that had been placed in a gold-plated copper sample cup and placed within the calorimeter cavity. The cups were sealed with plastic film to minimize evaporation of water. Each reactant was allowed to equilibrate separately to the appropriate temperature prior to mixing. The water was equilibrated in a syringe and, when equilibration had been achieved, the plastic film was penetrated and the water injected over the reactants. The rates of heat evolution, dQ/dt in mWatts, were measured and recorded using a computer data acquisition system. Integration of the areas under the rate curves allowed calculation of the total heats evolved. A trapezoid integration was utilized for such analyses. Calorimetric data were obtained at various temperatures and this allowed activation energies for the reactions of interest to be determined by calculating Arrhenius activation energies.

Solution Chemistry

Variations in solution pH were measured with an Orion 920 pH meter that utilized an automatic temperature-compensating probe. Ion concentrations were determined by DC plasma spectrometry. Solids were removed by filtration through 0.2 μm filters and the remaining liquids were analyzed.

Electron-optical Analyses

The morphologies and chemical compositions of the hydrates were determined by using scanning electron microscopy (SEM, ISI-DS 130 Dual Stage Scanning Electron Microscope) and

energy-dispersion x-ray spectrometry (EDX). Microstructural development was further observed by environmental scanning electron microscopy (ESEM, Electroscan Environmental Scanning Electron Microscope). The ESEM allows observation of microstructure and microstructural development under reduced pressure but does not require high vacuum. In the present case water pressures of 3-4 torr were used. This eliminates the problem of charging in porous and/or nonconducting materials. this technique has been particularly useful in the observation of cementitious materials in their natural states.

Mechanical Properties

The splitting strength was measured on an Instron machine. The splitting strength was calculated using the expression: S.S. = $2P/(\pi dt)$, where d is the diameter and t the thickness.

X-ray Diffraction

X-ray diffraction analyses were performed on a Scintag automated x-ray diffractometer interfaced with a microVAX computer.

Summary of Results

HAC-CONDENSED PHOSPHATE SYSTEMS

High strength was achieved in high alumina cement (HAC) through the incorporation phosphate-based additions at levels of approximately 10%. When sodium phosphates were incorporated with high alumina cements it was observed that they fluidified the fresh mix. This is desirable in that improvement of rheology reduces the water requirement. This, in turn, improves strength.

In order to further establish the mechanism which results in higher strength, the effects of a variety of condensed sodium phosphates $(NaPO_3)_n$, $(NaPO_3)_n{\cdot}Na_2O$, $Na_5P_3O_{10}$, and $(NaPO_3)_3$ were studied. The influence of these additions on the kinetics of hydration were studied using isothermal calorimetry. The phosphatic additions enhanced reactivity. X-ray diffraction analyses did not reveal evidence of new crystalline phosphate-containing hydration products. Microstructural evolution was examined in real time using environmental SEM and hydration products exhibiting distinct morphologies were observed. The features exhibited ranged from indistinct to polygonal shapes, plates, and fibers. These frequently formed between crystalline calcium aluminate hydrate grains and by doing so appear to provide a means to enhance the strengths of these cements. In spite of the morphological variations, companion energy dispersive X-ray analysis showed that the compositions of these products did not vary widely. Their range of compositions are 52-60 wt% Al_2O_3, 20-26 wt% P_2O_5, and 20-24 wt% CaO. Phosphate modification of HAC accelerates hydration. However, the total heat evolved in the hydration of unmodified HAC is actually greater. The phosphate-containing products formed in this system are x-ray amorphous. Although compositionally quite similar, ESEM shows that the hydration of HAC modified by different phosphates can result in morphologically distinct hydration products. The phosphate-based additions do not tend to promote the crystallization of calcium aluminate hydrates during the high alumina cement hydration. The amorphous C-A-P-H gel formed by reaction between HAC and the sodium phosphates serves as the bond interlinking the other constituents which are present. This CAPH phase provides enhanced structural integrity to high alumina cement. The presence of the phosphate-containing hydrates appear to reduce the strength losses associated with the conversion to hexagonal hydrates.

The flexural strength is greatly improved by addition of various sodium-based inorganic polymers and calcium phosphate. The short-term flexural strengths of samples containing 20 wt.% of these constituents can reach over 40 MPa, while that of corresponding pure cement cured under the same conditions is approximately 14 MPa. After ten months of curing, the strengths of the modified samples continue to be more than twice as high as that of pure cement. The mechanism responsible for strength increase in this material was studied by X-ray diffraction and mercury intrusion porosimetry. Experimental results indicate that these phosphate-based compounds do not form crystalline hydration products but provide structural integrity to high alumina cement by decreasing the porosity.

Sodium phosphate and calcium phosphate have different effects on mechanical properties. Silica fume replacement offers advantages in reducing the loss in strength. A low water:cement ratio is required to achieve high strength in the long term. Mechanical properties varied depending on the phosphate addition level. The increase in flexural strength is related to the decrease in pore size and in porosity.

OPC-CONDENSED PHOSPHATE SYSTEMS

New cementitious compositions were sought by reactions involving ordinary portland cement (OPC) and sodium and calcium phosphates. The phosphate modified cements produced more heat and exhibited much faster hydration rates than did OPC. The phosphate-containing products formed at room temperature are X-ray amorphous, but SEM shows that the hydration of OPC modified by different phosphates can result in morphologically distinct hydration products. Hydrothermal treatment at 160°C of OPC modified by $CaHPO_4$ led to phase transformations of a poorly crystalline phosphate containing product phase into crystalline hydroxyapatite. Generally, the presence of sodium and calcium phosphates resulted in improved flexural strengths; an exception was when $(NaPO_3)_n \cdot Na_2O$ was used. The effects of different sodium and calcium phosphates, processing by warm-pressing, W/C ratio, and curing conditions on mechanical properties were also explored. High strength can be achieved by ordinary portland cement with phosphate-based additions. The exception is OPC modified with $(NaPO_3)_n \cdot Na_2O$. With the mixing procedure used in this study, modest W/C needed is needed for OPC-phosphate system to develop high strength. Warm pressed samples have higher strengths than those pressed at room temperature. Temperature of curing is an important factor in influencing the strength. The strength data obtained suggests that this sodium phosphate-modified OPC is not very sensitive to water.

Phosphate modification of OCP accelerates hydration. However, the total heat evolved in the hydration of unmodified cements is actually greater except for calcium phosphate modified OPC. A relationship exists (except calcium phosphate modified OPC) between the strength and the rate of hydration reaction; the faster the reaction is, the higher the strength the sample exhibits. However, when the rate of heat evolution becomes excessive, mechanical damage to the specimen limits the strength attained.

The phosphate-containing products formed in this system are X-ray amorphous. However, SEM shows that the hydration of OPC modified by different phosphates can result in morphologically distinct hydration products. The amorphous phase formed in calcium phosphate modified OPC has the morphology of hydroxyapatite but is poorly crystalline. Hydrothermal treatment results in the formation of crystalline hydroxylapatite.

MAGNESIUM PHOSPHATES

Magnesium phosphates are an important member of a class of compounds which are used as castable refractories and rapid setting cements. They are of interest for, in particular, for the rapid repair of runways. However, the mechanisms limiting the rate of strength development have not been fully elucidated. Therefore the phase in the ternary system $MgO-P_2O_5-H_2O$ at 25°C was explored. The magnesium phosphates represented were $Mg(H_2PO_4)_2 \cdot nH_2O$ (n=4,2,0), $MgHPO_4.3H_2O$, and $Mg_3(PO_4)_2 \cdot mH_2O$ (m=8, 22). Because of the large differences in the solubilities of these compounds, the technique which involves plotting the mole fractions of MgO and P_2O_5 as their 10th roots has been employed. With the exception of $MgHPO_4 \cdot 3H_2O$, the magnesium phosphates are incongruently soluble. Because incongruency is associated with a peritectic-like reaction, the phase $Mg_2(PO_4)_3 \cdot 8H_2O$ persists metastably for an extended period. It is the peritectic character of this reaction which limits the rate of strength development in these systems. The ternary $MgO-P_2O_5-H_2O$ diagram at 25°C also shows that the dissolution of $MgHPO_4 \cdot 3H_2O$ is congruent. This phase forms an invariant point with $Mg(H_2PO_4)_2 \cdot 4H_2O$ in acidic solutions. As solutions become more basic the solubility of this phase decreases by several orders of magnitude. Our data shows that $MgHPO_4 \cdot 3H_2O$ forms an invariant point with the metastable hydrate, $Mg_3(PO_4)_2 \cdot 8H_2O$. However, equilibrium appears to involve an invariant point between $MgHPO_4 \cdot 3H_2O$ and $Mg_3(PO_4)_2 \cdot 22H_2O$. Although the low temperature formation of $Mg_3(PO_4)_2 \cdot 4H_2O$ has been reported to occur in reactions involving ammonium-magnesium phosphates, it was not observed in this study.

PORE STRUCTURES

The structure of the porosity in cementitious materials strongly influences their performance. Specifically, porosity determines the rates at which aggressive species can enter the mass and cause disruption. Rates of intrusion are related to permeability. In the most general way, permeability depends on the total porosity. More importantly, however, permeability depends on way in which the total porosity is distributed. Porosity, in turn, is related to the original packing of the cement, mineral admixtures, and the aggregate particles, to the water-to-solids ratio, to the rheology, which is related to the degree of dispersion of the solids originally present, and to the conditions of curing.

A variety of models have been developed to predict permeability from pore structure. A common feature of these models is that a power law may exist between permeability and some characteristic pore dimension. The tortuosity factor has been included explicitly in all percolation-based models.

Each model has its rational base. Statistical models consider all pores, whereas some models only consider large pores. Selected models provide the basis for relating entry pore volume and true pore volume. Others have considered crack-permeability relationship and explicitly used f, the fraction of connected pores in their models. Alternatively, some avoid calculating f, which is difficult. Rather, they predict permeability from mercury porosimetry data. Even the traditional Carmen-Kozeny model has its advantages. This pore structure-permeability model requires as input is a pore size distribution. Although a pore size distribution is more easily determined than permeability per se, it usually assumes shape for pores. The Carman-Kozeny model uses the specific surface area of pores as input. This does not require any shape assumption and can, therefore, avoid a source of error. We have reviewed models developed to describe porosity both in cement paste and concrete with emphasis on permeability models developed for a variety of porous inorganic materials, relationships between pore structure and permeability are discussed in terms of their applicability to concrete.

From a pragmatic standpoint, porosity of a material is not of interest as an end in itself. Rather porosity is of interest because it directly influences both mechanical and transport properties of cementitious materials. For example, the pore shape-dependent relationship between porosity and strength, s, of the form:

$$s/s_o = \exp\text{-}(be)$$

is well known, where b is a shape-dependent parameter, e the porosity and s_o the ideal strength.

With respect to durability, the ability of conventional concrete to resist various forms of deterioration is often related to its impermeability. Analysis of the sources of porosity and its connectivity can frequently provide the means to understand the mechanisms by which aggressive species can intrude concrete. This is because the pore structure defines the paths along which liquid or vapor preferentially moves. This, in turn, is of obvious importance with respect to specific durability considerations including the transport of freezable water and electrolytes, such as chlorides, through concrete.

It is widely accepted that permeability is determined by microstructure. Microstructure in this context is defined in terms of pore and crack structures. A large number of models have been developed, particularly for sedimentary rocks, to predict the permeability from measurements of pore structures and cracks. For cementitious materials, it is well recognized that both total porosity and its distributions determine the permeability, and that only pores with diameters greater than a specific value contribute significantly to permeability. For example, the dependence of permeability on the porosity has been illustrated. It has also been observed that the inflection point on the cumulative pore size distribution obtained by mercury porosimetry locates the minimum diameter of pores which form a continuous network through hydrating cement paste.

Large variations in permeability of concrete having nominally similar porosities are frequently observed. As a consequence, it is useful to enumerate the various types of porosity present and to establish their relative contributions to permeability. These types may be classified in terms of their origin or in terms of their anticipated effect on measurable parameters such as strength or permeability. Sources of porosity in concrete include:

1. gel pores
2. smaller capillary pores
3. larger capillary pores
4. large voids (also included in this category may be intentionally added voids such as by air entrainment)
5. porosity associated with paste-aggregate interfacial zones
6. microcracks and discontinuities associated with dimensional instabilities that occur during curing
7. porosity in aggregate

The diameter of a stable gel pore is assumed to be about 2 nm. The reason for the selection of this value is based on the assumption that hydration products cannot precipitate in pores having diameters smaller than about 2 nm. Because the gel porosity resides in the hydration products that accumulate between the liquid phase and the anhydrous cement grains, gel porosity has a major effect on hydration rates but only a minor effect on transport processes involving liquids.

However, there is at present no justification for ignoring the other types of pores listed above. Thus, the contribution of each of the remaining types of porosity to permeability must be considered. Unfortunately, deconvolution of the relative contributions of each of these sources of porosity to permeability has not been carried out. Therefore, conclusions reached regarding concrete permeability are frequently based on extrapolation of results obtained for cement pastes. However, it may be reasonable to subdivide the porosity in concrete into two classes: (1) that in the paste matrix and (2) that associated with the aggregate and paste interface.

The principle source of the matrix porosity contributing to permeability is that associated with residual space between cement grains which was originally filled with water. The contribution of this source of porosity may be amenable to assessment by investigations of cement paste. However, the contribution of the porosity associated with the interfacial zones between paste and aggregate and the microcracks that develop in this interfacial region, which extend into the paste, to permeability must be assessed by determinations carried out directly on aggregate-containing materials. Therefore an analysis technique which allows the pore structures of cements and cement-based systems to be modelled was developed.

Regardless of the compositions of the reactants, cements are particulate solids. To achieve optimal properties it is necessary to understand the manner in which these particle interact with each other. Condensed sodium phosphates can improve rheology in these particulate systems. The effects of rheological control can be assessed in a number of ways. One is to determine the distribution of porosity present after reaction has reached a substantial degree of completion. By establishing the pore size distributions it becomes possible to predict the homogeneity of mixing and to make assessments of the parameters which may limit the rates of reaction. Therefore, the pore size distributions in cement pastes and mortars, over the range of pore sizes determined by high pressure mercury intrusion porosimetry (MIP), can be described in terms of a multi-modal distribution by using lognormal simulation. The pore size distribution may be regarded as a mixture of lognormal distributions. Such a mixture is defined by a compound density function:

$$p(x) = \sum f_i \, p(x, \mu_i, s_i), \qquad \sum f_i = 1$$

where x is the pore diameter, f_i the weighting factor of the i-th lognormal sub-distribution of pore sizes, $p(x, \mu_i, s_i)$, μ_i and s_i location parameter and shape parameter of the i-th sub-distribution respectively. It may indicate that different origins and formation mechanisms exist for pores in different size ranges in cementitious materials.

Our work has shown that pore size distributions in cementitious materials determined by mercury intrusion porosimetry can be fitted to a compound distribution of three lognormal distributions. Pores of sizes ranging from about 1 nm to about 10 μm have been included in this compound lognormal model. The first sub-distribution is associated with coarse pores that may extend to voids. The third sub-distribution is associated with fine pores that may extend to gel pores. The middle distribution includes capillary pores. Pore size distributions for ordinary cement pastes, blended cement pastes and mortars, that have different compositions and degrees of hydration, have been examined to test the generality of the model. A graphical method can be applied to obtain initial estimates of the parameters in the compound distribution. Selected properties of the lognormal distribution, such as median pore diameter, inflection point and the mean squared pore diameter, have been used to calculate characteristics of pore size distribution. The median and inflection point can be used to check the quality of parameter estimation. The mean square pore diameter and inflection point may be used in permeability-pore structure relation

models. This appears to be the first time an analysis has provided the means to quantify the pore size distribution in terms of relative pore surface areas, or relative pore numbers. Relating the properties of the three distributions to the physical and mechanical properties of cementitious materials warrants further investigation.

ALKALI ZIRCONIUM PHOSPHATES

Because of the potentially attractive properties of phosphate-based cements, a study was done to determine whether alkali zirconium phosphates (NZP) of the generic composition: $NaZr_2(PO_4)_3$ would be formed by a cement-like reaction. By using an acid-base reaction analogous to the pozzolanic reaction, members of this class of materials were produced by a cement reaction.

Impacts and Relevance to the Air Force

The results of this program are believed to be relevant to the air force in at least four areas.

°The first of these is the establishment of the mechanistic paths which limit the rates of strength development in magnesium phosphate-based rapid hardening cements.

°The second is the chemistries of cementitious systems which involve sodium phosphates were established. This is relevant because it is likely that these chemistries could be used in the development of ultrahigh strength cements. Because these cements are likely to be stable when exposed to high humidity or moisture, they may used in conventional civil engineering applications. One example of such an application would be the fabrication of reinforcing bars. Because the bars need not contain metals, it may be possible to consider them for use in air force runways. Because such materials are more brittle than metals is possible that the problems encountered with metal rebars in bomb damage could be avoided.

°The use of the log normal model to describe the distributions in pore structure of cement-based systems was evaluated. This provides the basis for the assessment of rheological parameters governing the mixing of particulate solids and allows the prediction of permeability.

°A new family of materials, sodium zirconium phosphates or N-Z-P's, have been made by cement reactions. These compounds are highly stable thermally (to 1600°C) and their thermal expansion characteristics can be tailored.

°The chemistries evaluated in this program may be advantageous with respect to the immobilization of toxic and hazardous wastes.

ABSTRACT

It is generally recognized that conventional cements exhibit useful compressive strengths but have low tensile and flexural strengths. Generally, the behavior of cement-based materials is controlled by the compositions of starting materials, the manner in which these are mixed with an aqueous media, the chemical bonding of the reaction products and the microstructure of the final assemblage. A class of cements containing secondary constituents is high strength cement pastes called macrodefect free cements (MDF cements). These have generated a high level of interest recently. However, their applications in civil engineering are very limited because MDF cements are unstable when immersed in water or even when exposed to high humidity. A different approach to improving the properties of cementitious materials is the addition of phosphatic materials. The purpose of this study was to build on the general concepts from MDF cement technology by identifying cement-based composites eliminating organic polymer as an admixture.

Phosphates have a long history of use as binding agents in ceramic systems. Their reactions have resulted in the formation of materials which have been used in such diverse applications as alumina refractories and bioceramics. Cementitious materials modified by phosphate-based additions show high strength and durability. Application of MDF cement concepts to this combination of materials affords the opportunity to develop advanced cement-based systems which do not suffer from such problems as water sensitivity.

Thus, this material offers the potential for use in a range of applications.

Two systems -- the high alumina cement-phosphate system and the ordinary portland cement-phosphate system -- are investigated in this study. A novel method has been developed for processing cement-phosphate composites. The flexural strength is greatly improved by reinforcing high alumina cement and ordinary portland cement with phosphate-based reactants. The mechanisms influencing the mechanical properties of this material are investigated. The results obtained are expect to provide information on the microstructure of cement-inorganic composites and how it affects the mechanical properties of this material.

The kinetics of hydration, and the compositions and morphologies of the products which form in the phosphate-modified cement system have been studied. Isothermal calorimetry was used to explore the rates of hydration. The heat evolved during hydration was measured for both phosphate modified and pure cement. The hydration products were identified and characterized by x-ray diffractometry. Morphological development was determined using conventional high vacuum scanning electron microscopy (SEM) and environmental scanning electron microscopy (ESEM). Hydration product compositions were determined by energy dispersive x-ray analysis (EDX).

TABLE OF CONTENTS

LIST OF FIGURES

LIST OF TABLES

ACKNOWLEDGMENTS

I would like to extend a special thanks to my advisor, Dr. Paul W. Brown, whose guidance ranged from the general approach to the research to insights on the significance of the data. I would also like to thank the rest of my thesis committer, Dr. Della M. Doy and Dr. Michael W. Grutzeck. Their effort in reading and correcting the manuscript is greatly appreciated.

I extend my thanks to all faculty, friends who contributed their knowledge, interest and encouragement to this project in MRL. I gratefully acknowledge the support of the Air Force Office of Scientific Research, Aerospace Sciences Directorate.

Finally I wish to thank my family for all their love, encouragement and support throughout the years of my studies.

Chapter 1
INTRODUCTION

1.1 Introduction

In recent years new cementitious materials have been developed which have strengths that are much greater than those of conventional hydraulic cements; many of whose properties are closer to those of ceramics than to those of concrete. The new materials have attracted much attention partly because they can be made at relatively low temperatures (generally less than 400°C) instead of at high temperatures (> 1000°C) which are typical of traditional ceramics. They constitute one major family of so-called "Chemically Bonded Ceramics (CBC)" coined by Roy in 1984. The different routes to generating strong cementitious materials, which are summarized by Roy (1987), include warm pressing, chemical modification, high-shear mixing with polymer additions, and the incorporation of fibrous and particulate second phases.

One approach to improvement of the properties of cementitious materials is the addition of secondary constituents. Very early reports indicate that different investigators have tried to use secondary constituents in concrete to make high strength materials. The

available literature of interest dates back to the beginning of this century. Chandra and Flodin (1987) traced the earliest known reference to 1909, and more work was done in this field in the 1920s. In the 1940s, products were developed based on poly (vinyl) chloride which were used for improving the bond strength between old and new concrete and for making concrete pipes. Since then various admixtures have been used for different purposes in different fields. Air entraining admixtures and water reducers are good examples of admixtures widely used in concrete.

A class of cementitious materials containing secondary constituents is the high strength cement pastes called macrodefect free (MDF) cements, and was pursued originally by Birchall et al. (1981) at Imperial Chemical Industries in England. These have generated a high level of interest recently because of their superior mechanical properties. MDF cements were produced initially with high alumina cement, and then with ordinary portland cement, in combination with a water soluble organic polymer of low molecular weight. However, their applications in civil engineering are very limited because MDF cements are unstable when immersed in water or even when exposed to high humidity.

A different approach to improve the properties of cementitious materials is the addition of phosphatic materials. The purpose of this project is to build on the general concepts from MDF cement technology by identifying cement-inorganic polymer composites instead of composites using an organic polymer as the admixture. The combination of these two materials leads to the probability of strength generating bonding or hydration reactions and to the possibility of an

entirely new class of materials which shows the advantages of MDF cements, and will not be water strongly sensitive.

1.2 Objectives

1.2.1 Specific Goals

It is the specific goal to apply the fundamental basis of MDF cement technology for the development of an entirely new class of cement-based materials. Cementitious materials modified by phosphate-based additions show high strength and durability (Roy, 1989). Application of MDF cement concepts to this combination of materials affords the opportunity to develop advanced cement-based systems which do not suffer from problems such as water sensitivity so much. Thus, this material offers the potential for use in a range of applications.

1.2.2 Methodology and Anticipated Results

Two systems, the high alumina cement-phosphate system and the ordinary portland cement-phosphate system, are investigated in this study. A novel method has been developed for processing cement-phosphate composites. The flexural strength is greatly improved by reinforcing high alumina cement and ordinary portland cement with phosphate-based reactants. The mechanisms influencing the mechanical properties of this material are investigated. The results obtained are expect to provide the information of the microstructure of cement-inorganic composites and how it affects the mechanical properties of this material.

The kinetics of hydration, and the compositions and morphologies of the products which form in the phosphate-modified cement system have been studied. Isothermal calorimetry was used to explore the rates of hydration. The heat evolved during hydration was measured for both phosphate modified and pure cement. The hydration products were identified and characterized by x-ray diffractometry. Morphological development was determined using conventional high vacuum scanning electron microscopy (SEM) and environmental scanning electron microscopy (ESEM). Hydration product compositions were determined by energy dispersive x-ray analysis (EDX).

1.3 Literature Survey

1.3.1 Introduction

By definition, cement is a bonding material developed from a liquid or plastic state by chemical reactions that can provide strength and elasticity to a hardened body often containing large amounts of fillers. Three types of cement were identified by Sarkar (1990) according to this definition:

- Hydraulic cements, such as portland and alumina cements, set by hydration reactions when they react with water
- Precipitation cements set primarily by ion-exchange reaction
- Acid-base cements set by reaction between an acid and a base

The reaction product for the third type of cement, usually a salt or a hydrogel, forms the cement matrix in which the fillers are embedded. Sarkar summarized that the acids can be mineral (e.g.

phosphoric acid), Lewis (e.g. magnesium chloride or sulfate), or even an organic chelating agent (e.g. polyacrylic acid or eugenol). The bases used for these cements are generally metal oxides such as magnesium oxide, gel-forming silicate minerals, or an acid-decomposible aluminosilicate-type glass. Phosphate cements for commercial applications are generally based on the reactions between a metal oxide and acid salt or derivatives of phosphoric acid and are classified as acid-base cements.

Two materials, MDF-cement and phosphate chemically bonded ceramics, are surveyed in this section. One major aspect of this literature survey was to obtain information on MDF cement which mostly belongs to the first type of Sarkar's (1990) classification and phosphate cement which belonged to the third. This information includes their strength mechanism, microstructure, interaction of organic polymers or phosphates on cementitious materials, and applications.

The use of phosphate based materials in combination with portland cement and high alumina cement is very limited, and less information about their use in chemically bonded materials is available. Actually no citations have been found in the technical literature about behavior of high alumina cement (HAC) and ordinary portland cement (OPC) modified by phosphatic materials.

1.3.2 MDF-Cement

1.3.2.1 Introduction

By using high energy processing, the mixture of polymer, cement and low water content for MDF cement is prepared to gain a very dense state. The high strength is generally attributed to the lack of defects, such as large pores, which are usually present in conventionally mixed cement pastes. Although various investigators looked at many cement-polymer combinations, the one that gave the best results was a combination of a HAC with a polyvinyl alcohol/acetate copolymer (Young, 1991). Fracture behavior of MDF cements is shown in Table 1.

Unfortunately, even though these cements have superior mechanical properties, their use in civil engineering applications appears to be quite limited because MDF-cements are unstable not only to liquid water but also to high humidity.

In the following section, the role of polymer in the cement matrix and water sensitivity of MDF cement are mainly discussed.

1.3.2.2 Mechanism of Polymer Reinforcement

The strength mechanism of MDF cement has been investigated by varies researchers and it seems that no satisfactory model has been found to be able to describe it properly. Chandra and Flodin (1987) summarized that there are two theories for the mechanism of action of polymers in cement. According to the first theory there is no interaction between polymer and cement. During hydration the hydrophilic part of the polymer is oriented towards the water phase

Table 1. Fracture behavior of OPC and HAC based MDF cements (data from Alford et al., 1982)

Fabrication	Polymer Type	Addition (Wt.%)	W/C	Flexural Strength (MPa)	Total Porosity
OPC	~	~	0.15	28	15%
MDF (OPC)	HPMC[1]	2.7	0.13	58	18%
	Polyac[2]	2.7	0.13	72	19%
	HPMC	4.9	0.15	67	31%
MDF (HAC)	PVA[3]	7	0.11	150	<1%

[1]HPMC = Hydroxypropylmethylcellulose.
[2]Polyac = Polyacrylamide.
[3]PVA = Polyvinylalcohol.

whereas the hydrophobic part heads towards the air phase (pores and capillaries not filled with water). On drying, the water is taken away, the hydrophobic particles coalesce together and form a film. The other theory is that the polymer interacts with the components of the cement hydration products and makes complexes. This creates a type of reinforcement in the cementitious materials and produces semipermeable membranes. Birchall (1983) thought that the polymer assists in the packing of particles of the paste in two main stages, first by acting as an interparticles to closer packing during mixing the components of the paste and second by drawing the particles closer together as the polymer dehydrates after the forming operation.

Although the critical flaw approach implies that the polymer is used only as a processing aid (to eliminate macro-defects), and does not contribute to the properties of the materials, there are several lines of evidence that contradict this hypothesis (Young 1991). In short, it is becoming more generally accepted that the polymer is playing an important role in improving the properties of the materials.

In order to investigate the effects of the polymer, several studies (Kendall and Birchall, 1985; Young, 1991) have looked at results of removing it by igniting the material at an elevated temperature. Kendall and Birchall (1985) made samples of MDF cement paste and then heated them to 500°C to decompose and remove the polymer. Therefore, the final materials were made containing no organic additives. They found that this highly packed composition showed remarkably low porosity (1.06%), high elastic modulus (75 GPa), and good bending (80 MPa) and compressive (300 MPa) strengths. Based on the thought that hydraulic cement pastes exhibit an "intrinsic

strength" (Eden and Bailey, 1984) at zero porosity, they concluded that the bending strength of these materials depended on flaw size in a brittle fashion, and that the toughness increased as the volume porosity fell. On the contrary, according to Young's review (1991), a strength loss of 90% is found when the polymer is removed by igniting the material at 500°C. The level of residual flexural strength is still significant for a cement-based material. Thus, he concluded that the binding matrix must be composed of both polymer and a hydrated phase.

Eden and Bailey (1984) suggested that the much increased strength of the new polymer-containing cements must result from improvements to the microstructure other than the simple elimination of voids. TEM results (Sinclair and Groves, 1985) show that the microstructures of two MDF cement, Secar 71 and OPC-based, are essentially composed of either clinker or clinker and hydrate grains embedded in a continuous amorphous polymeric matrix. High strength OPC pastes contain the normal hydration products calcium hydroxide (CH) and ettringite (AFt), whereas HAC based cement is unusual in that it does not display any crystalline hydrate phases. Energy dispersive microanalysis revealed that all amorphous materials in HAC based MDF pastes contain both calcium and aluminium and are aluminium rich while in OPC pastes interstitial amorphous material is very rich in calcium. These results indicate that the polymer additive reacts with the cement rather than existing as an entirely inert lubricant.

The effect of different polymer contents on the microstructure of OPC based MDF-cement was studied by Poon and other researchers

(Poon and Groves, 1988; Brackenburg, 1988). They found the morphology and composition of the gel matrix of the material with a low polymer content is significantly different from that of material with a high polymer content. The former consists mainly of gelatinous material with some microcrystallites and with some porosity. The latter consists of mainly pure non-porous polymer gel with little metallic content. The mechanical results showed that strength of MDF cement increases with polymer content, but the samples with high polymer content were extremely unstable after immersion in water. They concluded that the difference in microstructure could be attributed to the instability after immersion of the materials in water.

The chemical reactions occurring in a cement-polymer systems were studied by various investigators (Rodger et al., 1985; Chandra and Flodin, 1987). Rodger et al. (1985) found that the addition of small amounts (1.6%) of polyvinyl (alcohol/acetate) to the high alumina cement Secar 71 significantly retarded the normal hydration reactions. At much larger doses (10% PVA) the crystalline hydrates were completely suppressed and the polymer reacted with the cement solution to form calcium acetate and a crosslinked polymeric product. In the case of high strength OPC/polyacrylamide pastes the high pH of the cement solution converted the polymer to polyacrylic acid which reacted with the cation from the hydrated cement to form a crosslinked-metal-polyacrylate. Chandra and Flodin (1987) explained the interaction of polymers on portland cement hydration and concluded that polymers interact with the components of portland cement when they came in contact with water. The interaction was due to ionic bonding, causing cross-links which inhibit

the film formation property of polymers and influence considerably the crystallization process during the hardening of cement. This theory gave a good explanation; however, it is not backed by experimental data.

Based on the properties of MDF cements, their use in structural (Bache, 1988), and some other applications (Alford and Birchall, 1985), such as acoustics, cryogenics, armour, and electro-magnetic radiation screening, were discussed. Alford (1984) gave a list of the potential applications of MDF cement.

Since the Young's modulus of elasticity and strength of MDF cements are greatly improved, reinforcement seems unnecessary. The main purpose of reinforcing MDF cement with fibers is to enhance toughness and impact performance. Alford and Birchall (1985) gave the results that small volume fractions of fiber (~ 2%) in the MDF cement matrix produce composites with excellent toughness and impact properties.

1.3.2.3 Water Sensitivity

The influence of moisture on MDF cement is now well established and has been reported in several studies (Poon and Groves, 1988; Sinclair and Groves, 1985; Kataoka and Igarashi, 1987; and Young, 1991). On immersion in water, the strength of HAC/PVA drops dramatically (Figure 1), particularly in the first two weeks. Young (1991) reported that this phenomenon could be attributed to the dissolution of cement and the subsequent formation of hydration products in the surrounding water; there may also be physical loss of polymer. The change in strength of OPC/ polyacrylamide MDF cement

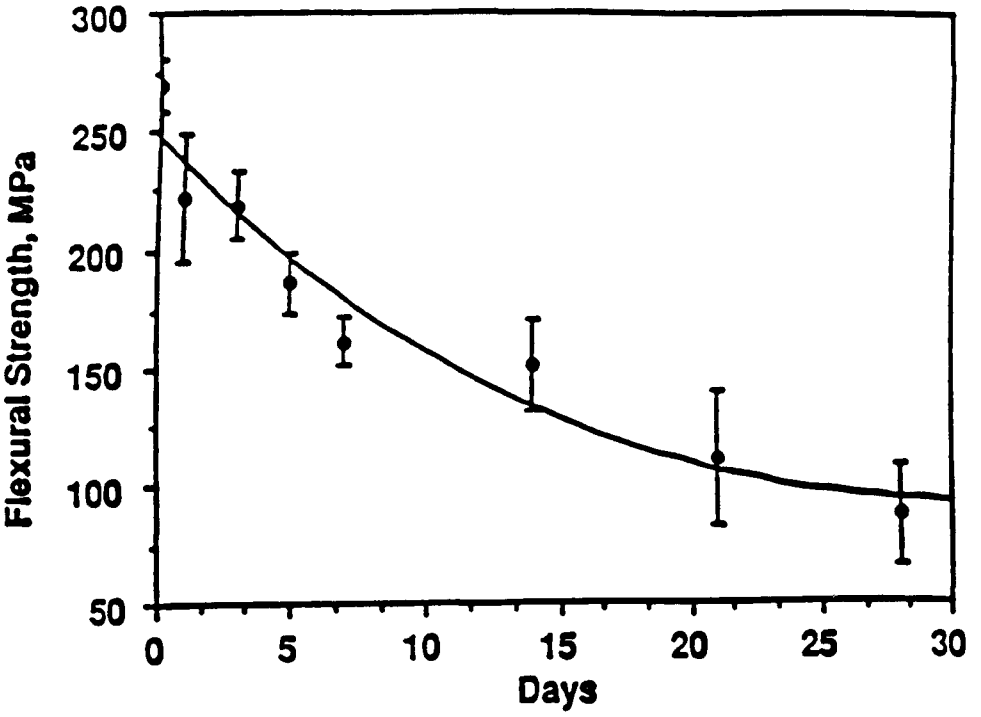

Figure 1. Effect of immersion in water on the flexural strength of HAC/PVA MDF cement. (from Young, 1991)

is less pronounced when initial moist curing is extensive and when polymer contents are lower (Young, 1991).

Under hot, wet conditions it is well known that conventional high alumina cements lose nearly all strength due to the "conversion" of the metastable hexagonal hydrates CAH_{10} and C_2AH_8 to the stable cubic hydrate C_3AH_6. Sinclair and Groves (1985) emphasized that the loss of strength of HAC based MDF pastes cannot be attributed to the conversion reaction of a conventional HAC paste since the hexagonal hydrates CAH_{10} and C_2AH_8 are not initially present. Uchiyama (1989) found strength can be regained if the cement is dried (Figure 2), and suggested that softening is possibly due to the absorption of water by the polymer.

The samples with high polymer content underwent substantial expansion and strength loss after water immersion (Poon and Groves, 1988). The effects of water on the lower polymer content samples were less harmful. Poon and Groves suggested that in the low polymer content samples, the gel is stabilized by the presence of metallic ions which crosslinked the polymer chain and formed certain crystalline products.

The expansion of the MDF cement pastes immersed in water increases with the content of polymer (Kataoka and Igarashi, 1987). Since the hydration of remaining unhydrated cement is not a cause of the expansion in itself, the expansion is attributed to the water soluble polymer, and such property restricts strongly the use of MDF cement.

In summary, although our understanding has increased dramatically over the past ten years, much work remains to be done. Young (1991) thought that the risks attendant in developing

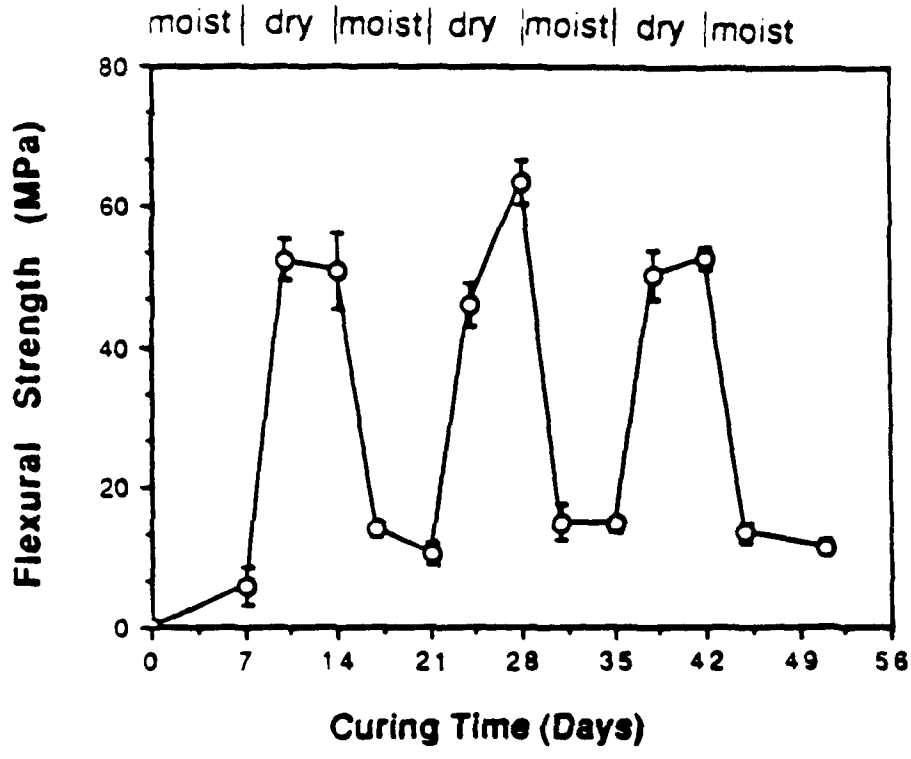

Figure 2. Flexural strength versus curing time of OPC/Polyacrylamide MDF cement subjected to three successive moist-dry cycles (from Uchiyama, 1989)

applications for these novel materials are rapidly diminishing, and he predicted the next ten years should see a gradual introduction of components made from MDF cements into the market place.

1.3.3 Phosphate Chemically Bonded Ceramics

A wide range of materials have been studied by various investigators in the development of phosphate-bonded materials. Formulations for concrete repair have been developed by trial and error and are either recorded in patents or kept as trade secrets (Sarkar, 1990). Phosphates have a long history of use as binding agents in ceramic systems. The reactions have resulted in the formation of materials which have been used in diverse applications, such as alumina refractories (Cassidy, 1977) and bioceramics (Brown and Fulmer, 1991).

The PO_4 group provides a basic building block that results in a series of compounds that are analogous to silicate compounds formed on the basis of SiO_4 building blocks (Roy, 1989). Various phosphate-based chemically bonded ceramics (CBC's) were studied by Roy (1989). In that study HAC was mixed with phosphoric acid and cured at elevated temperature. Tensile splitting strengths reached 27 MPa after 1 day curing at 90°C in a water vapor atmosphere. She summarized some typical values found for the phosphate materials, in comparison with portland cement-based materials as shown in Table 2.

According to Kingery (1950), Phosphate bonding can be accomplished by :

- using siliceous materials with phosphoric acid

Table 2. Properties of chemically bonded ceramics (data from Roy, 1989)

Property	Silicates		Phosphates
	Super-plasticized	Polymer Modified	Phosphate Bonded
Tensile Strength (MPa) Maximum	31	18	27
Density (Kg/dm^3) Maximum	2.73	2.53	2.53
Porosity (%) Minimum	1	12	~
Dielectric Const. (100 KH at 25°C) Minimum	~	5.8	2
Loss Factor (tan Dx100 for 100 KH at 25°C) Minimum	~	0.42	0.05

- using metal oxides with phosphoric acid
- direct addition or formation of acid phosphates

Many of the problems (e.g. bond migration, low shelf life, bloating and low hot strength) that have limited the use of these materials (Cassidy, 1977). Cassidy summarized that those problems could be resolved by the development of new bond systems and by studies of bond-aggregate interactions.

The alkali polyphosphates are particularly useful in bonding basic aggregate. Sodium hexametaphosphate forms rubberlike polymers and yields high strength mortars with fireclay aggregates. These materials are used in high alumina refractories, and are particularly useful for bonding basic aggregates (Cassidy, 1977). Thus, sodium phosphate polymer $NaPO_3$ may be represented by the following (where n varies from 6 to 21):

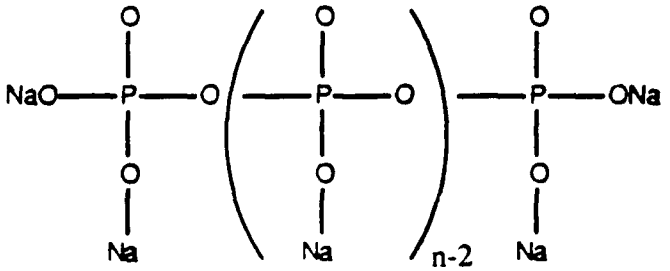

Cassidy summarized that very high strength could be achieved at high temperature. Sarkar (1990) thought that a weakly basic or amphoteric cation having a moderately small ionic radius was required so that a nonordered or glassy structure can be formed for optimum bonding.

The chemical reactions at room temperature between HAC and

$NH_4H_2PO_4$ - based fertilizer were studied by Sugama and Carciello (1991). They found that ammonium calcium pyrophosphate is the principal product responsible for the development of strength. Hydrothermal treatment at 200°C led to phase transformations into crystalline hydroxyapatite as the major phase and anorthite as the minor one and contributed to the development of compressive strength in excess of 70.0 MPa.

Powders prepared by sol-gel techniques at room temperature have been reacted to produce new setting cement materials in CaO-SiO_2-P_2O_5-H_2O system (Hu et al., 1987, 1988). The maximum splitting tensile strength was achieved up to 31 MPa at 100°C for 1 day of hydration in some compositions. They proposed that the high strengths were attributed to the ultrafine powders used and the formation of well developed gels of C-S-H and C-S-P-H which serve as the bond interlinking with crystalline grains. Steinke et al. (1989,1991) extended the above work with the purpose of obtaining optimum compositions that may provide good cementitious properties. They found that the characterization of the hydrated samples revealed that C-S-H phase is responsible for providing the strength to the material.

Many basic oxides will react with phosphoric acid or acid phosphate at ordinary temperature, forming a coherent mass and eventually setting with time, giving high compressive strength. However, the two components that have drawn most of the attention regarding quick-setting, road repairing compounds are magnesia and acid ammonium phosphate, but there have been few systematic studies made about the system (Sarkar, 1990). The magnesium phosphate

system has been investigated by various researchers. Sugama and Kukacka (1983) made a material which had a compressive strength of 48.2 MPa and was thermally stable in air at temperature > 1000°C.

1.4 Chemical and Physical Properties

1.4.1 Introduction

It is generally recognized that conventional cements exhibit useful compressive strengths but have low tensile and flexural strengths. Generally, the mechanical properties of cement-based materials are controlled by the compositions of the starting materials, the manner in which these are mixed with an aqueous media, the chemical bonding of the reaction products and the microstructure of the final assemblage. Strategies to improve the mechanical properties of cement-based materials have been addressed by a large number of studies. One approach to improvement of the properties of cement is the addition of secondary constituents.

The chemical and physical properties of cements, including ordinary portland cement and high alumina cement, and phosphatic materials are discussed in the following section.

1.4.2 Ordinary Portland Cement

Ordinary portland cement is admirably suitable for use in general concrete construction when there is no exposure to sulphates in the soil or in ground water. Over the years, there have been some changes in the characteristics of ordinary portland cement. In particular, modern cements have a much higher strength than they did a half

century ago (Neville, 1981).

The cement is made by heating a mixture of limestone and clay, ultimately to a temperature of about 1450°C. After the clinker is produced, it is mixed with a few per cent of gypsum which can control the rate of set and finely ground to make the cement. Portland cement normally contains four major phases (as listed in Table 3), these include tricalcium silicate (C_3S), dicalcium silicate (C_2S), tricalcium aluminate (C_3A) and tetracalcium aluminoferrite (C_4AF) (Czernin, 1980).

The compound composition of a cement and the manner in which each of its phases reacts with water govern its physical and chemical properties. Some knowledge of the hydration processes is therefore desirable for an understanding of the chemical reactions which can occur in cement and how they may be modified or counteracted by altering the composition of the cement or by adding materials which have greater chemical resistance (Eglinton, 1987).

The hydration reactions of portland cement have been studied for many years. The investigation of the cement hydration process with these various chemical and physical aids traces something like the following pattern of events. After the portland cement has been mixed with water, the latter will have become saturated or indeed supersaturated with calcium hydroxide. The tricalcium silicate in the cement passes into solution. The aqueous solution soon decomposes into hydrated calcium silicate and calcium hydroxide respectively. In similar fashion, though to a less extent, dicalcium silicate also forms calcium hydroxide. The hydrated calcium silicates which are precipitated in gel form on the surface of the grains, are considered to

Table 3. The composition of the main compounds in portland cement (data from Czernin, 1980)

Description	Formula	Abbreviation	Composition (per cent)			
			CaO	SiO_2	Al_2O_3	Fe_2O_3
Tricalcium Silicate	$3CaO \cdot SiO_2$	C_3S*	73.7	26.3	~	~
Dicalcium Silicate	$2CaO \cdot SiO_2$	C_2S	65.1	34.9	~	~
Tricalcium Aluminate	$3CaO \cdot Al_2O_3$	C_3A	62.3	~	37.7	~
Tetracalcium Aluminoferrite	$3CaO \cdot Al_2O_3 \cdot Fe_2O_3$	C_4AF	~	~	~	~

* It is customary in cement chemistry to indicate the individual clinker minerals by the following abbreviated notation:

$CaO = C$, $SiO_2 = S$, $Al_2O_3 = A$, $Fe_2O_3 = F$

Thus, the compound $3CaO \cdot SiO_2$ is referred to as C_3S, and $2CaO \cdot SiO_2$ as C_2S, etc.

conform to the following approximate overall formula: $3CaO{\cdot}2SiO_2{\cdot}3H_2O$. The following reaction pattern can be established for the calcium silicates of cement (Czernin, 1980):

$$2(3CaO{\cdot}SiO_2) + 6H_2O \rightarrow 3CaO{\cdot}2SiO_2{\cdot}3H_2O + 3Ca(OH)_2$$

$$2(2CaO{\cdot}SiO_2) + 4H_2O \rightarrow 3CaO{\cdot}2SiO_2{\cdot}3H_2O + Ca(OH)_2$$

As for the hydration of the aluminate components, this process is initially attended by vigorous participation of the sulphate in the mixing water. This sulphate derives primarily from the gypsum added to the clinker in cement grinding, but also from the alkali sulphates. With this sulphate component the tricalcium aluminate first forms the compound $3CaO{\cdot}Al_2O_3{\cdot}3CaSO_4{\cdot}32H_2O$, mineralogically known as "ettringite," which is believed to attach itself to the surface of the aluminate, slow down the access of water to the latter, and thus prevent too-rapid setting of the cement. After about 24 hours, the gypsum is found to have disappeared from the mixing water in the paste, it has been entirely consumed in forming ettringite and has come to the end of its role as a setting retarder. Then ettringite is converted into "monosulphate," a phase containing less sulphate and also substantially less water of crystallization (Czernin, 1980):

$$2(3CaO{\cdot}Al_2O_3) + 3CaO{\cdot}Al_2O_3{\cdot}3CaSO_4{\cdot}32H_2O + 4H_2O$$

$$\rightarrow 3(3CaO{\cdot}Al_2O_3{\cdot}CaSO_4{\cdot}12H_2O)$$

The ferric oxide in tetracalcium aluminoferrite $4CaO{\cdot}Al_2O_3{\cdot}Fe_2O_3$ can enter into entirely analogous compounds in the way that alumina does. However, the reaction of tetracalcium aluminoferrite is much slower than that if tricalcium aluminate (Czernin, 1980):

$$4CaO{\cdot}Al_2O_3{\cdot}Fe_2O_3 + 4Ca(OH)_2 + 22H_2O$$

$$\rightarrow 4CaO{\cdot}Al_2O_3{\cdot}13H_2O + 4CaO{\cdot}Fe_2O_3{\cdot}13H_2O$$

It has been found that reaction that occur during the first few hours, or the first day or so, are of particular importance in their influence of the final properties of the concrete.

The differences in behavior of the four main compounds make it possible for a range of portland cements to be produced, each having its own special properties. These are mainly physical, affect such properties as the rate of hardening, of strength development and of evolution of heat on hydration (Eglinton, 1987).

1.4.3 High Alumina Cement

High alumina cement differs from portland cement in composition and exhibits properties that severely limits its use. The SiO_2 deficient side of the CaO-Al_2O_3-SiO_2 ternary phase diagram is given in Figure 3. The phases present in this ternary system at room temperature form the basis for both portland cement and high alumina cement, which are shown on the diagram in the approximate general compositional ranges. The main cementitious compounds of HAC are the calcium aluminates CA, CA_2 and very small proportion of $C_{12}A_7$. CA_2 is relatively slow to react and thus primarily contributes to long-term hydration and strength development. The hydration of CA, which has the highest rate of strength development, initially results in the formation of CAH_{10}, a small quantity of C_2AH_8, and of alumina gel.

One of the outstanding feature of high-alumina cement is its very high rate of strength development. About 80 per cent of its ultimate strength is achieved by 24 hours. The high rate of gain of strength is due to rapid hydration of CA, which in turn means a high rate of heat development. The hydration of CA results in the formation of several

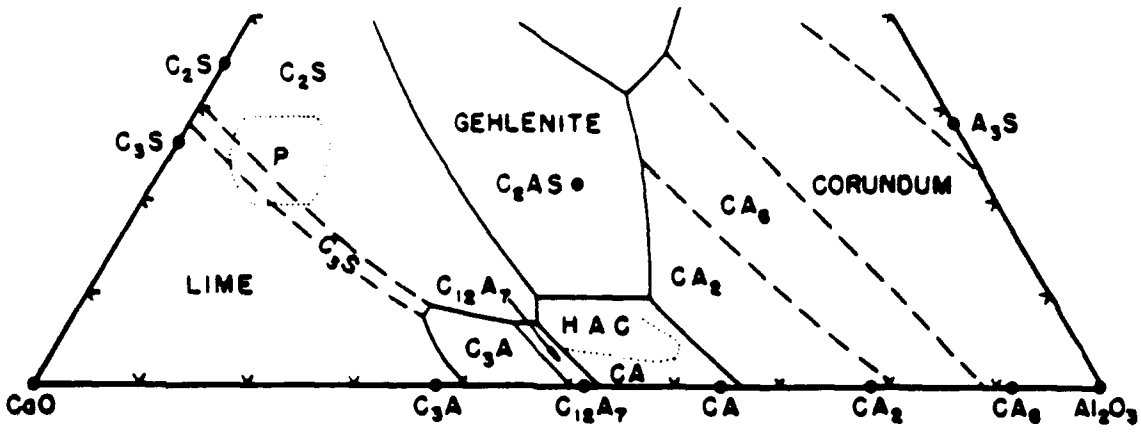

Figure 3. The SiO_2 deficient side of the CaO-Al_2O_3-SiO_2 ternary phase diagram with compositional ranges marked for portland cement (P) and high alumina cement (HAC). S = SiO_2, C = CaO, A = Al_2O_3 (from Robson, 1962)

hydration products by the following reaction:

$$CA + H_2O \rightarrow CAH_{10} + C_2AH_8 + AH_x$$

A factor severely limiting the use of HAC is the strength loss which occurs in applications at room temperature and above or in humid conditions because of the conversion of the hexagonal hydrates CAH_{10} and C_2AH_8 to the more dense cubic hydrate C_3AH_6. With time, these hexagonal CAH_{10} and C_2AH_8 crystals, which are chemically unstable both at normal and higher temperatures, transform into cubic C_3AH_6 and alumina gel. This change is know as conversion. The transformation is encouraged by a higher temperature and a higher concentration of lime or a rise in alkalinity. Thus, at room or higher temperatures only the cubic form of the calcium aluminate hydrate is stable. Because the hexagonal crystals CAH_{10} and C_2AH_8 spontaneously and slowly convert to the cubic form C_3AH_6, they can be said to be unstable at room temperature. In addition, AH_3 as gibbsite or hydrargillite is the stable phase over the aluminous gel phase. The final products of the reactions of hydration are the cubic form as in the following (Sliva, 1988):

$$3CAH_{10} \rightarrow C_3AH_6 + 2AH_3 + 18H$$

$$3C_2AH_8 \rightarrow 2C_3AH_6 + AH_3 + 9H$$

$$AH_x \text{ (aluminous gel)} \rightarrow g\text{-}AH_3 \text{ (gibbsite)} + (x\text{-}3)\,H$$

The practical interest in conversion lies in the factor that it leads to a loss of strength of high-alumina cement. The most likely explanation by Neville (1981) why this is so is in terms of the densification of the calcium aluminate hydrates. typically the density would be 1.72g/ml for CAH_{10}, 1.95 for C_2AH_8 and 2.53 for C_3AH_6. Thus, under condition such that the overall dimensions of the body are constant, conversion

results in an increase in the porosity of the paste. It is reported by Neville that porosity increase of 5 per cent can reduce the strength by more than 30 per cent. and a 50 per cent increase in strength would be caused by a porosity reduction on the order of 8 per cent.

In summary, high alumina cement (HAC) rapidly develops strength and offers modest strength and stiffness in compression but is weak in flexural and impact strengths. The strength losses which HAC may show at room temperature or in hot and humid conditions are because of the conversion of the hydration products. It is a valuable material for repair work of limited life and in temporary works but no longer used in structural concrete above or below ground.

1.4.4 Phosphate-Based Inorganic Polymers

Early studies demonstrated that organic polymers contain large numbers of simple molecular units (monomers) covalently linked together to form extremely long, and in many cases infinite, chains. It has been well established that many organic materials can be polymerized to form long-chain compounds and a careful study has been made of the principles of such polymerization processes, the structures, and properties of the polymer formed. The formation of organic polymers may be attributed to the ability of the tetrahedral carbon atom to undergo unlimited covalent combination with other carbon atoms. However, this ability is not restricted to carbon, and many other elements of the Periodic Table are capable of similar behavior. This so-called "Inorganic Polymer" mostly has a hetero-chain structure (Gimblett, 1963).

The concept of a "condensed phosphate" embraces a group of pentavalent phosphorus compounds in which various numbers of tetrahedral PO_4 groups are linked together by oxygen bridges according to the scheme (Thilo, 1962):

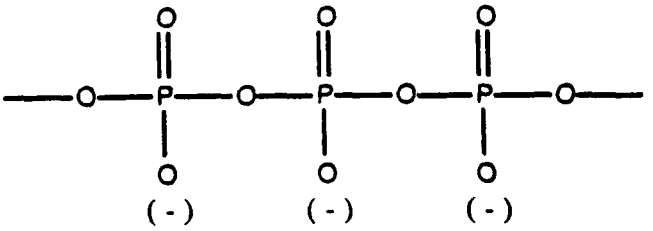

The analogy has led to attempts to synthesize inorganic analogs of carbon-based linear polymers in the hope of achieving highly flexible, highly thermally stable inorganic polymers. Unfortunately, the effort seems not to have been wholly successful since polyvalent inorganic species tend to form highly ordered crystalline compounds or in some instances to cross-link and form rigid glassy structures. While this is undesirable if one is attempting to develop inorganic polymers for textiles, it provides considerable promise if one wishes to develop a high strength composite (Brown and Roy, 1992).

Alkali phosphates, such as sodium phosphate glasses, can polymerize by condensation and form linear polymers as follows:

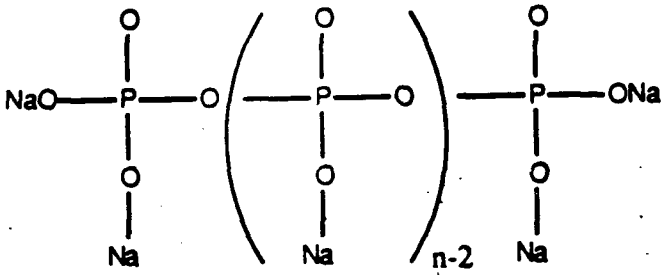

These polymers can possess the properties of elastomers, and high strength can be achieved at high temperature (Cassidy, 1977). The methods of preparation can use reactions at high temperature with metal oxides, metal salts, or less condensed metal phosphates. The phosphate-based inorganic polymers, such as $(NaPO_3)_n$ and $(NaPO_3)_n{\cdot}Na_2O$ can be made by this method. Reaction in solution at room temperature is another way for preparation. This method can be used to produce $Na_5P_3O_{10}$ which is virtually insoluble in water.

Pyrophosphoric acid is the condensed phosphoric acid which can be prepared in crystalline form, and the crystals, in contrast to other condensed phosphoric acids, contain a single type of phosphate. At acid concentrations higher or lower than the theoretical composition, the crystallization products will contain either long chain or orthophosphoric acids. Extensive x-ray data and paper chromatographic analysis demonstrated the existence of intermediates which often are polyphosphates of unspecified composition.

In short, much progress in phosphate chemistry and technology has been made in recent years. The development of research on phosphates as industrial materials is particularly remarkable.

Chapter 2
EXPERIMENTAL PROCEDURES

2.1 Introduction

Several starting materials were used in this investigation and can be grouped for discussion purposes as cement and phosphate.

A variety of characterization techniques were used to determine the physical and chemical properties of the materials prepared during this investigation. The physical properties included density, surface area, particle size distribution, flexural and tensile strength, porosity and pore size distribution, and microstructure. The chemical properties were investigated using isothermal calorimetry, x-ray diffraction analysis and energy-dispersion x-ray spectrometry.

The preparative procedures for the samples include: mixing, molding/or compacting, and curing. Preparation for different technical measurement will be discussed in different instrument sections.

2.2 Starting Materials

High alumina cement and ordinary portland cement were employed as starting materials in this study. Silica fume was added to some of the samples.

The phosphate materials used include four condensed sodium phosphates and two calcium phosphates: sodium hexametaphosphate $(NaPO3)_n$, sodium metaphosphate $(NaPO_3)_n Na_2O$, sodium tripolyphosphate $Na_5P_3O_{10}$, sodium trimetaphosphate $(NaPO_3)_3$, calcium phosphate $CaHPO_4$, and calcium pyrophosphate $Ca_2P_2O_7$. The following sections describe physical and chemical properties of each of these materials.

2.2.1 Cement and Silica Fume

The physical properties and some general information for ordinary portland cement, high alumina cement and silica fume are described in following section.

2.2.1.1 Portland Cement

Table 4 contains the chemical analyses of the raw materials as weight percent oxide carried out by means of a D.C argon plasma spectrometer and titrimetric analysis at the Mineral Constitution Laboratory of The Pennsylvania State University. The mineralogical compositions of the portland cement was calculated from the chemical composition by Bogue calculations [Taylor, 1964] as shown in Table 5. The physical properties of the materials, such as density, surface area and particle size distribution, are listed in Table 6.

Table 4. Chemical analyses of starting materials (wt%)

	OPC	Secar 71	Silica Fume
SiO_2	19.20	0.68	95.32
Al_2O_3	6.25	71.30	0.02
Fe_2O_3	2.45	0.09	0.08
CaO	61.10	26.80	0.38
TiO_2	0.30	0.01	<0.01
MgO	3.21	0.46	0.19
Na_2O	0.43	0.37	0.08
K_2O	0.77	0.02	0.55
L-O-I	2.80	0.70	3.05
SO_3	3.60	0.04	0.24
Total %	100.11%	100.47%	99.92%

Table 5. Bogue calculations for Keystone Type-I OPC used in this study

C_3S	47.10
C_2S	19.51
C_3A	12.42
C_4AF	7.46
MgO	3.21
Anhydrite	7.74
Others	2.68

Typical cement notation is employed here; thus, the compound $3CaO \cdot SiO_2$ is referred to as C_3S, and $2CaO \cdot SiO_2$ as C_2S, etc.

Table 6. Density, surface area and particle size distribution data of starting materials

	Density (g/cm^3)	Surface Area (m2/g)	Size Distribution Range (μm)
OPC	3.11	0.87	1.2-50
HAC	3.00	0.96	0.9-45
Silica Fume	2.05	17.2	0.1- 9

Ordinary portland cement (OPC), assigned the Materials Research Laboratory (MRL) identification File No. I-23, was obtained from Keystone Cement Co. It has density of 3.11 g/cm^3 and BET surface area of 0.87 m^2/g. The particle size distribution range determined by micromeritics sedigraph is given in Figure 4.

2.2.1.2 High Alumina Cement

The high alumina cement (MRL File No. S-07), also known as calcium aluminate cement, used in this study was Secar 71 cement, which was obtained from Lonestar Lafarge, Inc. This material used primarily in refractories and repair applications. Table 4 shows the chemical composition of the cements as weight percent oxide content.

X-ray powder diffraction indicated that the cement contains CA, CA_2 and $C_{12}A_7$. It is difficult to quantitatively measure the relative proportions of this phases because variations were observed from one sample to another. Bushnell-Watson and Sharp (1986) suggested that this was associated with different particle size distributions of the various phases. BET surface area of Secar 71 was found to be 0.96 m^2/g, and density 3.0 g/cm^3. The particle size distribution range determined by micromeritics sedigraph is about 0.9~45.0 μm (Figure 5).

2.2.1.3 Silica Fume

The silica fume, an extremely fine powder (MRL File No. G-15), used in this study was obtained from Elkem Chemical, Co. The chemical analysis of silica fume used in some experiments to replace a

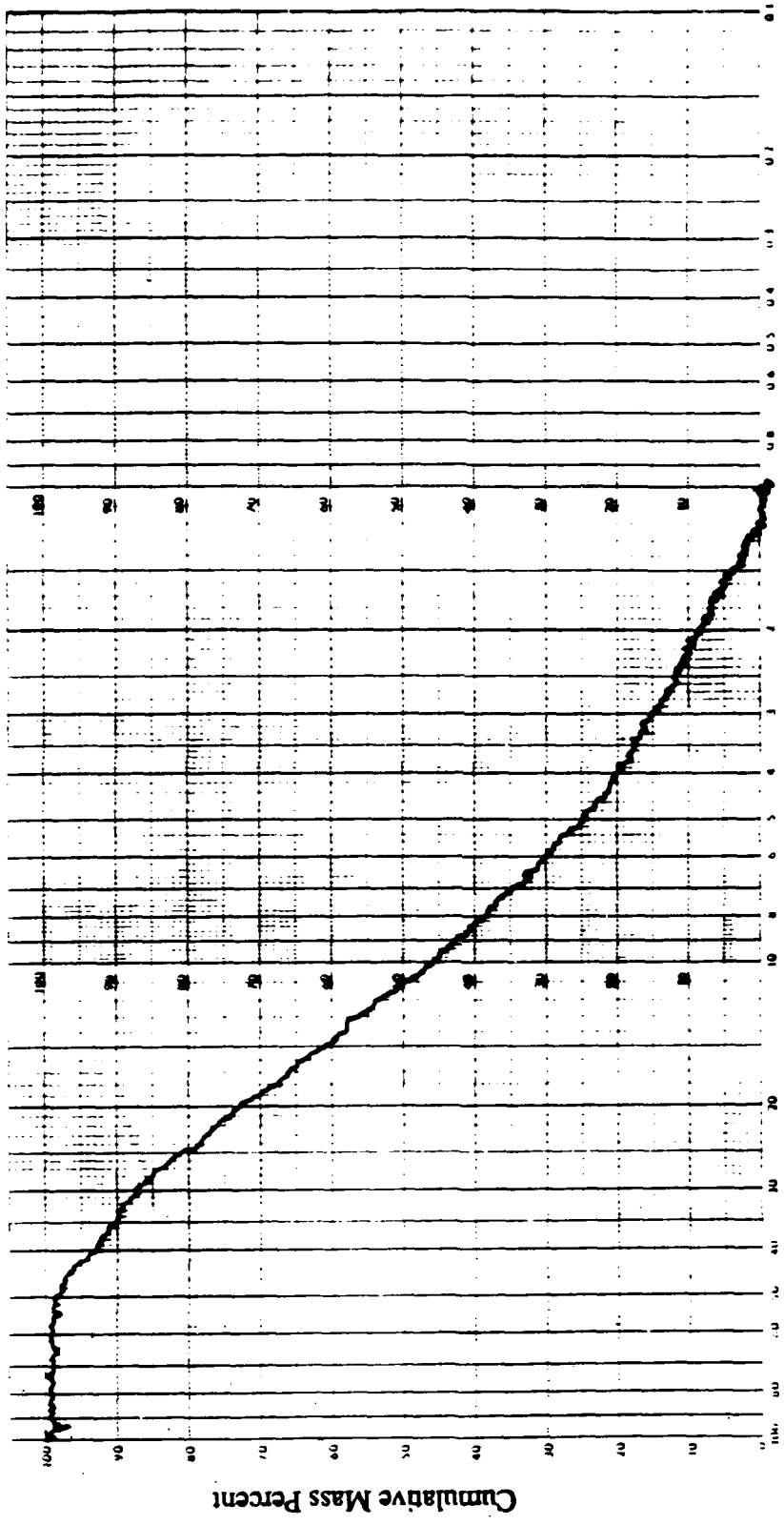

Figure 4. Particle size distribution of ordinary portland cement as determined by sedigraph analysis (Keystone Type-I, No. 1-23)

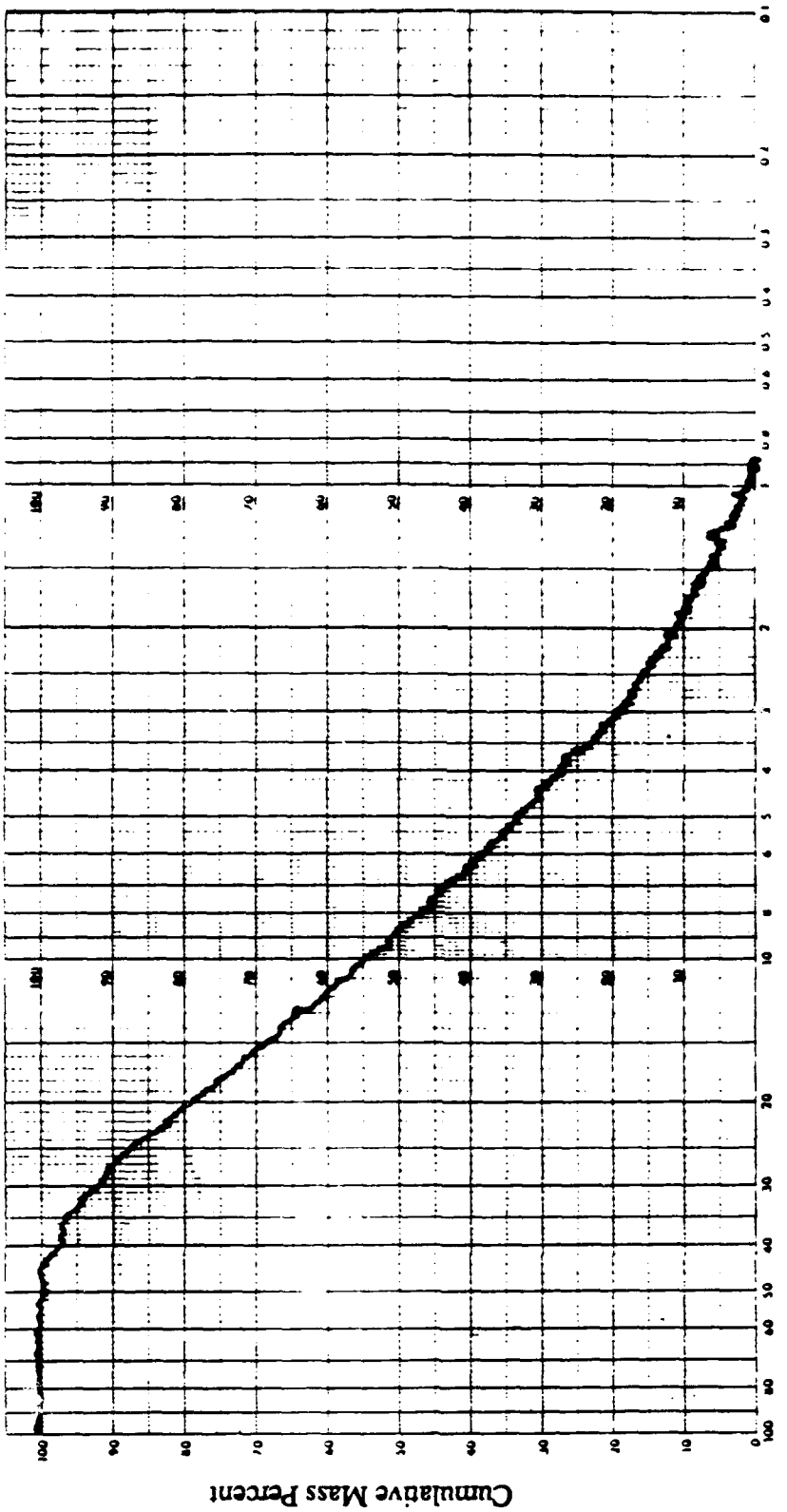

Figure 5. Particle size distribution of high alumina cement as determined by sedigraph analysis (Secar 71, No. S-07)

portion of the cement is given in Table 4. The density is 2.05 g/cm^3, BET surface area 17.2 m^2/g. The particle size distribution is given in Figure 6.

2.2.2 Phosphate

Sodium phosphate and calcium phosphate are grouped for discussion purposes in the following section.

2.2.2.1 Sodium Phosphate

Four sodium phosphates were used in this investigation: sodium hexametaphosphate $(NaPO_3)_n$, sodium metaphosphate $(NaPO_3)_n \cdot Na_2O$, sodium tripolyphosphate $Na_5P_3O_{10}$, and sodium trimetaphosphate $(NaPO_3)_3$.

$(NaPO_3)_n$ and $Na_5P_3O_{10}$ was obtained from Aldrich Chemical Company, Inc, $(NaPO_3)_n \cdot Na_2O$ from Fisher Scientific Co., and $(NaPO_3)_3$ from Johnson Matthey Electronics.

X-ray powder diffraction indicated that $(NaPO_3)_n$ and $(NaPO_3)_n \cdot Na_2O$ exhibit amorphous, while $Na_5P_3O_{10}$ and $(NaPO_3)_3$ are well crystallized.

2.2.2.2 Calcium Phosphate

Calcium phosphate $CaHPO_4$ and dicalcium pyrophosphate $Ca_2P_2O_7$ were used in this study. $CaHPO_4$ was obtained from Fisher Scientific Co., and $Ca_2P_2O_7$ from Sigma Chemical Co. X-ray powder diffraction indicated that both of them are well crystallized.

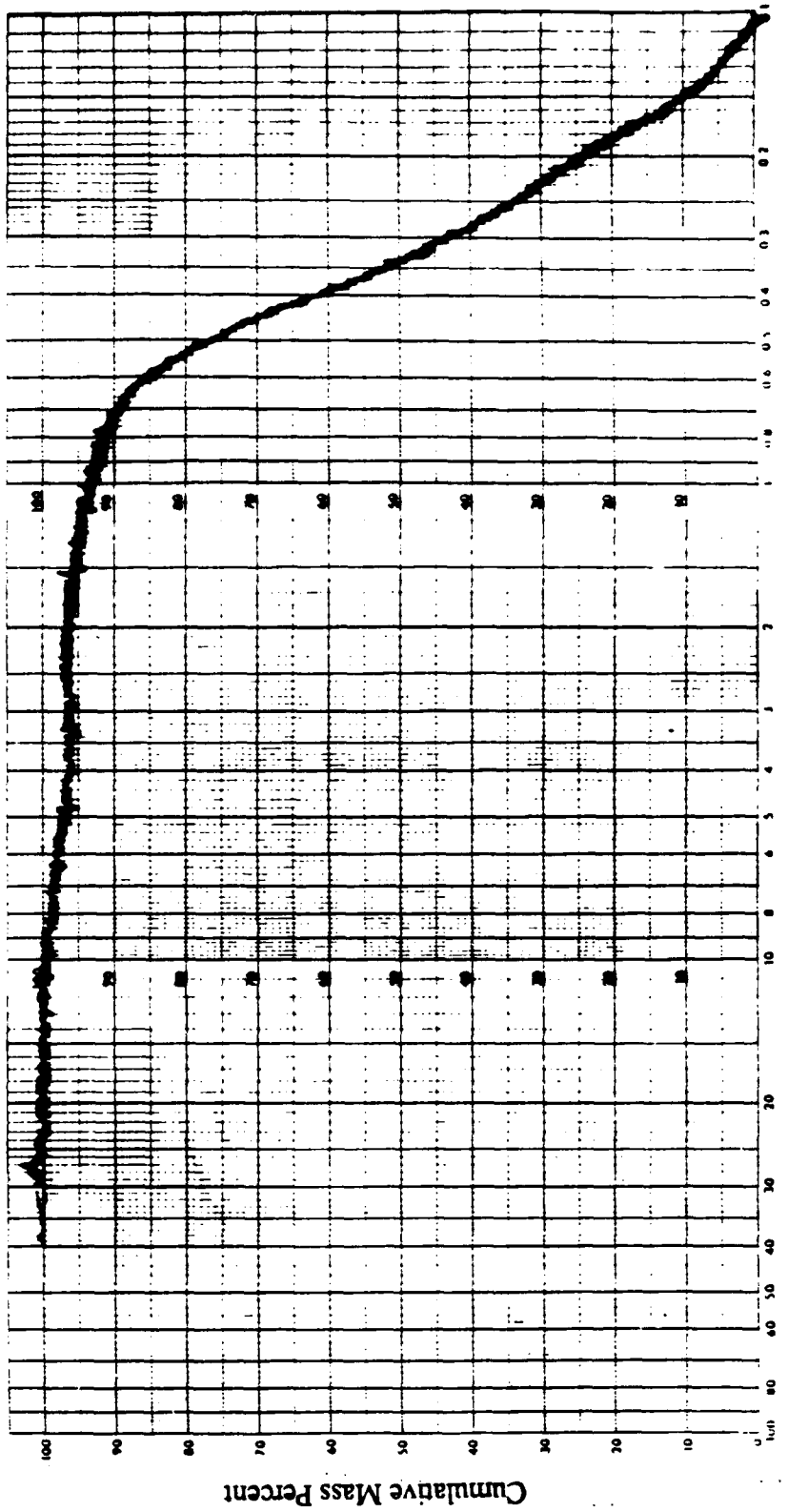

Figure 6. Particle size distribution of silica fume as determined by sedigraph analysis (No. G-15)

2.3 Instrumentation and Characterization Studies

The following section describes a variety of characterization techniques were used to determine the physical and chemical properties of the materials prepared during this investigation.

2.3.1 Mechanical Property Measurements

Three point bend test determinations were made using an Instron testing machine at a loading rate of 0.01 cm/minute. Figure 7(a) schematically shows the condition of the three point bending test, and the flexural strength or modulus of rupture (MOR) was calculated using the expression (Timoshenko and Goodier, 1982, pp.354-78)

$$MOR = \frac{3LP}{2Wt^2}$$

where P is the maximum load, L the distance between the supports (= 0.96 cm). W and t are the width and depth of the specimen, respectively. The splitting (tensile) strength was also measured on an Instron machine as shown in Figure 7(b). The splitting strengths were calculated using the expression (Timoshenko and Goodier, 1982, pp.122-27)

$$S.S = \frac{2P}{\pi dt}$$

where d is the diameter and t the thickness.

The results given are typically the average values of six specimens.

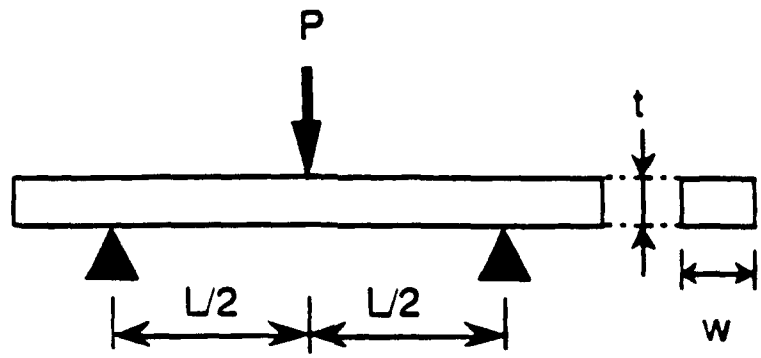

(a)

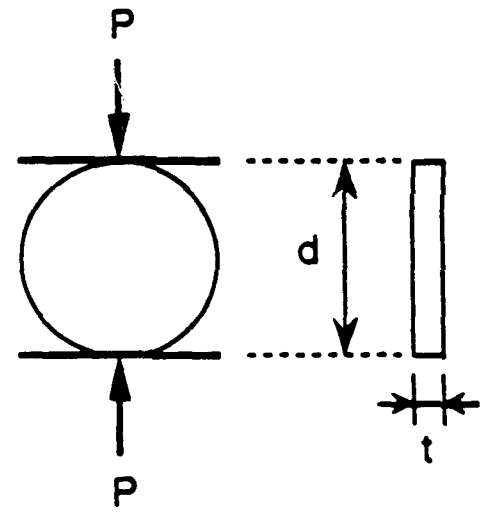

(b)

Figure 7. Schematic diagram and conditions of (a) the 3-Point Bending Test and (b) Tensile (Splitting) Test (from Uchiyama, 1989)

2.3.2 Isothermal Calorimetry

Calorimetric studies were performed to test reactivities of the materials by determining the rates of heat evolution during the reactions. In the method used, a known amount of cement (typically 3 grams) is placed in a gold plated copper calorimetric sample holder. This is then thermally equilibrated to the temperature of reaction. An aqueous reactant is separately equilibrated to the same temperature. Once equilibrium has been achieved, the liquid is inoculated onto the solid and the rate of heat evolution is measured. Configuration of the isothermal calorimeter used in this study is shown in Figure 8. A computer is connected to the thermopiles to collect data. Preparation of samples consisted of placing about 3g of powder into a gold-plated cup, putting the cup in, and injecting about 1.7 cc DI water in a syringe. Each reactant was then allowed to equilibriate separately at 25°C for about half an hour prior to mixing. The heats of hydration of the samples were recorded for 48 hours. With some samples, data were collected only for the first 24 hours.

2.3.3 X-ray Diffraction

X-ray diffraction analyses were performed on a Scintag Automated X-ray diffractometer interfaced with a microVAX computer. This diffractometer is equipped with a copper target with Cu $K\alpha_1$ radiation (λ=1.540598Å) being used to determine the d-spacings. The phase identification software package has several major features that include crystalline peak identification and an automated search and match routine that compares the generated x-ray diffraction of a phase by visual comparison of the generated pattern with any JCPDS (Joint

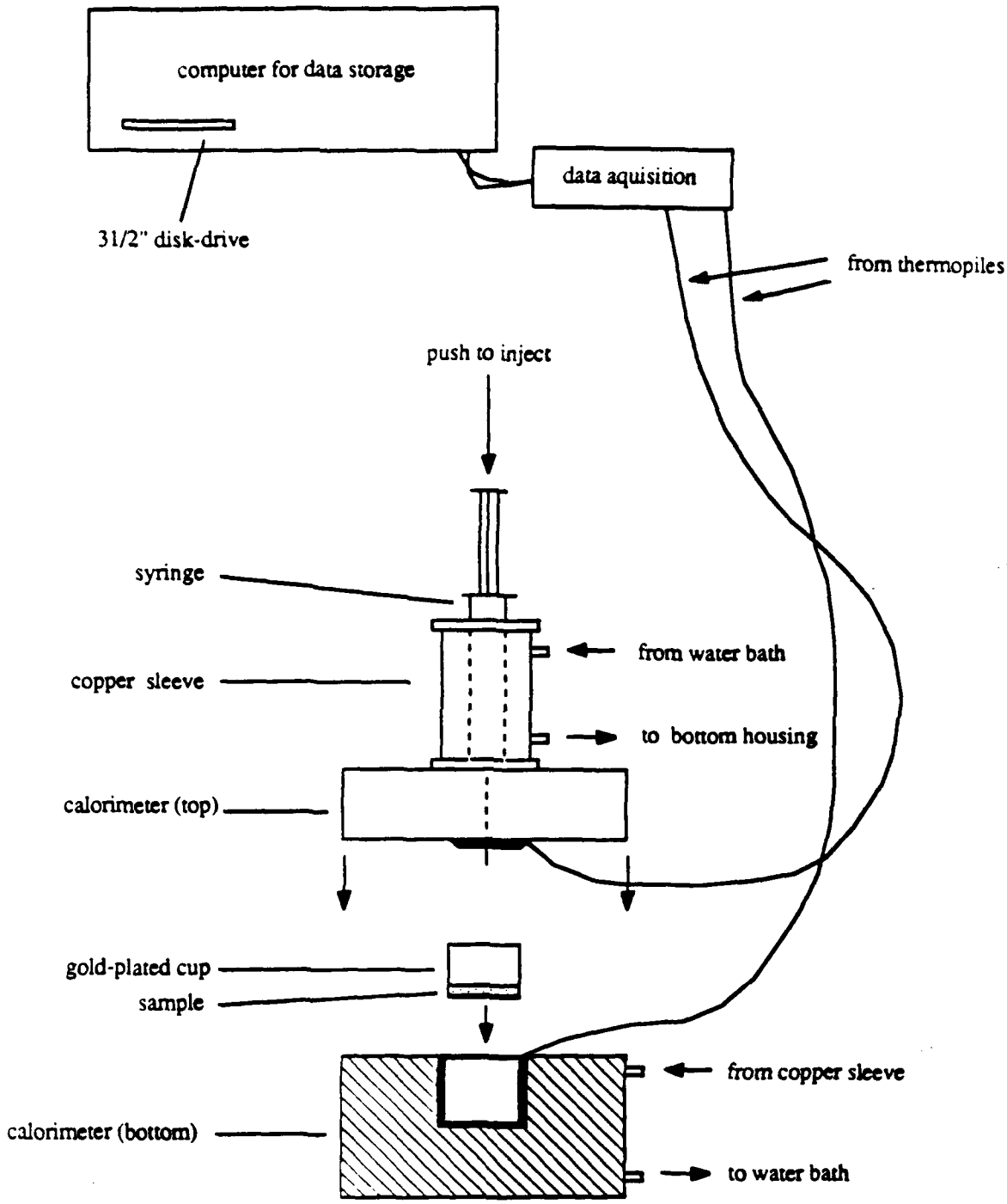

Figure 8. Configuration of the isothermal calorimeter used in this study (from Bothe, 1991)

Committee on Powder Diffraction Standards) card file. The software also allow the pattern background to be stripped from the experimental data.

The most frequently used scan rate for phase identification of as-received materials was used 2°2θ per minute. Scan rates to 4°2θ per minute were also used.

Preparation of solid samples consisted of grinding the sample in a mortar and pestle, and mounting a portion on a glass slide. A few drops of acetone were mixed into the powder with a stainless steel spatula. The slide then trembled on the table until it was spread out. Early hydrated samples have a certain fluidity, and sample preparation therefore is different from hardened samples. Samples taken after short times of hydration were put in acetone to stop reaction and then mounted on a glass slide until the acetone evaporated. All diffraction patterns were obtained at room temperature.

2.3.4 Mercury Intrusion Porosimetry

Porosity analyses were performed on a Quantachrome Corporation scanning mercury porosimeter with a recorder which was used to plot the volume of mercury intruded as a function of pressure. In this technique, an evacuated sample of a porous material is immersed in liquid mercury. The mercury is then forced into the pores of the material under pressure. The pore diameter is therefore inversely proportional to the required pressure. The porosimeter's available pressure range was 24 to 60,000 psi (0.17 to 414 MPa). This corresponds to pore dimensions in the range from 7.5 mm to 1.8 nm.

Preparation for samples consisted of cutting the samples into about 4 or 5 mm and freeze drying for 16 hours.

2.3.5 Scanning Electron Microscopy

Microstructures of samples were observed using an International Scientific Instruments ISI-DS 130 dual stage Scanning Electron Microscope (SEM) with a Kevex Energy Dispersive X-ray analyzer (EDX) for chemical determinations. This system utilizes five lenses to allow examination of a wide range of sample sizes. A tungsten filament acts as the electron source. The system is capable of detecting secondary electrons, back scattered electrons and X-rays.

Samples were prepared by carefully cutting the pellets with a razor blade. A small, relatively flat surface piece was then placed on the holder with silver paint. The sample was then sputtered with gold to provide a path for charge built up on the surface.

2.3.6 Energy-Dispersion X-ray Spectrometry

The chemical compositions of the hydrates were determined by using Kevex Energy-Dispersion X-ray Spectrometry (EDX) which is coupled with SEM. This technique employs a cryogenically cooled Si(Li) detector and a multichannel analyzer to determine the presence of elements by their characteristic x-rays.

2.3.7 Environmental Scanning Electron Microscopy

Comparing traditional high vacuum SEM, the Environmental Scanning Electron Microscopy (ESEM) demonstrates the advantage of studying uncoated, non-conductive materials, and it allows specimens

to be observed in real time and microstructural evolution during hydration reactions has been observed. Using Model ESEM-30 (ElectroScan Corp., Wilmington, MA), wet samples remain hydrated during examination. Thus, the reaction process could be observed.

A relatively high water/cement ratio (usually 0.5) was used in order to keep the samples moist for an extended period of time. The samples were hand mixed then immediately placed in the ESEM.

2.3.8 Shear Mixing

High shear mixing was performed on C. W. Brabender, Inc. Preparation Center-Mixer which consists of a hardened steel mixhead capable of being heated through internal resistance heaters and cooled through forced air to room temperature. High shear, hardened steel cam blades were used for all mixing. The blades can be rotated up to 100 rpm. Temperature was monitored through a thermocouple inserted into the mixhead and a digital readout on the control console.

All batches were run at room temperature. The highest rate of the blades was used for 60 rpm in this study.

2.3.9 Density

The density of the cements and silica fume was determined following the standard ASTM C188 technique (1982). The standard LeChatelier flask was used with kerosene as the displacing fluid.

2.3.10 BET Surface Area

BET surface areas was obtained by using a Quantachrome BET Surface Area Analyzer. The theory utilizes a series of gas additions to

obtain several points from which the surface area can be derived. The nitrogen gas usually be used to be adsorbed as a monolayer on the surface of a materials. Powder samples were prepared by heating in air at 150°C for about half hour.

2.3.11 Particle Size Distribution

Particle size distribution for as-received cement and silica fume was done on a Micromeritics Sedigraph instrument. X-ray attenuation is a sedimentation technique wherein the powder is suspended in a liquid sedisperse in a sample cell and allowed to settle. As the particles settle, a collimated x-ray beam is passed through the chamber and the transmitted x-ray intensity detected. The concentration of particles remaining in suspension is measured as a function of time and sedimentation depth. Output is displayed as a cumulative mass percent versus equivalent spherical diameter (log scale). Preparation for samples includes dispersing the powder in sedisperse and sonication for 15 seconds.

2.4 Preparation of Materials

This section describes the details of sample processing. The preparation involves mixing, molding/or compacting, and curing. Figure 9 shows the precessing flowchart for this study.

2.4.1 Mixing the Cement Pastes

Mixing is based on the general concept from MDF technology, and high shear mixing was employed instead of standard mixing to improve the homogeneity. Thus, lower water to cement ratios can be

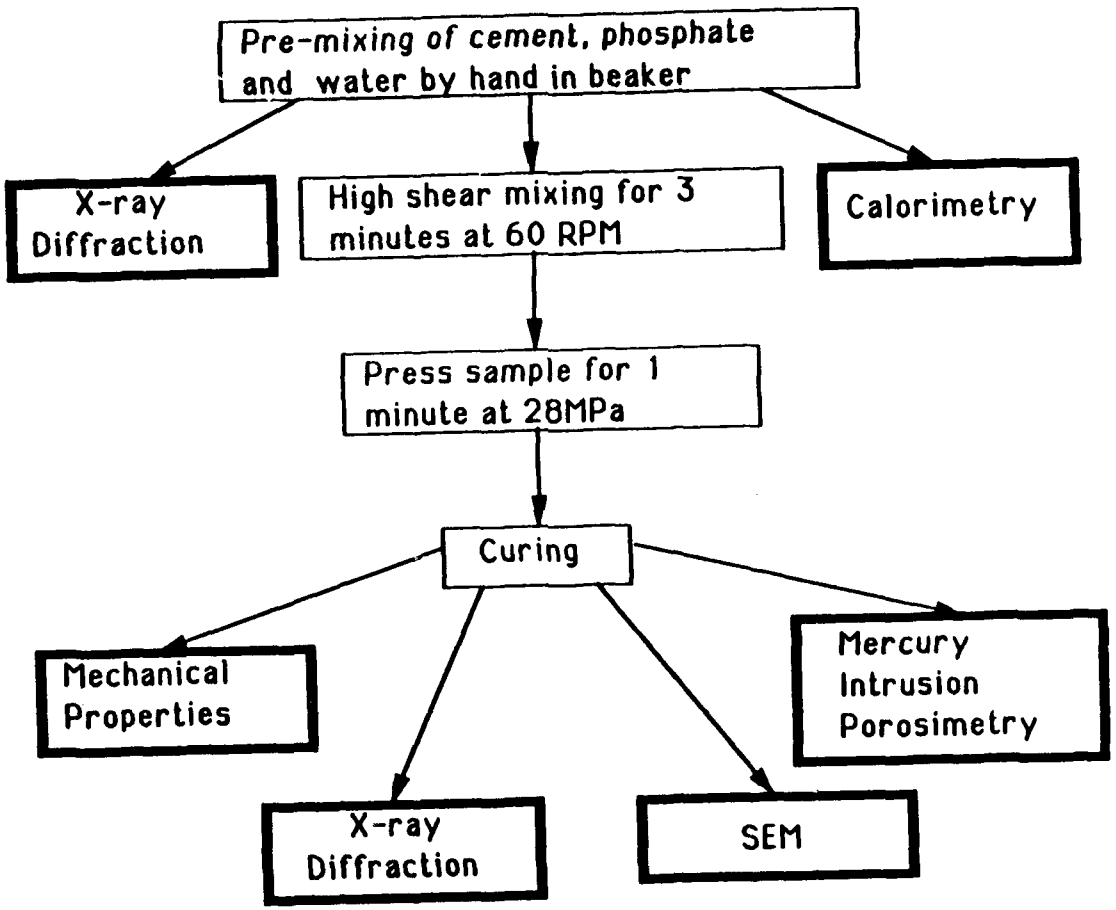

Figure 9. Processing flowchart

used. The high shear mixer used was a Brabender Laboratory Sample Preparation Center, manufactured by C. W. Brabender Instruments, Inc.

To prepare the cement pastes, cement and phosphate were mixed with deionized water by hand in a beaker for about 30 seconds. The mixture then was placed in a high-shear mixer cell and stirred at approximately 5 rpm. The remaining portion of the cement was gradually added while the paste was being stirred. After all the mixture had been added, the mixing speed was increased to 60 rpm and mixing was continued for 3 minutes. All samples were mixed at room temperature.

Tables 7 and 8 show the compositions (proportions of components) of the HAC and OPC based-phosphate mixtures used in this study along with their identifying numbers. Tables 9 and 10 show the processing, curing, and aging for the HAC and OPC based-phosphate mixtures, and Table 11 the notation for Tables 9 and 10.

2.4.2 Compacting of the materials

Compaction was used in an attempt to decrease the porosity and in increase the density of the hardened paste. After mixing, the specimens of the paste ware pressed in a rectangular or cylindrical die assembly which was designed and constructed at the Materials Research Laboratory. The size for the rectangular die is 2.5 x 1 cm and the cylindrical die is half inch (1.27 cm) in diameter. The mixture was pressed normally at 28-30 MPa for about 1 to 1.5 minutes.

Table 7. Contents of cement pastes prepared with HAC and different phosphates

	Batch (g)				Types of	Weight%
No.	HAC	Phosphate	water	W/S	Phosphate	Phosphate
01	80	8.00	16.00	0.18	$(NaPO_3)_n \cdot Na_2O$	10
03	80	0.00	16.00	0.18	~	0
05	80	19ml	~	~	$Al(H_2PO_4)3$	~
06	80	8.00	16.00	0.18	$CaHPO_4 \cdot 2H_2O$	10
07	80	8.00	12.00	0.14	$(NaPO_3)_n \cdot Na_2O$	10
08	80	8.00	12.00	0.14	$(NaPO_3)_n \cdot Na_2O$	10
09	80	8.00	12.00	0.14	$(NaPO_3)_n \cdot Na_2O$	10
10	80	8.00	12.00	0.14	$(NaPO_3)_n \cdot Na_2O$	10
13*	80	8.00	13.60	0.15	$(NaPO_3)_n \cdot Na_2O$	10
14	80	8.00	13.60	0.15	$(NaPO_3)_n \cdot Na_2O$	10
18	80	8.00	13.60	0.15	$(NaPO_3)_n \cdot Na_2O$	10
21	80	8.00	16.00	0.18	$Na_5P_3O_{10}$	10
23	80	8.00	16.00	0.18	$(NaPO_3)_n$	10
25	80	8.00	16.00	0.18	$(NaPO_3)3$	10
27**	70	7.00	21.00	0.25	$(NaPO_3)_n$	10
28	85	4.25	17.85	0.20	$(NaPO_3)_n$	5
29	85	0.85	17.17	0.20	$(NaPO_3)_n$	1
30	85	2.55	17.51	0.20	$(NaPO_3)_n$	3
31	85	4.25	17.85	0.20	$(NaPO_3)_n$	5
32	85	0.00	17.00	0.20	~	0
33	85	8.50	18.70	0.20	$(NaPO_3)_n$	10
34	85	17.00	20.40	0.20	$(NaPO_3)_n$	20
35	85	25.50	22.10	0.20	$(NaPO_3)_n$	30
36	85	4.25	17.85	0.20	$(NaPO_3)_n$	5
37	85	8.50	18.70	0.20	$(NaPO_3)_n$	10
38	85	17.00	20.40	0.20	$(NaPO_3)_n$	20
39	85	25.50	22.10	0.20	$(NaPO_3)_n$	30
40	85	0.00	17.00	0.20	~	0

Table 7. (Cont.)

41	85	12.75	17.55	0.20	$(NaPO_3)_n$	15
42	85	21.25	21.25	0.20	$(NaPO_3)_n$	25
43	85	17.00	18.36	0.18	$(NaPO_3)_n$	20
44	85	17.00	16.32	0.16	$(NaPO_3)_n$	20
45	85	17.00	14.28	0.14	$(NaPO_3)_n$	20
46	85	17.00	12.24	0.12	$(NaPO_3)_n$	20
55	85	8.00	24.00	0.26	$2CaO \cdot P_2O_5$	9.4
56	85	20.00	24.00	0.23	$2CaO \cdot P_2O_5$	23.5
57	85	0.00	24.00	0.28	~	0
58	75	30.00	29.00	0.28	$2CaO \cdot P_2O_5$	40

* 2.67g gypsum added

** 7g silica fume added

Table 8. Contents of cement pastes prepared with OPC and different phosphates

No.	Batch (g)			W/S	Types of Phosphate	Weight% Phosphate
	OPC	Phosphate	water			
02	80	8.00	16.00	0.18	$(NaPO_3)_n \cdot Na_2O$	10
04	80	0.00	16.00	0.18	~	0
11	80	8.00	16.00	0.18	$CaHPO_4$	10
12	80	8.00	16.00	0.18	$CaHPO_4$	10
15	80	8.00	20.00	0.23	$CaHPO_4$	10
16	80	8.00	20.00	0.23	$CaHPO_4$	10
17	60	25.20	15.00	0.18	$CaHPO_4$	10
19	80	0.00	20.00	0.25	~	0
20	60	25.20	21.30	0.25	$CaHPO_4$	42
22	80	8.00	16.00	0.18	$Na_5P_3O_{10}$	10
24	80	8.00	16.00	0.18	$(NaPO_3)_n$	10
26	80	8.00	16.00	0.18	$(NaPO_3)_3$	10
50	80	4.00	24.00	0.29	$CaHPO_4$	5
51	80	12.00	24.00	0.26	$CaHPO_4$	15
52	80	0.00	24.00	0.25	~	0
53	85	26.72	24.00	0.21	$2CaO \cdot P_2O_5$	33.4
54	85	26.72	24.00	0.21	$2CaO \cdot P_2O_5$	33.4

Table 9. Processing, Curing and Aging for cement pastes prepared with HAC and different phosphates

No.	Processing	Curing	Aging	Drying	Remarks
01	CP	Air, RT	1,3,7,14,28,300	Dry/No dry	
03	CP	Air, RT	3,7,14,28,90,300	Dry/No dry	Pure HAC
05	CP	Air/Water, RT	1,3,7	Dry/No dry	5.5g/ml$Al(H_2PO_4)_3$
06	CP	Air/Water, RT	1,3,7	Dry/No dry	
07	CP/WP	Air/Water, RT	1,3	Dry/No dry	
08	CP/WP	Air/Water, RT	1,3	Dry/No dry	
09	WP	Air, RT		Dry/No dry	
10	WP	Air/Water, RT	7,14	Dry/No dry	
13	CP			Dry	2.67g gypsum
14	CP	Air, RT	1,3,7,14,28	Dry	
18	CP	Water, RT	1,3,7,14,28,90,300	Dry/No dry	
21	CP	Air, RT	1,3,7,14,28,90,300	Dry/No dry	
23	CP	Air, RT	1,3,7,14,28,90,300	Dry/No dry	
25	CP	Air, RT	1,3,7,14,90,300	Dry/No dry	
27	CP	Air, RT	1,3,7,14,90,300	Dry	7g Silica Fume
28	CP	Air, RT	1,7	Dry	Solution mixed
29	CP	Air, RT	1,7	Dry	Solution mixed
30	CP	Air, RT	1,7	Dry	Solution mixed
31	CP	Air, RT	1,7	Dry	Solution mixed
32	CP	Air, RT	1,7	Dry	Pure HAC
33	CP	Air, RT	1,7	Dry	Solution mixed
34	CP	Air, RT	1,7	Dry	Solution mixed
35	CP	Air, RT	1,7	Dry	Solution mixed
36	CP	Air, RT	1,7	Dry	Dry mixed
37	CP	Air, RT	1,7	Dry	Dry mixed
38	CP	Air, RT	1,7	Dry	Dry mixed
39	CP	Air, RT	1,7	Dry	Dry mixed
40	CP	Air, RT	1,7	Dry	Pure HAC
41	CP	Air, RT	1,7	Dry	Dry mixed
42	CP	Air, RT	1,7	Dry	Dry mixed

Table 9. (Cont.)

43	CP	Air, RT	1,3	Dry	
44	CP	Air, RT	1,3	Dry	
45	CP	Air, RT	1,3	Dry	
46	CP	Air, RT	1,3	Dry	
55	CP	Air/Water, RT	1,3,7,28	Dry	
56	CP	Air/Water, RT	1,3,7,28	Dry	
57	CP	Air/Water, RT	1,3,7,28	Dry	Pure HAC
58	CP	Air/Water, RT	1,3,7,28	Dry	

Table 10. Processing, Curing and Aging for cement pastes prepared with OPC and different phosphates

No.	Processing	Curing	Aging	Drying	Remarks
02	CP	Air, RT	1,3,7,14,28,90,365	Dry/No dry	
04	CP	Air, RT	3,7,14,28,90,365	Dry/No dry	Pure OPC
11	CP/WP	Air/Water, RT	3,7,14,28	Dry	
12	CP/WP	Air/Water, RT	3,7,14,28	Dry	
15	CP/WP	Air, RT	1,3,7,14,28	Dry/No dry	
16	CP/WP	Air, RT	1,3,7,14,28,90,365	Dry/No dry	
17	CP	Air/Water, RT	1,3,7,14,28,90,365	Dry	
19	CP	Air/Water, RT/80°C	3,7,14,90,365	Dry	Pure OPC
20	CP	Air/Water, RT/80°C	3,7,14,90,365	Dry/No dry	
22	CP	Air, RT	1,3,7,14,28,90,365	Dry/No dry	
24	CP	Air, RT	1,3,7,14,28,90,365	Dry/No dry	
26	CP	Air, RT	1,3,7,14,90,365	Dry/No dry	
50	CP	Air/Water, RT/80°C	3,7,14	Dry	
51	CP	Air/Water, RT/80°C	3,7,14	Dry	
52	CP	Air, RT	3,7,14	Dry	Pure OPC
53	CP	Air/Water, RT/80°C	3,7,14	Dry	
54	CP	Air, RT	3,7,14	Dry	

Table 11. Notation for Tables 9 and 10

Processing	CP	Cool-pressed
	WP	Warm-pressed
	CP/WP	Some are cool-pressed, the other warm-pressed for the same batch
Curing	Air	Curing in air
	Water	Curing in water
	Air/Water	Some are cured in air, the other in water for the same batch
	RT	Room temperature
	RT/80°C	Some are cured at room temperature, the other at 80°C for the same batch
Aging	1,3,7,.....	Number refers to day(s)
Drying	Dry	Drying sample for 4 hours at 80°C before measuring
	Dry/No dry	Some are dried at 80°C, the other are not for the same batch
Remarks	Solution mixed	Making the phosphate solution first, and then mixing
	Dry Mixed	Mixing phosphate powder with cement first, and then adding the water

The cool-pressed (25°C) and warm-pressed (80°C) conditions were used to investigate the influence on strength by different processing. The pressure used in the higher temperature processing was the same as that of cool-pressing (28-30 MPa), but the pressing time of the former was extended to about one hour.

2.4.3 Curing and Aging

The cement pastes were sealed in plastic bags for about 12 hours at room temperature after compacting. The samples were then cured in room humidity, water vapor atmosphere conditions or by directly immersing in water. The water vapor atmospheric was usually used to prevent loss of moisture from the specimens to the atmosphere during curing, but the main purpose in this research is to compare the different curing conditions, and try to find the effect of water on the materials.

The curing temperatures used were 25°C and 80°C. Some other higher temperatures were also tried, but no satisfactory results could be observed.

After curing for 1, 3, 7, 14, 28, 90, and 300 days (some up to 1 year), they were cut into bars with the dimensions of about 0.2 x 0.2 x 0.8 inches (0.5 x 0.5 x 2 cm) by a low speed diamond saw for flexural strength measurement. Cylindrical specimens 0.5 inch in diameter were made for splitting tensile strength measurement.

Some of samples were dried at 80°C for three hours before the mechanical testing, others were not. The influence of drying on strength was determined.

Chapter 3
RESULTS AND DISCUSSION

3.1 High Alumina Cement and Phosphate Systems

3.1.1 Mechanical Properties

The effects of different factors on the mechanical properties are discussed in this section. The studied factors include using different sodium and calcium phosphates, addition of silica fume, W/C ratio, and phosphate addition level. The most frequently used mechanical property for discussion in this section is flexural strength. Splitting strength also used in some cases.

3.1.1.1 Flexural Strength of HAC Modified by Sodium Phosphate

The flexural strength of the hardened cement pastes were measured after curing for up to ten months at room temperature. Table 12 shows the results for pure HAC and samples modified with four sodium phosphate compositions. All samples were hydrated at a water/solid ratio of 0.182, and a phosphate/cement ratio of 0.1. It was found that the reactivities of these formulations are high and leads to rapid setting after mixing and rapid strength gain. It can be seen from

Table 12. Flexural strength for pure HAC and samples modified with sodium phosphate

No.	Materials	Amount (g)	Flexural Strength (MPa) 1D	3D	7D	14D	28D	90D	300D
03	HAC	80	7.3	9.4	13.7	12.3	11.0	11.9	12.1
	DI Water	16							
	HAC	80							
01	$(NaPO_3)_n \cdot Na_2O$	8	20.1	34.5	33.8	24.5	27.3	~	34.5
	DI Water	16							
	HAC	80							
21	$Na_5P_3O_{10}$	8	26.6	23.8	33.4	23.6	19.7	19.1	29.1
	DI Water	16							
	HAC	80							
23	$(NaPO_3)_n$	8	33.7	39.3	33.7	32.5	18.3	20.7	27.3
	DI Water	16							
	HAC	80							
25	$(NaPO_3)_3$	8	23.8	28.8	28.5	23.6	~	29.4	27.7
	DI Water	16							

Figure 10 that all of the phosphate modified cements have higher strengths than pure HAC.

As shown in the figure, strengths increased very rapidly with age for about 3 to 7 days for both pure HAC and modified cements. After 7 days, the strengths began to decrease until 28 days of hydration. The values slowly increased again after 28 days of hydration until ten months. The differences between pure HAC and the modified cements are significant. The maximum strength of pure HAC was 14 MPa at 7 days, while the $(NaPO_3)_n \cdot Na_2O$, $(NaPO_3)_n$ and $(NaPO_3)_3$ modified samples attained maximum strengths of 35, 40, 29 MPa, respectively, at 3 days (the $Na_5P_3O_{10}$ modified sample reached a maximum strength of 34 MPa at 7 days). The modified cements had strengths between 2 and 3 times that of the pure cements. However, the modified cements followed the same trend as pure cement in that their strengths began to decrease after reaching maxima. Between one month and three months of curing, the strengths of all the samples were lower than the strengths exhibited during the first thirty days. After ten months of hydration, $(NaPO_3)_n \cdot Na_2O$, $(NaPO_3)_n$, $Na_5P_3O_{10}$ and $(NaPO_3)_3$ modified cements attained strengths of 35, 27, 29 and 28 MPa, respectively, while pure cement only reached 12 MPa.

As the strength data shown in Figure 10 illustrate, while strength regression also occurs in phosphate modified formulations, the strengths of the modified cements always exceed those of the unmodified cement. These data suggest that it may be possible to develop an HAC-based cementitious material exhibiting desirable chemical reactions and physical properties.

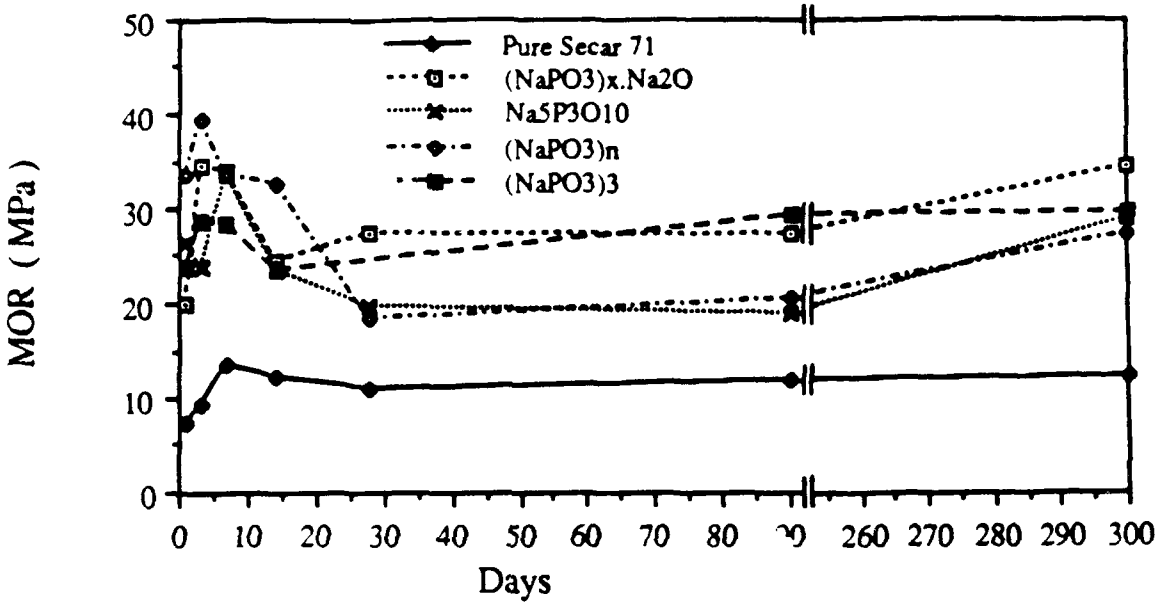

Figure 10. Flexural strength for pure HAC and sodium phosphate modified samples with curing time

The reason for the loss in strength is probably related to the same mechanism in all cases. The initial products of HAC hydration under room temperature are hexagonal calcium aluminate hydrates CAH_{10}, C_2AH_8, and alumina gel. These three products are all metastable. With time, both hexagonal CAH_{10} and C_2AH_8 crystals, which are unstable both at normal and higher temperatures, slowly convert to C_3AH_6 and alumina gel with a consequent increase in porosity and strength loss.

3.1.1.2 Flexural and Splitting Strengths of HAC Modified by Calcium Phosphate

The effects of calcium phosphate additions were also studied as shown in Table 13 and 14. Proportions of phosphate used were: 10%, 25% and 40%, and samples were cured in air or water at room temperature. As seen in the table, no matter how much calcium phosphate is added, the affect on the flexural strength at early ages is small. However, in the long term, the more calcium phosphate that is added initially, the higher the strength. The splitting strengths showed the same trend, as shown in Table 14. It was found that calcium phosphate was not as effective as sodium phosphate in achieving increases of strength of HAC. For samples cured in water, as shown in Figure 11(b), strengths were reduced significantly. This indicates that the calcium phosphate modified HAC composite is sensitive to water.

Table 13. Flexural strength of HAC modified by calcium phosphate

No.	Materials	Amount (g)	Curing Condition	Flexural Strength (MPa) 1D	3D	7D	28D
57	HAC	85	In Air	15.0	14.7	18.3	22.9
	DI Water	24	In Water	11.2	13.9	10.5	11.2
	HAC	85	In Air	15.0	10.9	16.9	25.1
55	$Ca_2P_2O_7$	8	In Water	17.5	10.5	10.1	12.5
	DI Water	24					
	HAC	85	In Air	14.6	14.0	15.5	28.1
56	$Ca_2P_2O_7$	20	In Water	17.9	11.7	11.6	13.0
	DI Water	24					
	HAC	75	In Air	11.0	14.1	27.0	35.0
58	$Ca_2P_2O_7$	30	In Water	10.1	9.2	9.1	10.1
	DI Water	29					

Table 14. Splitting strength of HAC modified by calcium phosphate

No.	Materials	Amount (g)	Splitting Strength (MPa) 1D	3D	7D	28D
57	HAC	85	5.6	6.1	8.0	11.8
	DI Water	24				
	HAC	85				
55	$Ca_2P_2O_7$	8	5.3	7.6	7.8	11.9
	DI Water	24				
	HAC	85				
56	$Ca_2P_2O_7$	20	6.1	5.9	9.0	13.1
	DI Water	24				
	HAC	75				
58	$Ca_2P_2O_7$	30	6.3	7.2	10.1	17.5
	DI Water	29				

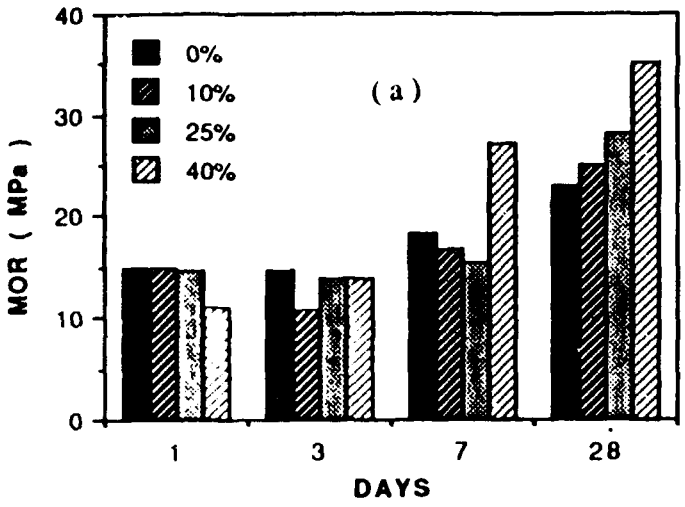

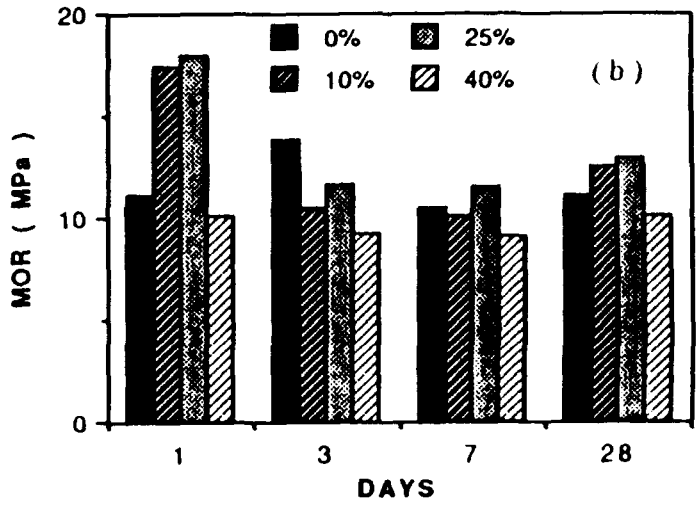

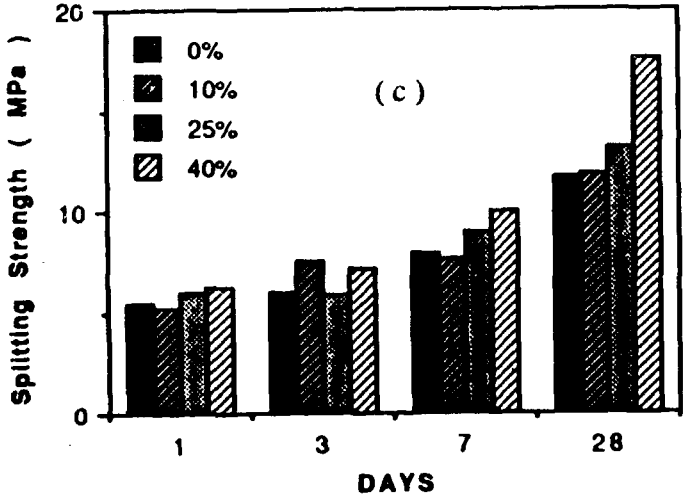

Figure 11. Flexural strength and splitting strength of HAC modified by calcium phosphate. (a) Flexural strength at room humidity, (b) Flexural strength at wet condition, and (c) Splitting strength at room humidity. Notation: 0% --> Pure HAC, 10% --> 10% $2CaO \cdot P_2O_5$, 25% --> 25% $2CaO \cdot P_2O_5$, 40% --> 40% $2CaO \cdot P_2O_5$

3.1.1.3 Effects of Addition of Silica Fume

10% silica fume was used to replace the same amount of HAC. The resultant strength of the samples exhibited the same trend as the samples shown before (Figure 10). The strength is very high at early ages as shown in Figure 12, but the flexural strength decreased from 48 MPa to 24 MPa between one and three days. Figure 12 compares the pure cement, $(NaPO_3)_n$ modified cement and $(NaPO_3)_n$ modified cement but with about 10% HAC replaced by silica fume. In the phosphate modified cement, the strength is higher than that of pure HAC. After 10 months of curing, the strength of silica fume replaced sample was still twice as high as that of pure cement. Furthermore, strength loss in silica fume replaced samples is less than in samples without silica fume, although they have the approximately same strength at the end of 10 months curing. Thus adding silica fume retards the loss in strength.

3.1.1.4 Effects of W/C Ratio

It was found that fluidity increased by adding the sodium phosphate to HAC during sample processing. Therefore a lower W/C can be used to obtain the same fluidity. It can seen in Figure 13 that samples with lower W/C (W/C = 0.17) exhibits lower strength than samples with higher W/C (W/C = 0.20) during the early stages. However, with time, the lower W/C samples develops higher strengths than samples with higher W/C. After about seven days of hydration, the strengths of samples with higher W/C decrease while those with lower W/C maintain their strengths and show minimal

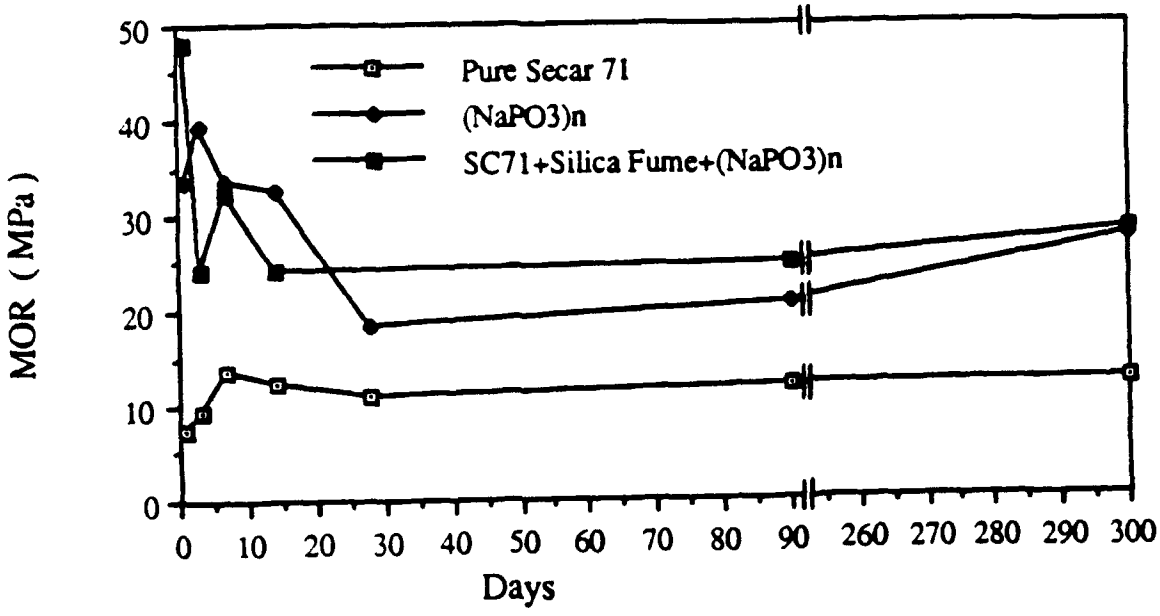

Figure 12. Effect of silica fume addition on flexural strengths

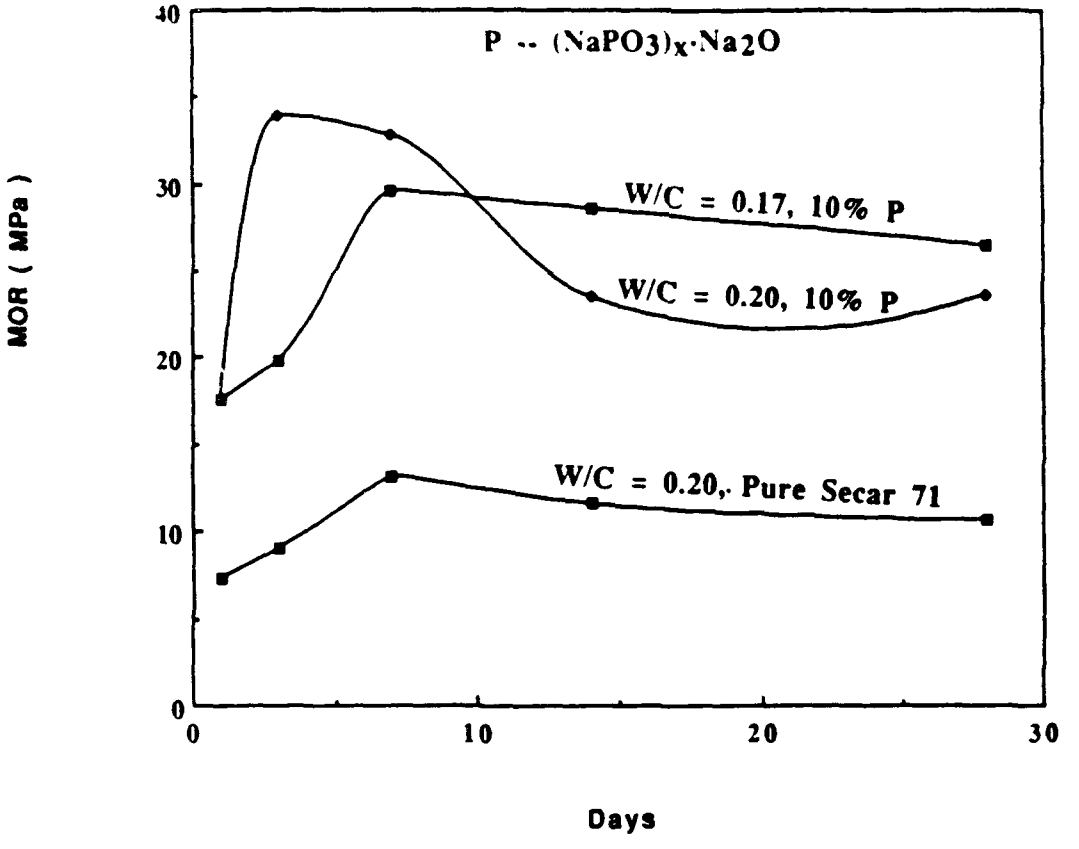

Figure 13. The loss in flexural strengths is reduced by a low W/C ratio

strength loss. This indicates that using a lower W/C is an effective way to minimize the conversion reaction and to retard the loss in strength.

3.1.1.5 Effect of Phosphate Addition Level

In order to determine the effect of addition level on strength, sodium hexametaphosphate $(NaPO_3)_n$ was added to HAC in 5 Wt.% increments from 5 Wt.% to 30 Wt.%. The effect on strength is shown in Figure 14. As shown in the figure, the one and seven day strengths increased with amount of added phosphate until 20%, and then decreased rapidly at higher addition levels. It can be concluded that the amount of phosphate strongly affects the mechanical properties of HAC.

3.1.2 Calorimetric Measurements

The changes in mechanical properties raise a question as to why some of the phosphates are more effective than others. Isothermal calorimetry was used to study the major effects on the hydration of HAC by phosphate additions.

The heat evolved during hydration was studied for both modified and pure cement by isothermal calorimetry during the first 48 hours of hydration. It was found that the phosphate modification accelerates the initial hydration rates regardless of phosphate composition, but different types or different addition level of phosphates hydrate with different rates and exhibited different mechanical properties. Figure 15 shows the heat evolved for both pure cement and $2CaO{\cdot}P_2O_5$ modified samples during the first 48 hours of hydration. Different amounts of phosphate were used. They were 10%, 25% and 40%.

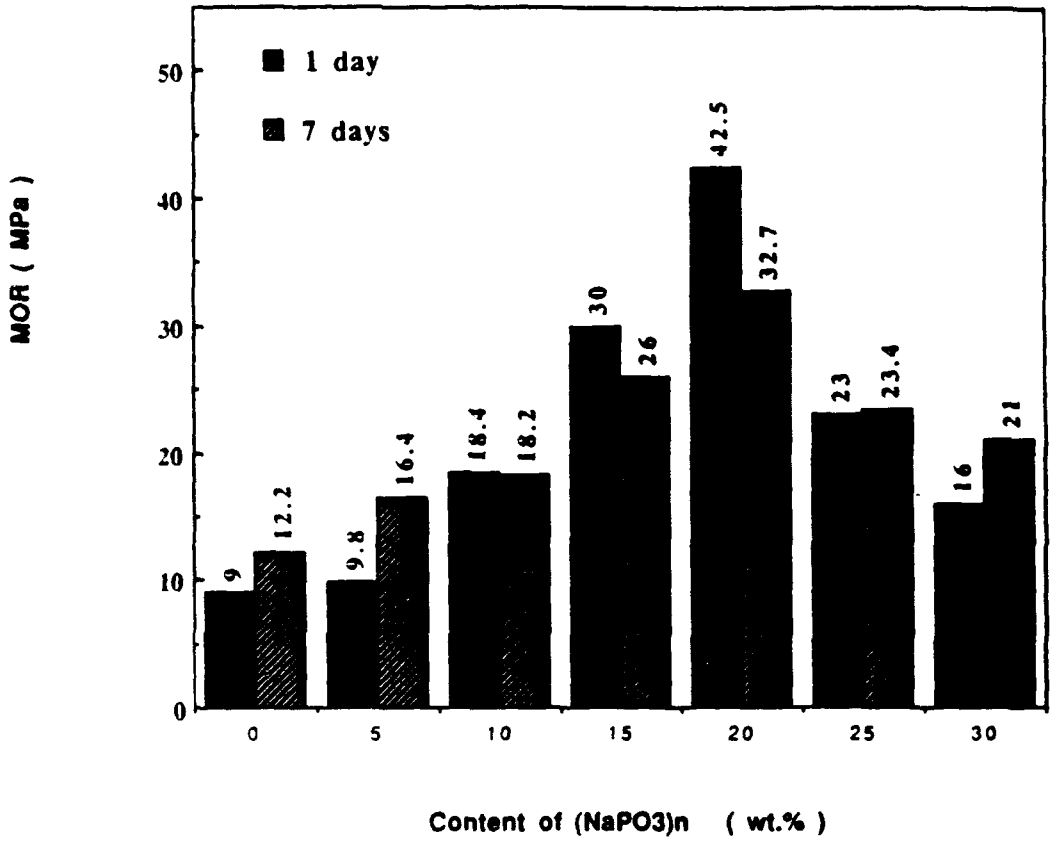

Figure 14. Flexural strength depending on the amount of phosphate added

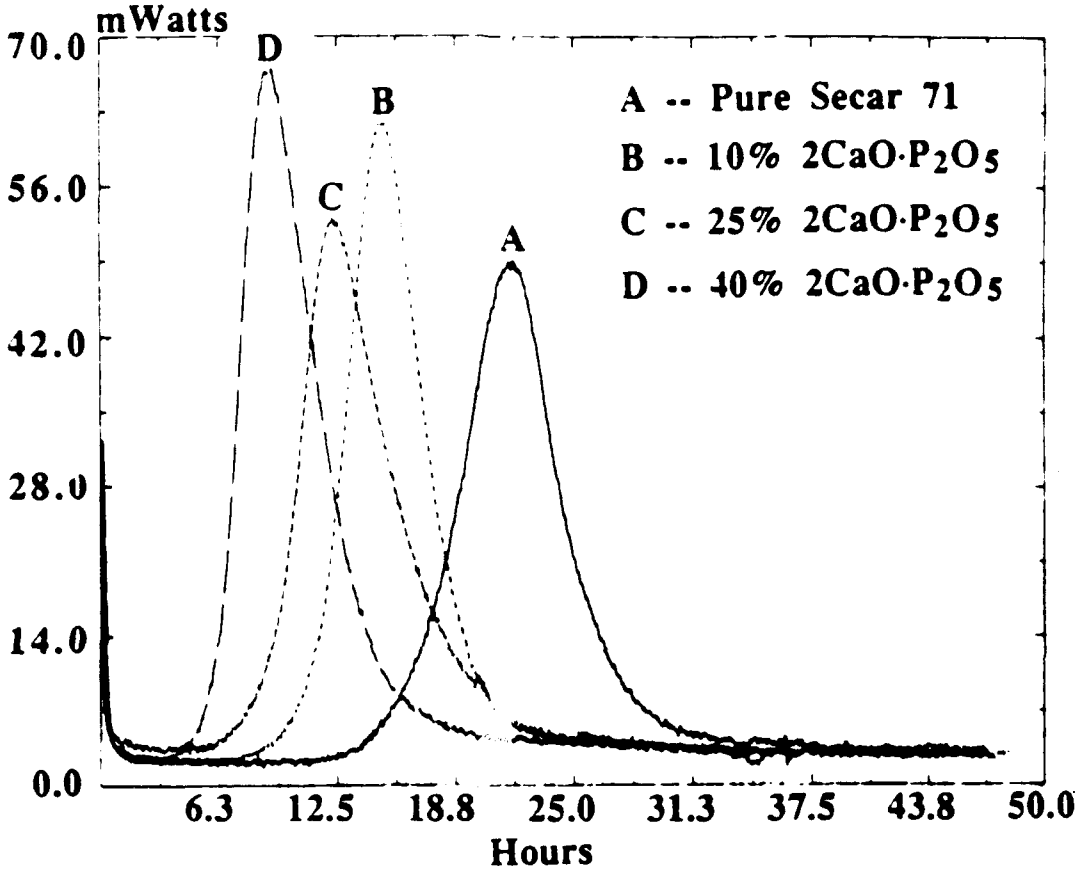

Figure 15. Heat evolved for both pure HAC and modified samples by $2CaO \cdot P_2O_5$ during the first 48 hours of hydration

The data indicate that the more calcium phosphate added, the faster is the reaction. However, the total evolved heat for each of the samples, as shown in Figure 16, becomes approximately the same after 48 hours.

It can be seen from Figure 11 that the amount of calcium phosphate affects the strength especially at later stage. The more calcium phosphate added, the higher is the strength attained. Therefore, a relationship exists between the strength and the rate of hydration reaction; the faster the reaction is, the higher strength the sample exhibits.

This can also be seen in sodium phosphate modified samples. As discussed before, sodium phosphate is more effective in high alumina cement than calcium phosphate. Therefore, the samples modified by sodium phosphate should have faster reaction rates than samples containing calcium phosphate. Experiments have confirmed this. Figure 17 compares the rates of heat evolved during the first 30 hours of hydration for pure cement, a calcium phosphate modified sample (the fastest one in Figure 15) and four sodium phosphate modified samples. It shows that all of four sodium phosphate modified samples have much faster hydration rates, even though only 20 wt.% sodium phosphate was added compared with 40 wt.% of added calcium phosphate. The samples with sodium phosphate exhibited hydration reactions almost immediately upon mixing, and the peaks occurred within the first three hours. However, the onset of this peak is delayed for about 16 hours in the absence of the phosphates. For clarity, the first six hours of hydration is shown in Figure 18. It can be seen easily that the four sodium phosphate-modified samples show

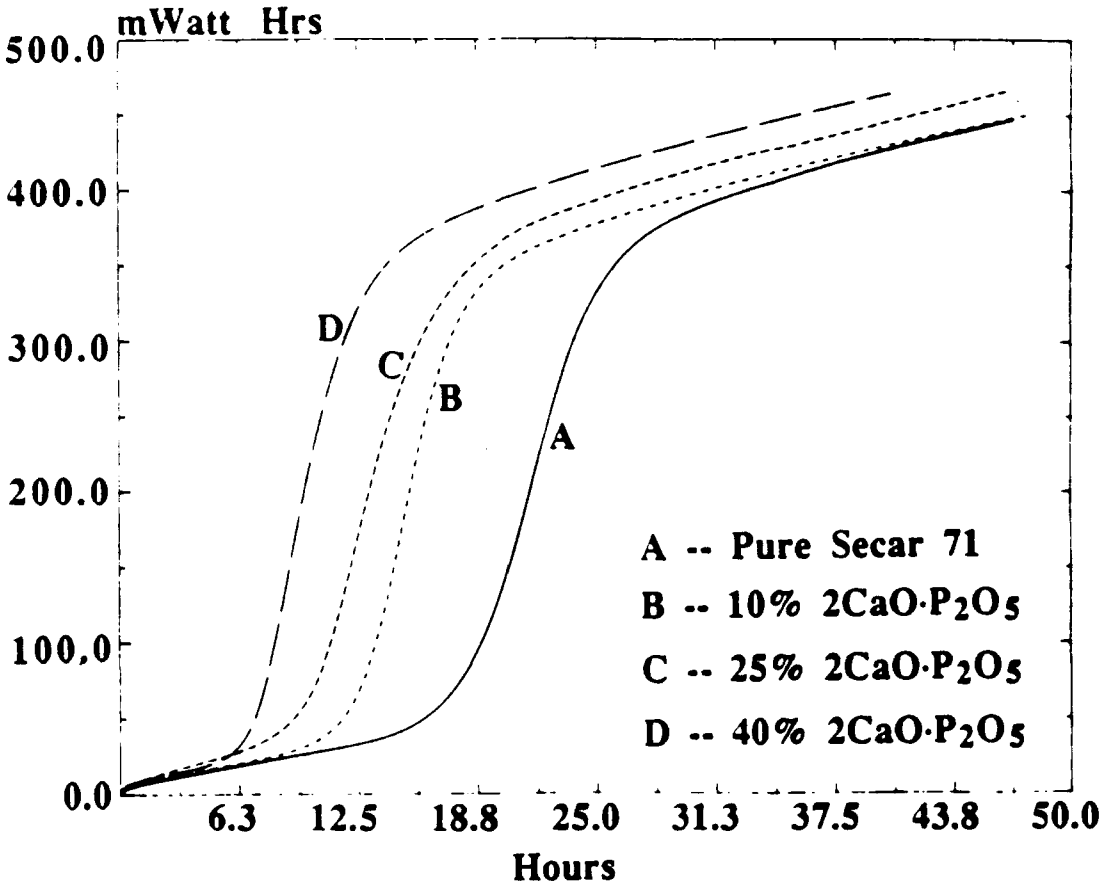

Figure 16. Total heat for both pure HAC and modified samples by 2CaO P_2O_5 during the first 48 hours of hydration

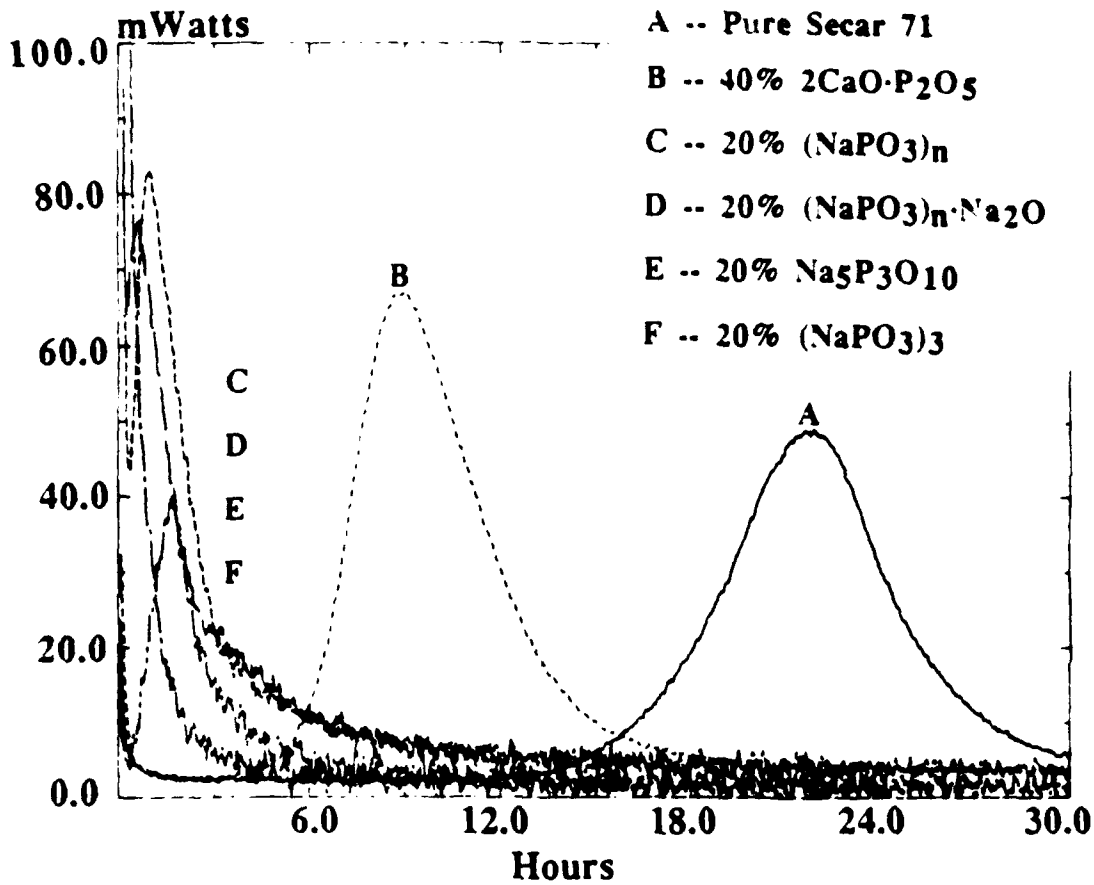

Figure 17. Comparison of the rate of heat evolved during the first 30 hours of hydration for pure HAC, a calcium phosphate modified sample and four different sodium phosphate modified samples

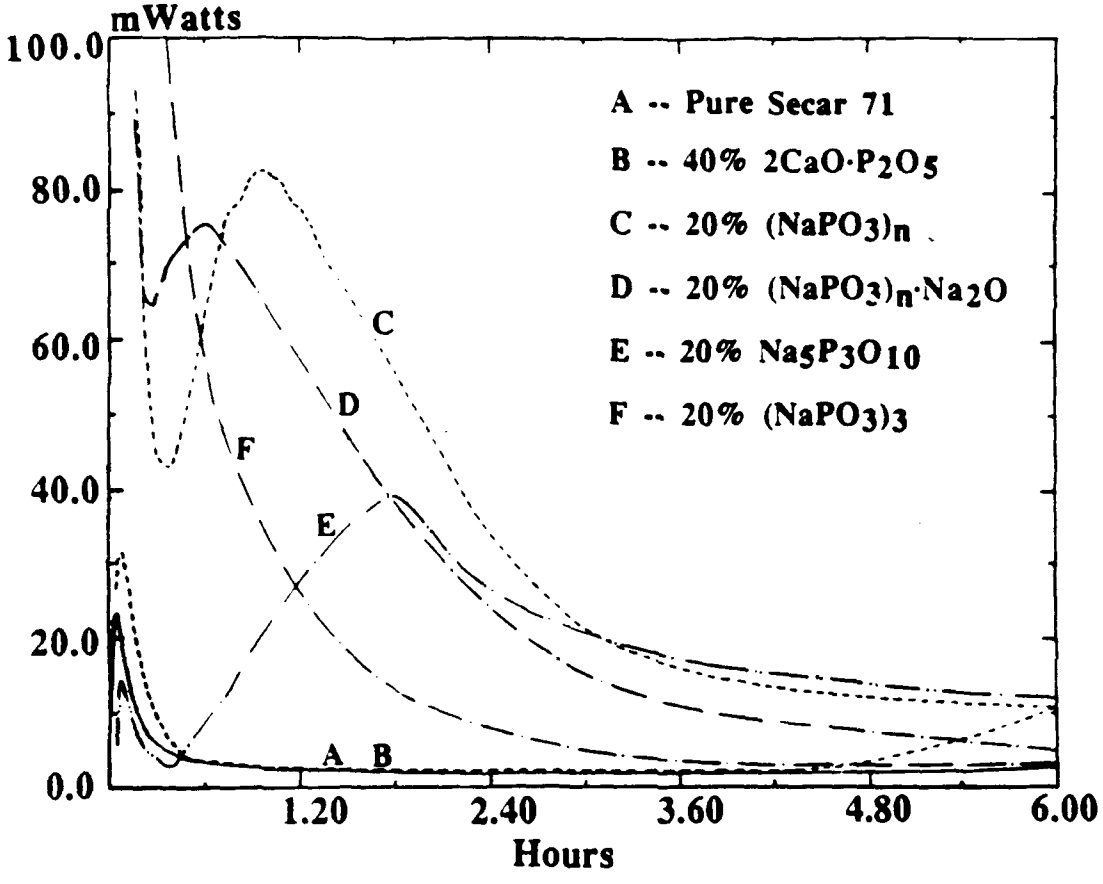

Figure 18. Heat evolved of the first six hours extended from Figure 17

peaks during this period while pure sample and calcium phosphate modified sample do not yet develop such peaks. Because only one peak was observed during the first 48 hours of hydration for all samples, it probably corresponds with reaction of CA. The total heats for these two figures are shown in Figure 19 and 20, respectively. It shows that significantly more heat is produced during the first several hours when the sodium phosphates are present. However, after 30 hours of hydration, the cumulative heats evolved when HAC is modified by the various phosphates are lower than that from unmodified HAC. However, the samples containing sodium phosphate produced higher heat at the beginning while those with calcium phosphate have lower heat as shown in both Figure 19 and 20. It can be concluded from these data that the phosphate modifiers have their greatest effect at the onset of hydration, and adding phosphate-based additions strongly accelerates the hydration reaction. The nature of the effects of phosphate modification were further studied by observing microstructural evolution during this period of rapid hydration.

3.1.3 Microstructural Analysis by ESEM

3.1.3.1 Unmodified HAC

The morphologies of hydration products of pure Secar 71 were firstly identified by ESEM. A relatively high water/cement ratio (0.5) was used in order to keep the samples moist for an extended period of time. The samples were hand mixed then immediately placed in the ESEM. It was observed that the crystalline calcium aluminate hydrate grows within the first 3 hours of reaction. No further changes were

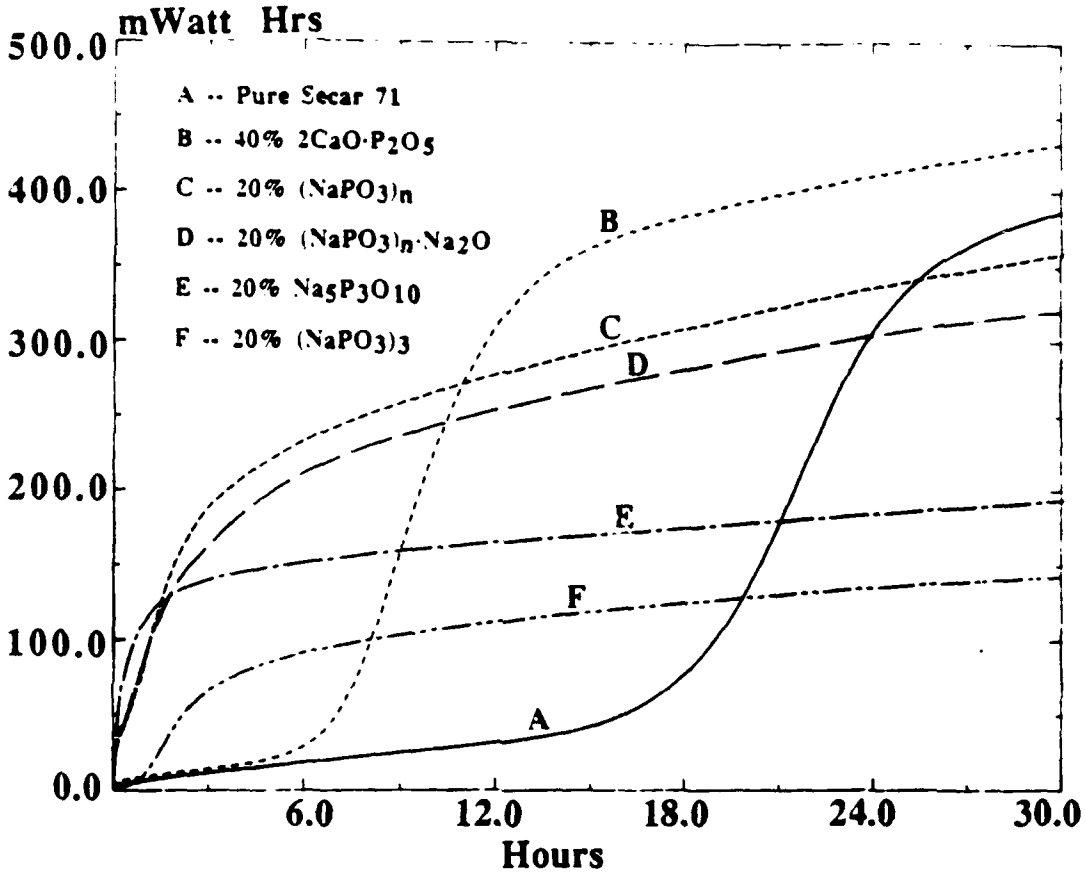

Figure 19. Total heat evolved for pure HAC, a calcium phosphate modified sample and four different sodium phosphate modified samples during the first 30 hours of hydration

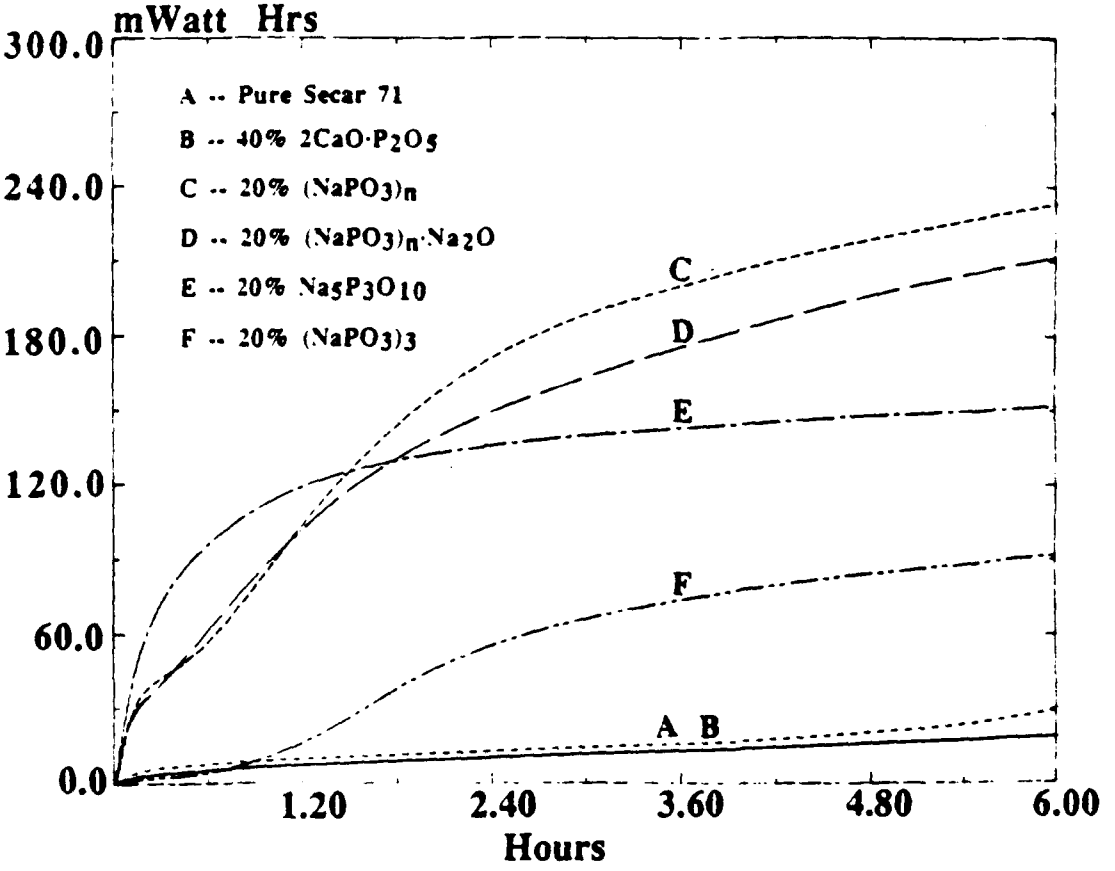

Figure 20. Total heat of the first six hours extended from Figure 19

found during the subsequent 15 hours of hydration. Figure 21 shows the morphology of the pure cement hydrated after about 20 hours. Polygonal crystallites of various sizes could be observed and the morphology is very different from the modified samples which will be discussed in the following section.

3.1.3.2 HAC Modified by $(NaPO_3)_3$

Figure 22 shows the microstructural evolution during the hydration of HAC modified by $(NaPO_3)_3$ using a phosphate/cement ratio of 0.1. The first noticeable change is the occurrence of microcracks after 11 minutes of hydration (a). The width of the cracks was about 2 μm. A significant change is observed after about one hour of hydration, associated with the appearance of fibrous phase. This can be seen by comparing to (a) with (b) which are photos of the same area. The fibers have diameters of 3-8 μm and attain various lengths as shown in (c).

The cracks shown in (d) enlarge to about 5 μm during the next 3 hours after they appeared. The experiments were carried out at a water vapor pressure of 2.5 torr. Although water is present throughout the hydration process, 2.5 torr is below the saturation vapor pressure for water in vacuum. Thus, it is likely that crack formation is due to shrinkage during specimen desiccation. During the 3 hour interval, a second new phase forms in the cracks (e). The morphology is shown at higher magnification in (f) and its morphology is very similar to that of hydroxyapatite. Therefore, two new phases were produced during early time of hydration in the HAC-$(NaPO_3)_3$ system, and they exhibit distinct morphologies. Significantly, the

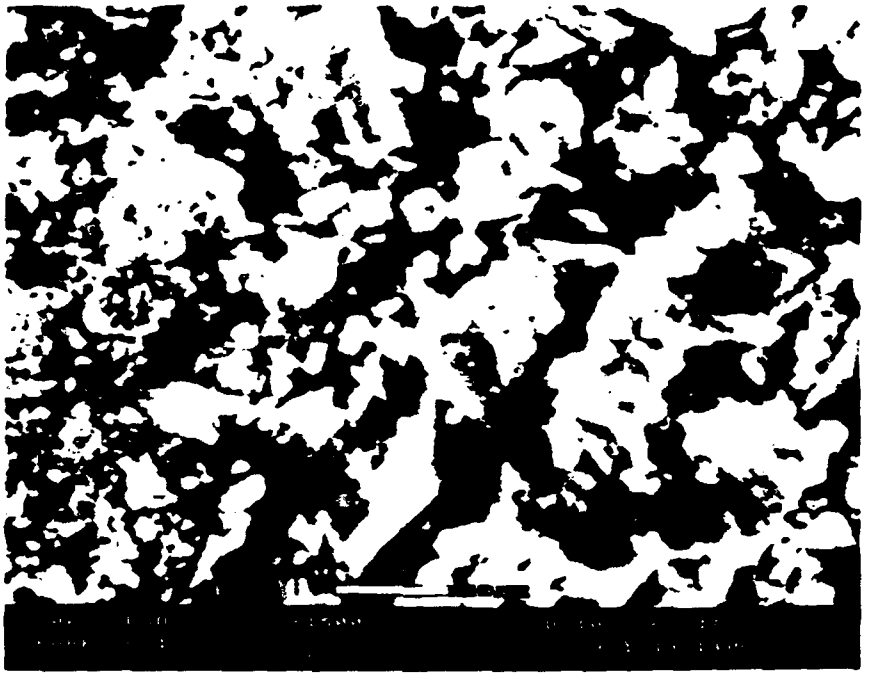

Figure 21. Microstructural development in pure HAC after 20 hours of hydration

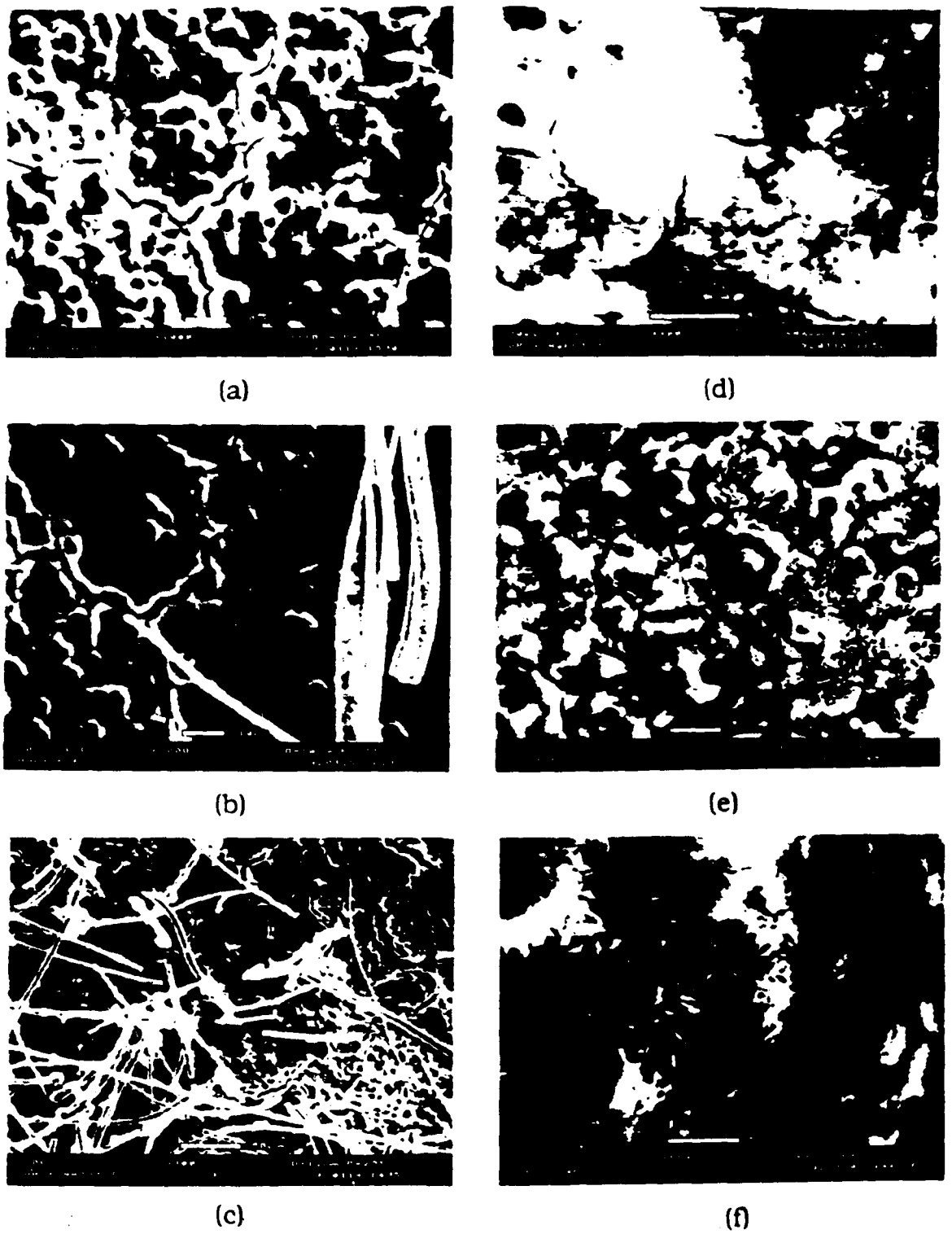

Figure 22. ESEM images of $(NaPO_3)_3$ modified HAC (a) after 10 minutes of hydration, (b) after 1 hours 9 minutes of hydration, (c) fiber-like phase, (d) after 11 minutes, (e) after 3 hours 13 minutes of hydration, (f) higher magnification of produced phase

formation of a fibrous phase may provide a mechanism by which a self-assembling composite, where microstructurally distinct phases form from a single solid precursor, may be created.

3.1.3.3 HAC Modified by $Na_5P_3O_{10}$

The sample modified by $Na_5P_3O_{10}$ exhibits morphological development which is different from that caused by $Na(PO_3)_3$. Figure 23 shows the evolution in morphology in the same area between 8 and 25 minutes of hydration. It can be seen that morphology changed very much during this period of time. After 25 minutes, the distinct phase embedded in a matrix which was basically an amorphous-like material.

3.1.3.4 HAC Modified by $(NaPO_3)_n$

The effect of the phosphate-based inorganic polymer $(NaPO_3)_n$ was also studied. The changes in microstructure were small during the first 20 hours of hydration with small difference in the photographs. The first noticeable change observed was the enlargement of cracks, and grains separated after 30 minutes of hydration. Small bubble-like features then appeared on the grain surfaces. These events are most likely the result of the slow evaporation of water from the specimen. No further changes were observed during the subsequent 20 hours of hydration. Considering microstructural observations and heat evolution characteristics together, the phosphate samples which evolve the most heat do not produce the greatest microstructural changes. The presence of $Na(PO_3)_n$ results in minimal microstructual evolution over the first 20 hours but causes the greatest amount of heat to be evolved. The

(a)

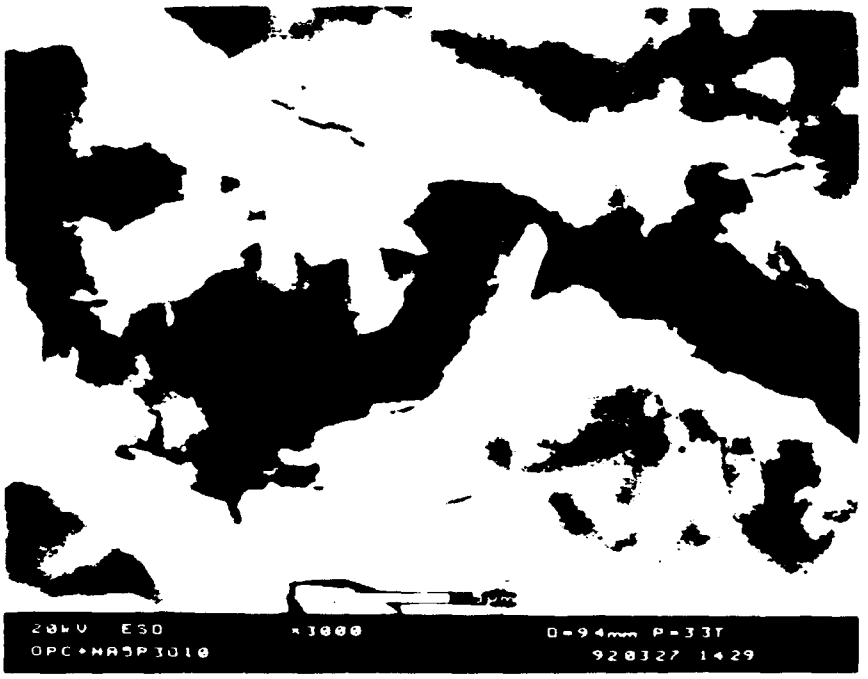

(b)

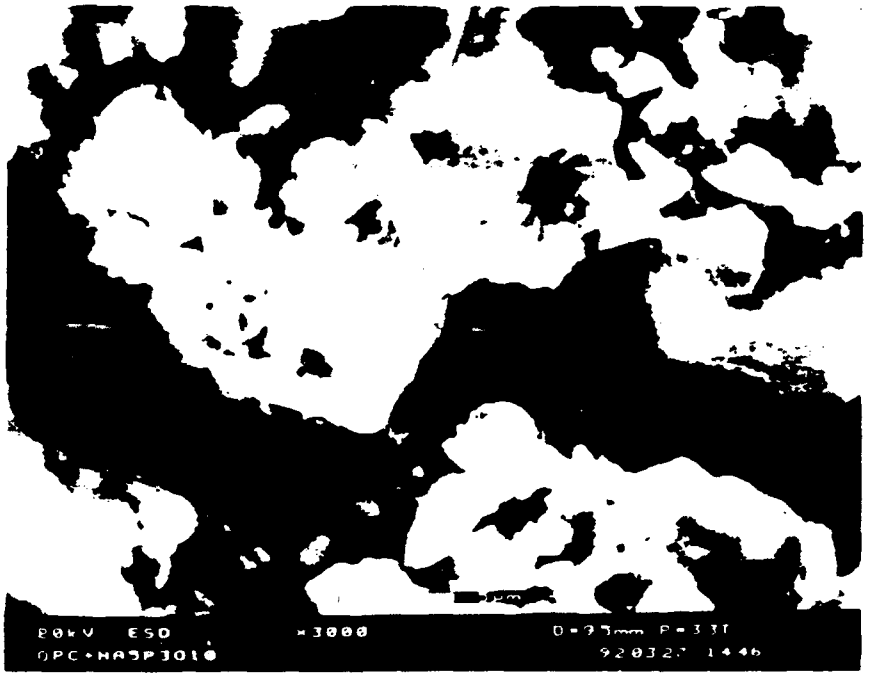

Figure 23. ESEM images of $Na_5P_3O_{10}$ modified HAC (a) after 8 minutes of hydration (b) after 25 minutes of hydration

previous work has shown that HAC achieves high early strengths as a result of modification by sodium phosphates. $Na(PO_3)_n$ modified HAC also attains the highest initial strength but shows the greatest loss of strength due to conversion of hexagonal hydrates to the cubic hydrate (Figure 10). This suggests that the formation of the hexagonal hydrates, C_2AH_8 and C_4AH_{13}, may not be responsible for the early strength development. Therefore, phases which form during early hydration were determined.

3.1.4 X-ray Diffraction Analysis

This section will focus on how phosphate affects the cement. The mechanism by which strength increased and the phases formed during the hydration of phosphate modified HAC were analyzed by x-ray diffraction (XRD) and energy dispersive x-ray analysis (EDX). Figure 24 shows sequential X-ray diffraction pattens of HAC-10% $Na(PO_3)_n$ when cured between 4 minutes and 2 hours. The most intense peaks in the figure result from calcium aluminate (CA). Although heat evolution is significant during the first 2 hours (Figure 17), no discernible crystalline phases can be observed. Figure 25 compares the diffraction patterns of pure Secar 71 and four modified samples with different phosphate additions after 24 hours of hydration. Although there are significant differences in the mechanical properties among these samples, the differences in the X-ray diffraction pattens are negligible. Two possible phenomena may explain this. One is that the new products are X-ray amorphous. The other is that phosphate-based additions only accelerate hydration but do not become incorporated into the hydration products. However,

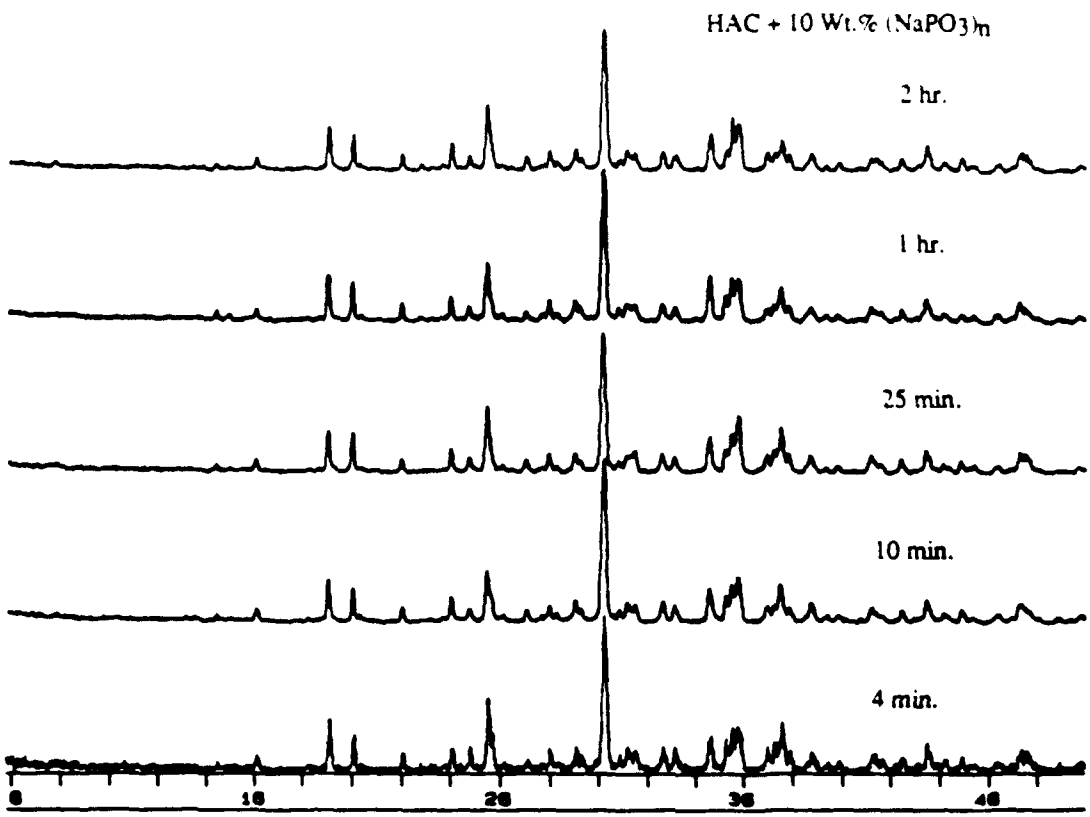

Figure 24. X-ray diffraction pattern of $(NaPO_3)_3$ modified HAC curing in sufficient water in the early stage at room temperature

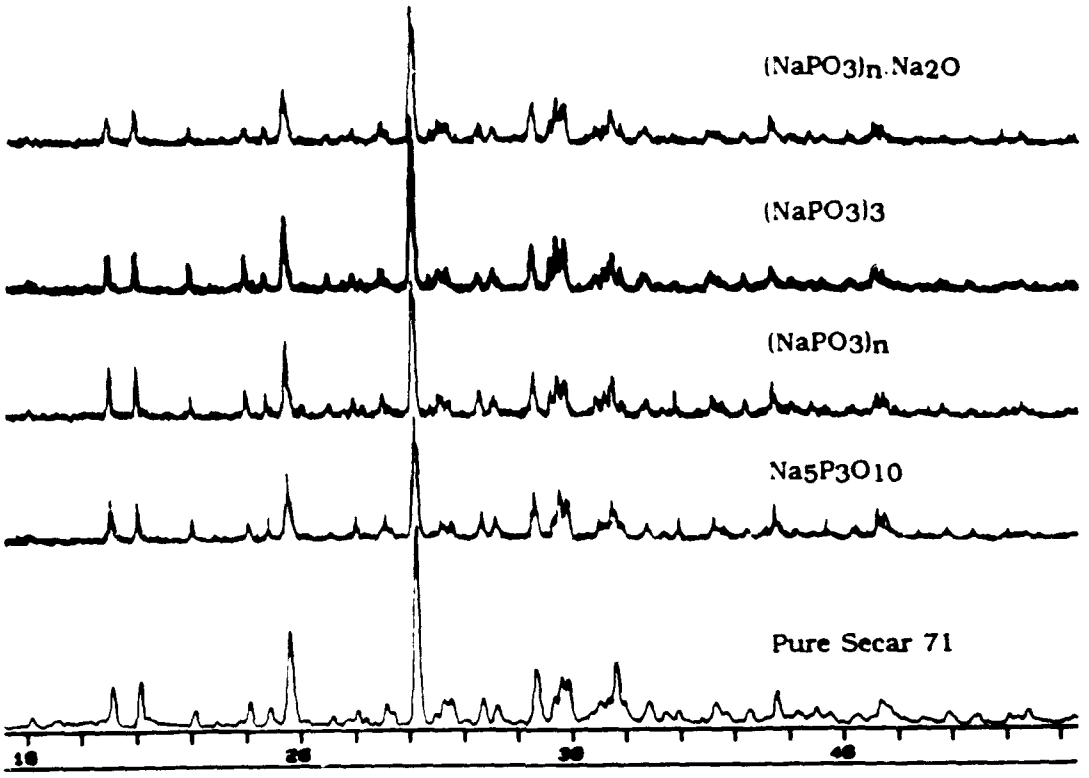

Figure 25. X-ray diffraction pattern of pure HAC and four phosphate modified compositions hydrated for 24 hours at room temperature (Blended samples contain 10 wt% phosphate)

the calorimetric data shown in Figure 17 indicates the less total heat is evolved when phosphates are present, and that the molecular weights of compositionally similar phosphates, $Na(PO_3)_3$ vs $Na(PO_3)_n$, have a significant effect on heat evolution. Therefore, although no x-ray detectable phase is produced, it is likely that phosphates are incorporated into the hydration products.

Figure 26 shows four x-ray diffraction pattens: pure HAC and three modified samples with 10 Wt.%, 20 Wt.% and 30 Wt.% $(NaPO_3)_n$ additions, respectively. All samples were cured in air for one day at room temperature. As discussed previously, there were large differences in the mechanical properties by using different amounts of phosphate (Figure 14), but the differences in the x-ray diffraction patterns are minimal. Nearly all the peaks remained in the same position. Figure 27 shows the patterns obtained after six hours of hydration of pure HAC and a modified sample containing 20 Wt.% $(NaPO_3)_n \cdot Na_2O$. The positions of the peaks do not change, but only differ in intensity. The highest peak in the figure refers to calcium aluminate (CA). It can be seen that the modified samples consume more CA, and further confirms that phosphate addition accelerates the hydration reaction.

Figure 28 compares the diffraction patterns obtained from pure Secar 71 and modified sample with a calcium phosphate addition of 40 Wt.% $2CaO \cdot P_2O_5$. The samples were cured in air for 28 days at room temperature. A similar conclusion can be made as before: CA consumption is accelerated, however, a new crystalline reaction product does not appear to form. Thus, a conclusion can be made as that a new crystalline reaction product does not seem to form at the

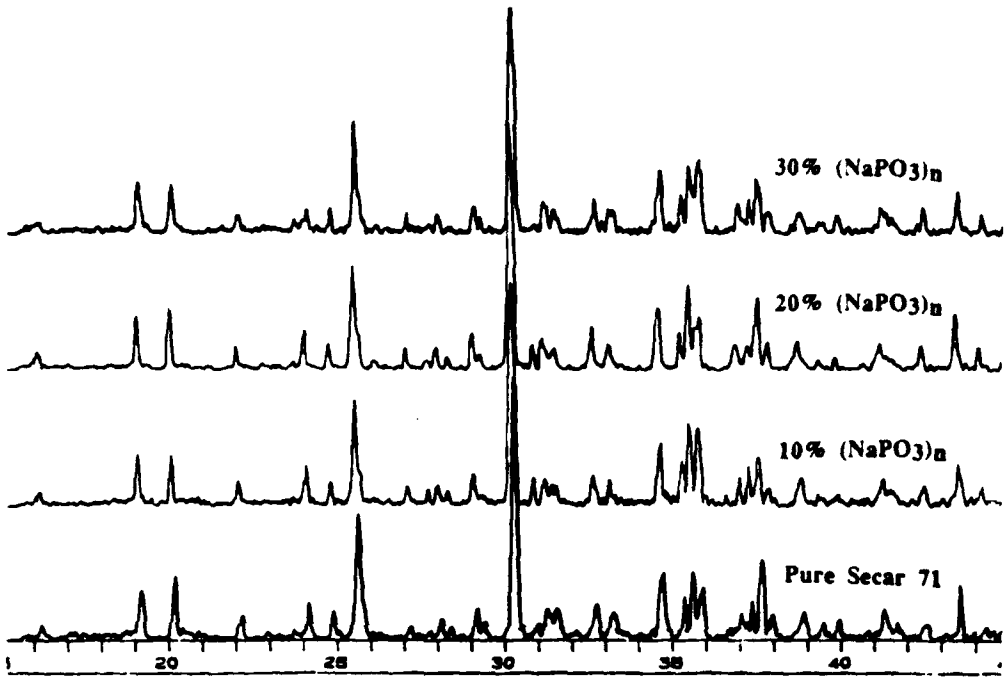

Figure 26. XRD of pure HAC and three modified samples containing three addition levels of $(NaPO_3)_n$ and cured in air for one day at room temperature

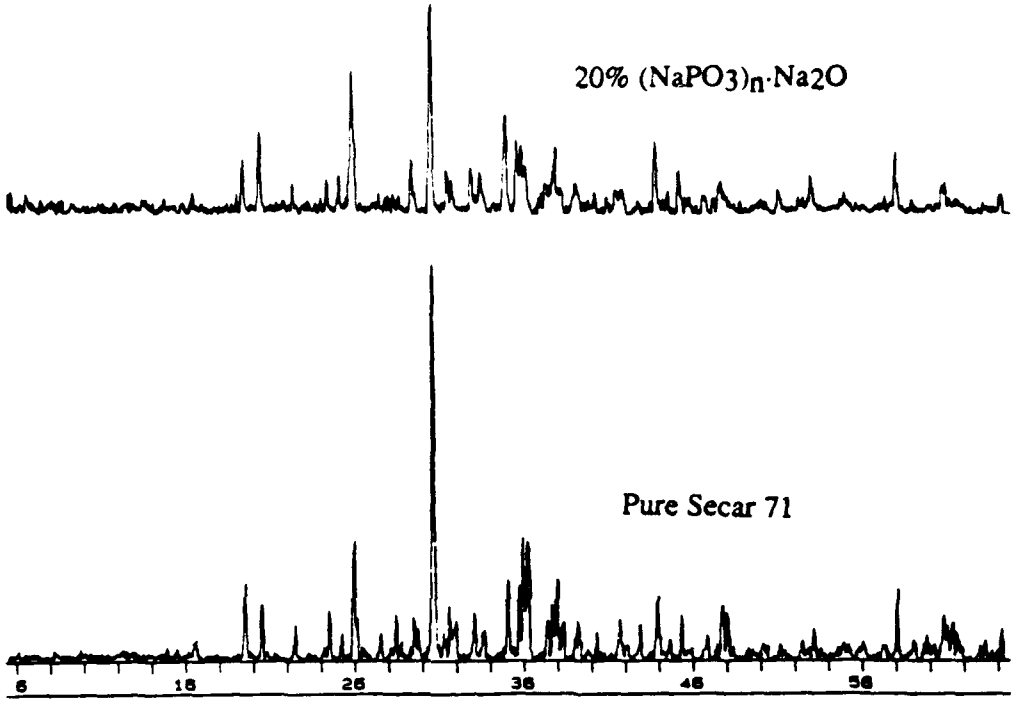

Figure 27. XRD of pure HAC and 20 Wt.% $(NaPO_3)_n \cdot Na_2O$ modified sample after curing in water for six hours at room temperature

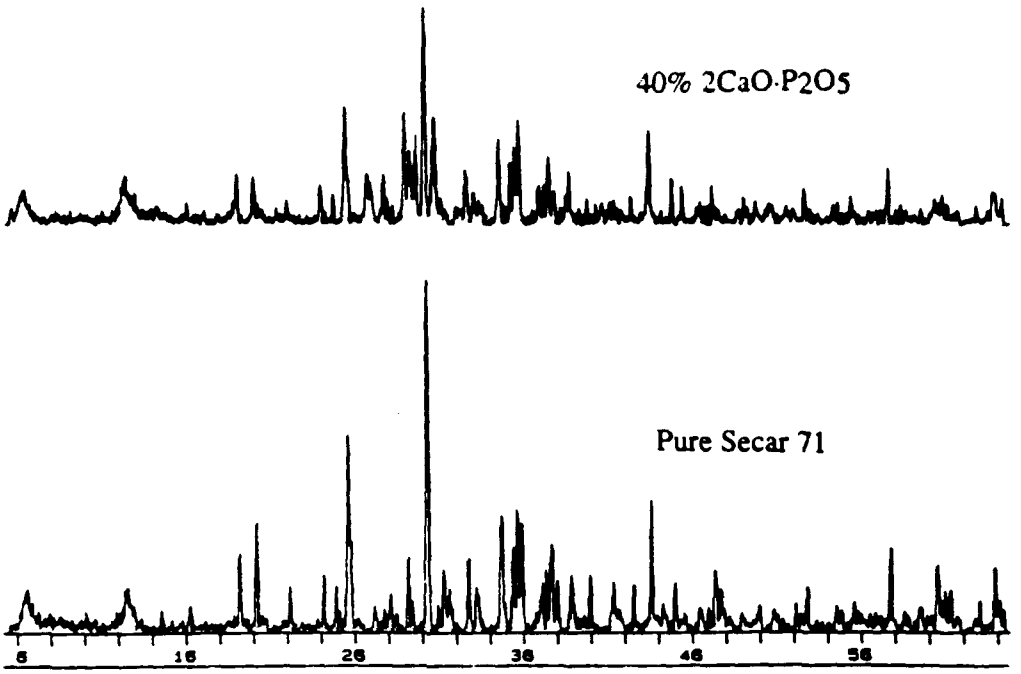

Figure 28. XRD of pure HAC and 40 Wt.% $2CaO \cdot P_2O_5$ modified sample cured in air for 28 days at room temperature

room temperature in these mixtures. The increase in strength may be related to formation of an amorphous phase which may be an aluminate-phosphate gel. If so, such a gel may be stronger than the aluminate gel which is produced by pure high alumina cement.

3.1.5 Identification of Gel Composition

EDX was used to study the compositions of the hydration products. Figure 29 shows SEM micrographs of HAC modified by 10 wt.% $(NaPO_3)_n$ (a) and 10 wt.% $(NaPO_3)_n \cdot Na_2O$ (b), and the corresponding EDX spectra of selected regions. The regions chosen were the hydration products. EDX shows the existence of aluminum, phosphorus and calcium in the amorphous phase. Figure 30 shows SEM micrographs and EDX spectra of HAC modified by 10 wt.% $Na_5P_3O_{10}$. There are hexagonal crystallites which tended to grow in the pores and are surrounded by other hydration products. The EDX spectrum for the crystal, marked "X", shows the chemical composition consists principally of calcium and aluminum. Only minor amounts of phosphorous and sodium are present. This crystalline phase is a calcium aluminate hydrate, the primary hydration product of HAC. The composition of the matrix, which contains aluminum, phosphorus and calcium, is similar to that observed in the other analyses.

For all four classes of phosphate modified HAC, the relative percentages of the constitutents in hydration products are very similar (Table 15). These data indicate that an amorphous calcium aluminate phosphate hydrate (C-A-P-H) gel is produced during hydration reaction in these systems. The microstructure of this phase varies with the different phosphate modifications. The CAPH from different

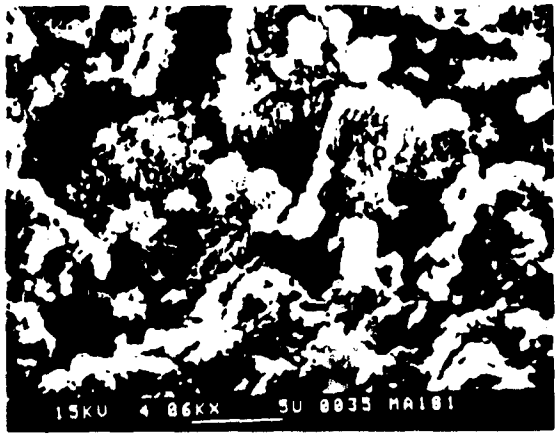

(a)

(b)

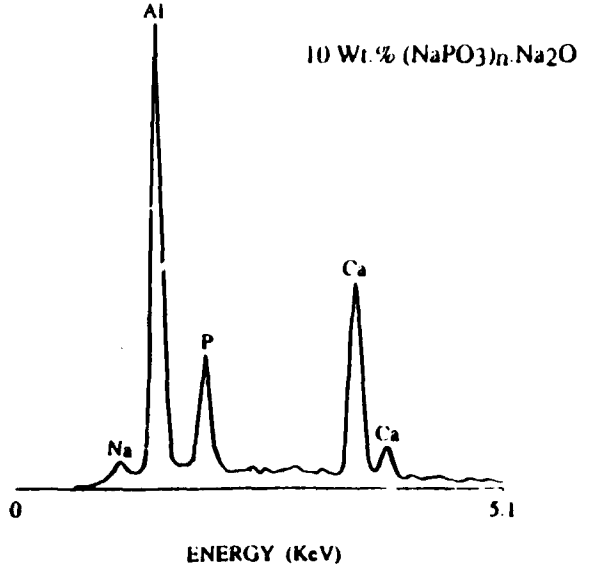

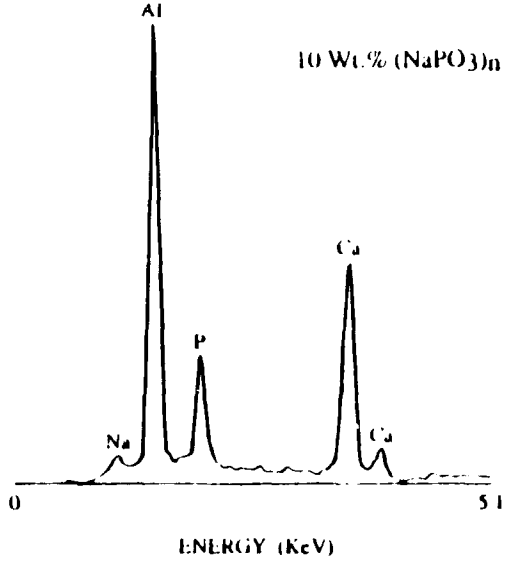

Figure 29. Morphologies and the associated EDX spectra for (a) $(NaPO_3)_n$ modified HAC (b) $(NaPO_3)_n \cdot Na_2O$ modified HAC

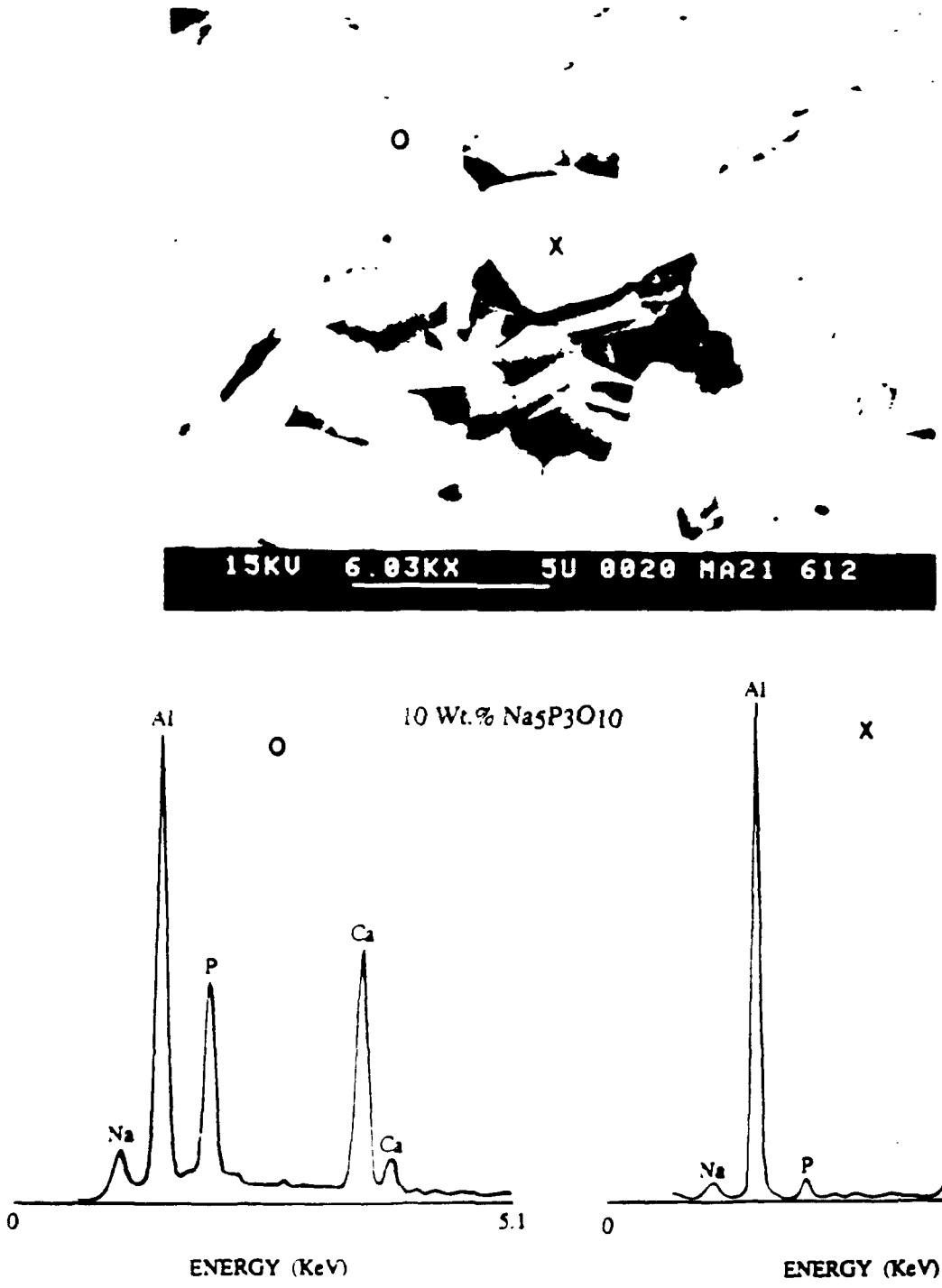

Figure 30. Morphologies and the associated EDX spectra for $Na_5P_3O_{10}$ modified HAC

Table 15. Percentage of the oxides of phosphates modified samples

Admixtures	Oxide Percentage		
(P/C = 0.1)	Al_2O_3	P_2O_5	CaO
$(NaPO_3)_n{\cdot}Na_2O$	60	20	20
$(NaPO_3)_n$	59	21	20
$(NaPO_3)_3$	54	22	24
$Na_5P_3O_{10}$	52	26	22

phosphate modifications is not compositionally identical, however, its composition lies within a narrow range (Table 15). The CAPH appears to bond both the anhydrous HAC grains as well as the calcium aluminate hydrates which form thus providing improved structural integrity to high alumina cement. Although there is still a regression in the strength as the the hexagonal calcium aluminate hydrates undergo conversion to the hexagonal hydrate, the losses in strength appear to be mitigated by the presence of this phosphate-containing hydration product.

3.1.6 Mercury Intrusion Porosimetry Results

Figure 31 shows the cumulative percentage of pore volume with respect to the total pore volume, for pure Secar 71 and for two modified samples containing 10 Wt.% and 20 Wt.% $(NaPO_3)_n{\cdot}Na_2O$. All samples were cured for one day at room temperature and room humidity. It is observed that modified cements have lower total porosity and pore distribution consisting of smaller pores than the pure cement. The sample with 20 Wt.% $(NaPO_3)n.Na_2O$ addition exhibits the lowest total porosity and the smallest pores. These porosity results are in accord with mechanical properties observed.

3.1.7 Microstructures

X-ray diffraction (XRD) results are not entirely consistent with micrographs of the mixture using the scanning electron microscope (SEM). While XRD does not indicate the growth of new crystalline phases in these mixtures, the micrographs indicate that there is some degree of order in the newly developed phases. Figures 32 to 35

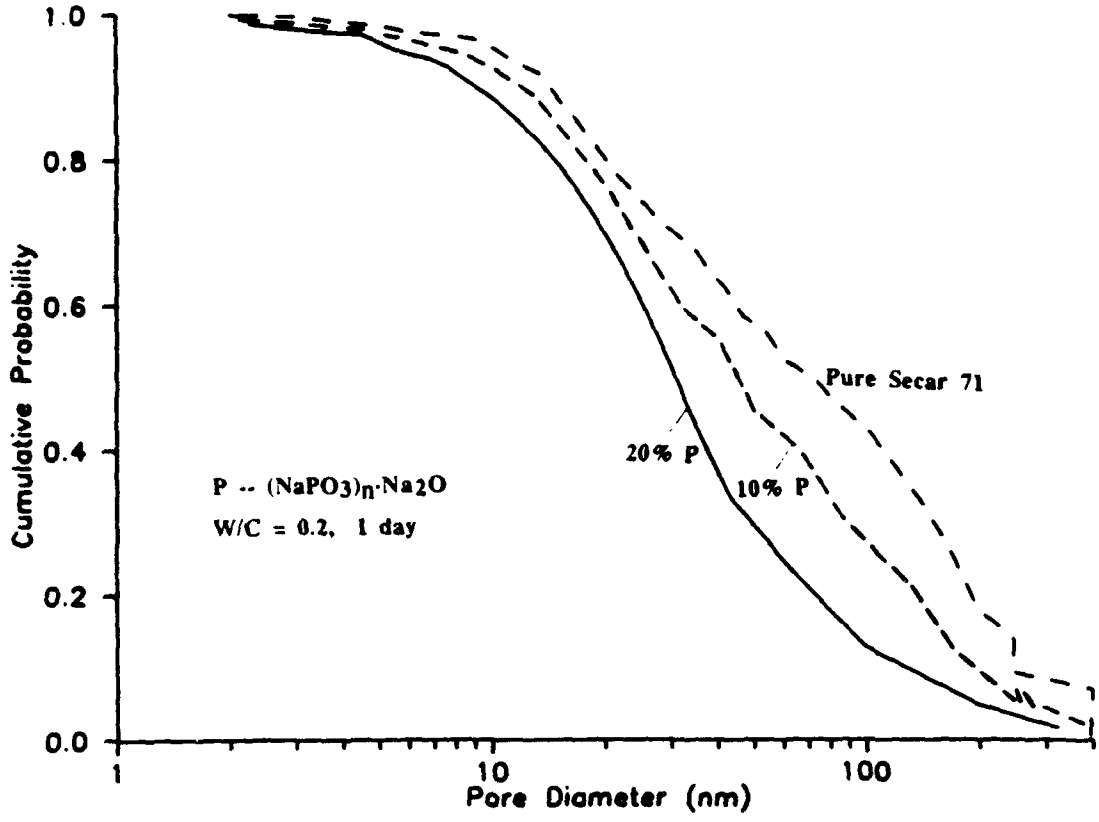

Figure 31. Cumulative probability distributions for HAC and $(NaPO_3)_n \cdot Na_2O$ modified samples

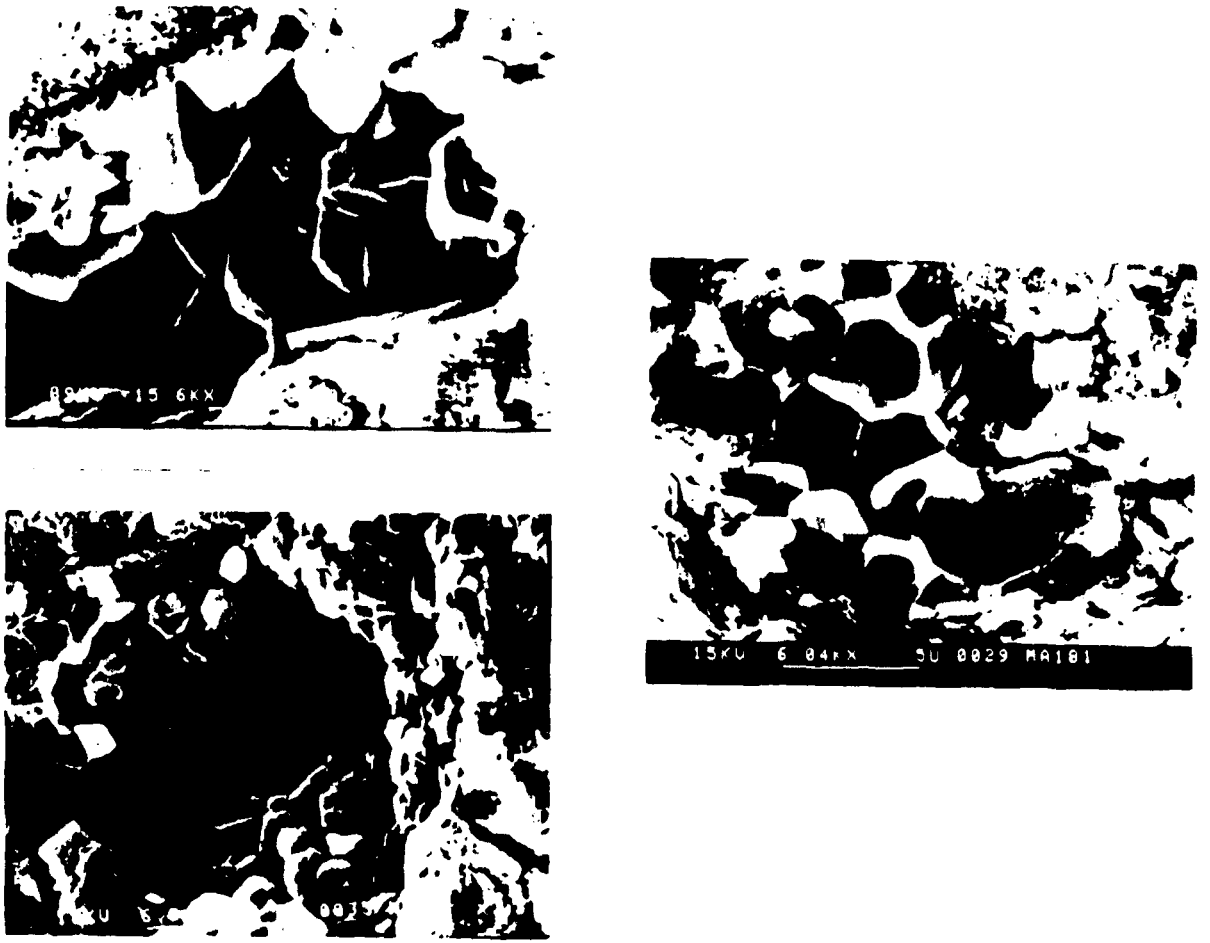

Figure 32. SEM images of $(NaPO_3)_n$·Na_2O modified HAC

Figure 33. SEM images of $Na_5P_3O_{10}$ modified HAC

Figure 34. SEM images of $(NaPO_3)_n$ modified HAC

Figure 35. SEM images of $(NaPO_3)_3$ modified HAC

contain micrographs of cements modified by the different sodium phosphates. All of the samples were cured for 28 days. Figure 32 shows a $(NaPO_3)_n \cdot Na_2O$ modified sample, while Figures 33, 34 and 35 show $Na_5P_3O_{10}$, $(NaPO_3)_n$ and $(NaPO_3)_3$ modified samples, respectively.

The microstructures of the fractured surfaces of the four materials appeared to be different. The microstructure of the fractured surface of a $(NaPO_3)_n \cdot Na_2O$ modified sample as seen in Figure 32 shows hexagonal crystal embedded in a matrix. Although large pores were removed during sample processing, small pores (~5 μm diameter) can still be seen. It is observed from $Na_5P_3O_{10}$ modified samples (See Figure 33) that these hexagonal crystal tended to grow along with the pore. The hexagonal crystals are shaped much like $Ca(OH)_2$ crystals. The $(NaPO_3)_n$ modified sample in Figure 34 shows columnar-like phases in the binding matrix, while in Figure 35 ($(NaPO_3)_3$ modified samples) showed much less crystallinity or smaller crystallite size in appearance than previous three samples.

While scanning the surface of the cement pastes modified by calcium phosphate, a large number of smooth, plate-like structures were observed in Figure 36. These structures have a smooth "glassy" appearance. It should be noted that the pores seem to contain this plate-like structure, and thus porosity can be decreased.

In order to investigate the existence of different crystals, the hardened samples were milled and dissolved in the water. After placing the solution in a 60°C chamber for 48 hours, the solid state was appeared in the solution, and microscopic sized crystals can be seen to have precipitated out of solution. SEM of these solids (see

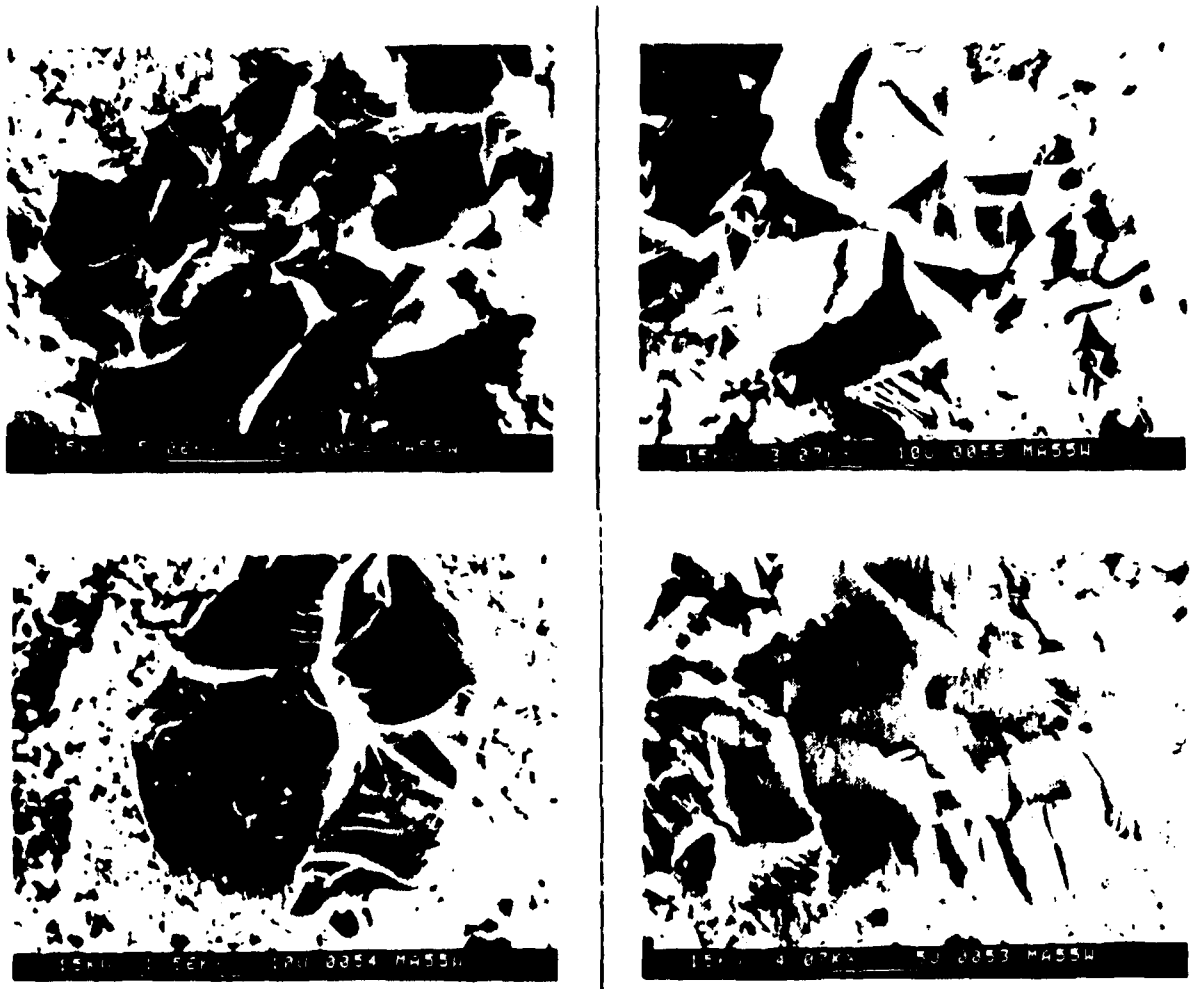

Figure 36. SEM images of $CaHPO_4$ modified HAC

Figure 37) showed that these solids are covered with some very fine crystals. However, the crystals can be seen only at high magnification.

3.2 Ordinary Portland Cement and Phosphate Systems

3.2.1 Mechanical Properties

The effects of different factors on the mechanical properties in the OPC-phosphate system are discussed as in the previous chapter. The factors discussed in this chapter include using different sodium and calcium phosphates, cool-pressed and warm-pressed processing, W/C ratio, and curing conditions.

3.2.1.1 Flexural Strength of OPC Modified by Sodium Phosphate

Table 16 lists the results of the flexural strength for pure OPC and modified samples using four sodium phosphate compositions. The hardened cement pastes were cured up to one year at room temperature. All samples were hydrated at a water/solid ratio of 0.182, and a phosphate/cement ratio of 0.1. It is observed from Figure 38 that all of the sodium phosphate modified samples except the one with $(NaPO_3)_n \cdot Na_2O$ have higher flexural strength than that of the pure one for almost all curing times.

The strengths of modified cements vary significantly during the first week depending on the phosphate used as shown in Figure 38. After 14 days of hydration, the strengths of the phosphate modified samples continue to increase until three months. The strength at one year for pure OPC was 26 MPa, while $Na_5P_3O_{10}$, $(NaPO_3)_n$, $(NaPO_3)_3$

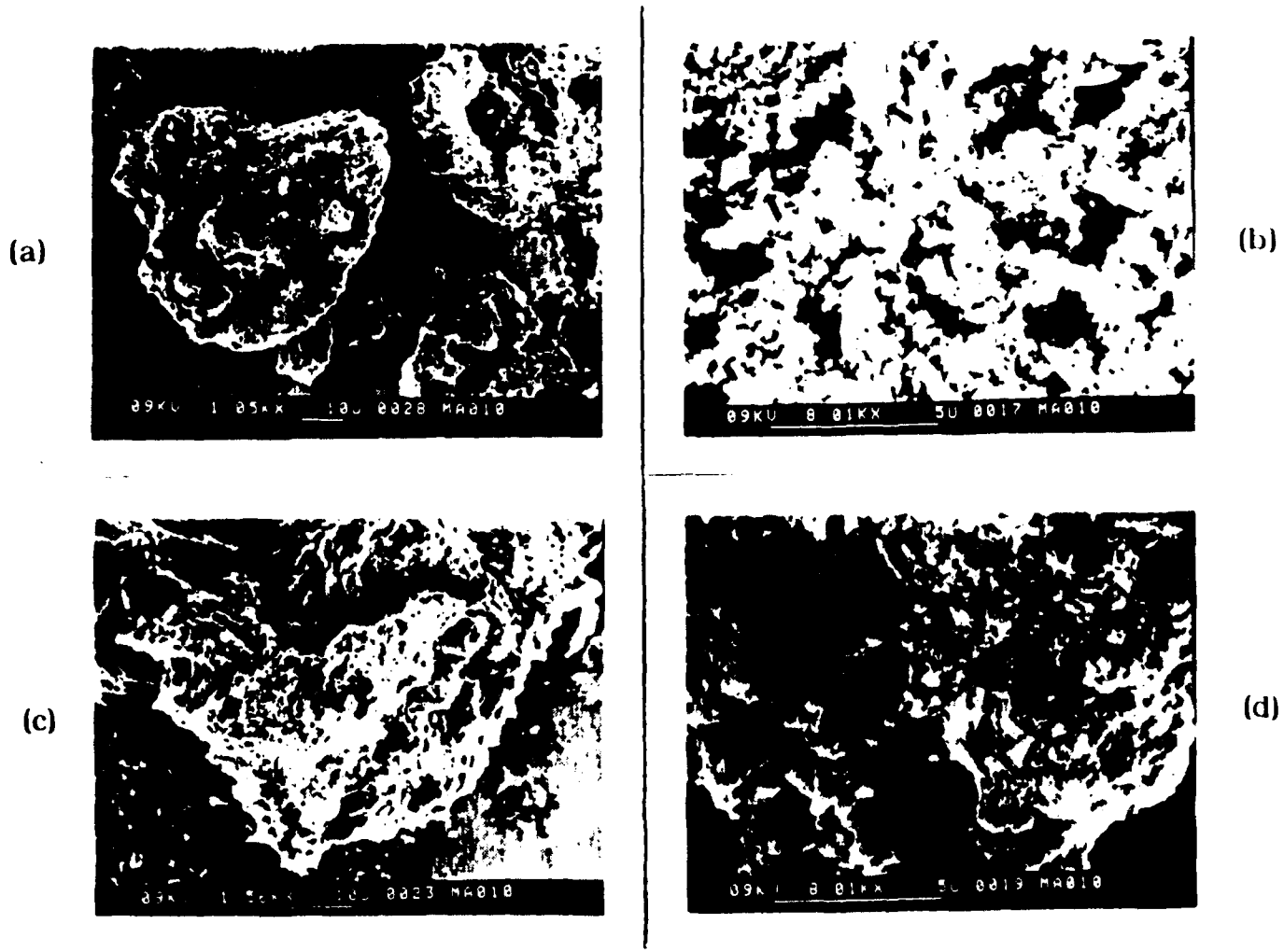

Figure 37. SEM images of morphology of solid state came from the solution of $(NaPO_3)_n \cdot Na_2O$ modified HAC. (a)(b)Low magnification, (c)(d)High magnification

Table 16. Flexural strength for pure OPC and sodium phosphate modified samples

No.	Materials	Amount (g)	Flexural Strength (MPa) 1D	3D	7D	14D	28D	300D	365D
04	OPC	80	~	18.3	18.4	20.7	23.9	26.7	25.6
	DI Water	16							
	OPC	80							
02	$(NaPO_3)_n.Na_2O$	8	13.6	12.4	13.0	11.4	12.4	23.9	23.1
	DI Water	16							
	OPC	80							
22	$Na_5P_3O_{10}$	8	18.0	25.9	21.1	27.8	29.3	31.2	32.2
	DI Water	16							
	OPC	80							
24	$(NaPO_3)_n$	8	18.2	21.5	16.3	24.3	36.5	38.9	38.4
	DI Water	16							
	OPC	80							
26	$(NaPO_3)_3$	8	24.3	28.5	32.1	30.0	~	32.6	33.0
	DI Water	16							

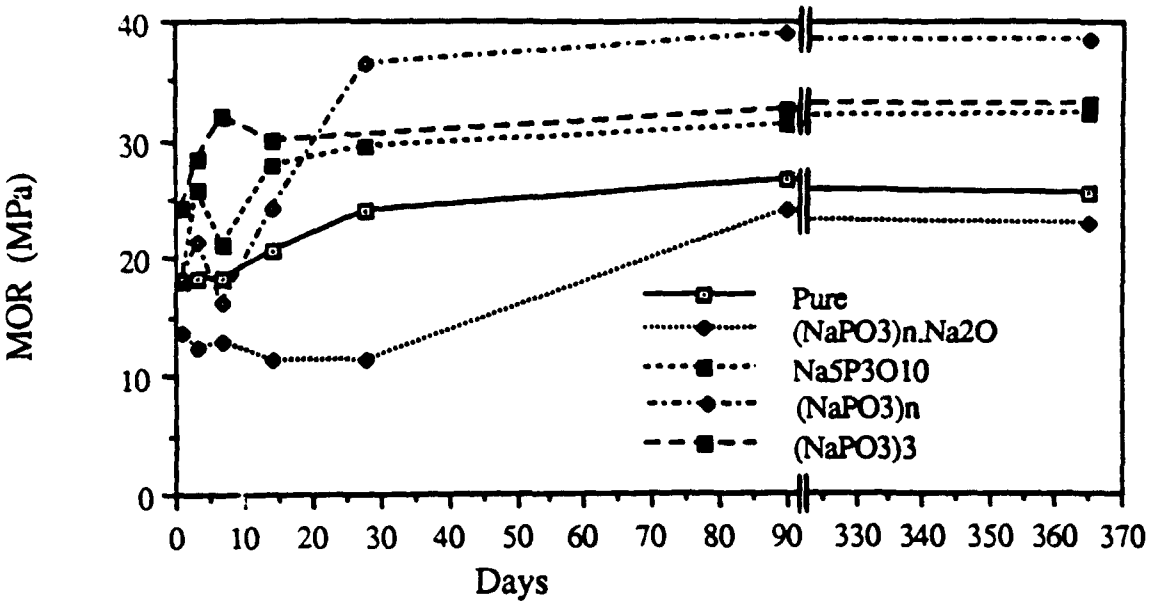

Figure 38. Flexural strength for pure OPC and sodium phosphate modified samples with curing time

and $(NaPO_3)_n \cdot Na_2O$ modified samples reached 32, 38, 33, and 23 MPa, respectively.

3.2.1.2 Flexural Strength of OPC Modified by Calcium Phosphate

The effects of calcium phosphate additions were studied as shown in Table 17. Proportion of phosphate and water/solid ratio were varied to establish their influence on the flexural strength. It was observed that the effect of W/S on the flexural strength at early ages is small no matter how much calcium phosphate was added. It seems that the strengths did not increase rapidly at the early ages, but had relatively high long term values. The samples with higher W/S ratios such as No.15 and 20, however, exhibited higher strengths throughout the entire experiment. Within a certain range, a change in the amount of phosphate doesn't change the strength very much.

3.2.1.3 Effects of Warm-Pressed Processing

Pressing samples is an important step in processing. Cool-pressed (25°C) and warm-pressed (80°C) processing were used to determine the influence on strength. The results are shown in Table 18. All the warm pressed samples have higher strengths than ones with cool pressed ones. Figure 39 (data from Nos.11 and 12) shows the development of strength of two groups of samples, one with cool pressure, the other with warm pressure. The samples were cured in air and water, respectively. It can be seen that in the air curing, warm pressed samples exhibit higher strengths than do cool pressed ones. The values of warm-pressed samples can reach about double that of cool pressed ones. On the other hand, when cured in water, warm-

Table 17. Flexural strength of OPC modified by calcium phosphate

No.	Materials	Amount (g)	W/S Ratio	P/C Ratio	Flexural Strength (MPa) 1D	3D	7D	14D	28D	90D	365D
	OPC	80									
12	CaHPO4	8	0.182	0.10	~	16.6	19.6	20.1	28.0	~	~
	DI Water	16									
	OPC	80									
15	CaHPO4	8	0.227	0.10	22.5	26.3	30.5	33.3	40.1	~	~
	DI Water	20									
	OPC	60									
17	CaHPO4	25.2	0.176	0.42	16.9	21.1	28.1	32.3	30.3	37.4	36.1
	DI Water	15									
	OPC	60									
20	CaHPO4	25.2	0.250	0.42	~	16.0	34.3	38.1	40.3	~	42.6
	DI Water	21.3									
	OPC	80									
50	CaHPO4	4	0.286	0.05	~	35.8	~	31.7	37.5	~	~
	DI Water	24									
	OPC	80									
51	CaHPO4	12	0.261	0.15	~	34.2	~	26.1	38.9	~	~
	DI Water	24									

Table 18. Comparison of flexural strength by using different processing

No.	Materials	Amount (g)	W/S Ratio	P/C Ratio	Curing Conditions	Sample Processing	Flexural Strength (MPa) 3D	7D	14D	28D
12	OPC $CaHPO_4$ DI Water	80 8 16	0.182	0.1	In Air	Cool Pressed	16.6	19.6	23.1	28.0
12	OPC $CaHPO_4$ DI Water	80 8 16	0.182	0.1	In Air	Warm Pressed	34.7	36.1	37.5	42.9
11	OPC $CaHPO_4$ DI Water	80 8 16	0.182	0.1	In Water	Cool Pressed	24.6	26.1	27.2	30.1
11	OPC $CaHPO_4$ DI Water	80 8 16	0.182	0.1	In Water	Warm Pressed	31.9	33.0	36.9	36.9
15	OPC $CaHPO_4$ DI Water	80 8 20	0.227	0.1	In Air	Cool Pressed	26.7	30.5	33.3	40.1
15	OPC $CaHPO_4$ DI Water	80 8 20	0.227	0.1	In Air	Warm Pressure	29.5	32.2	32.7	38.5

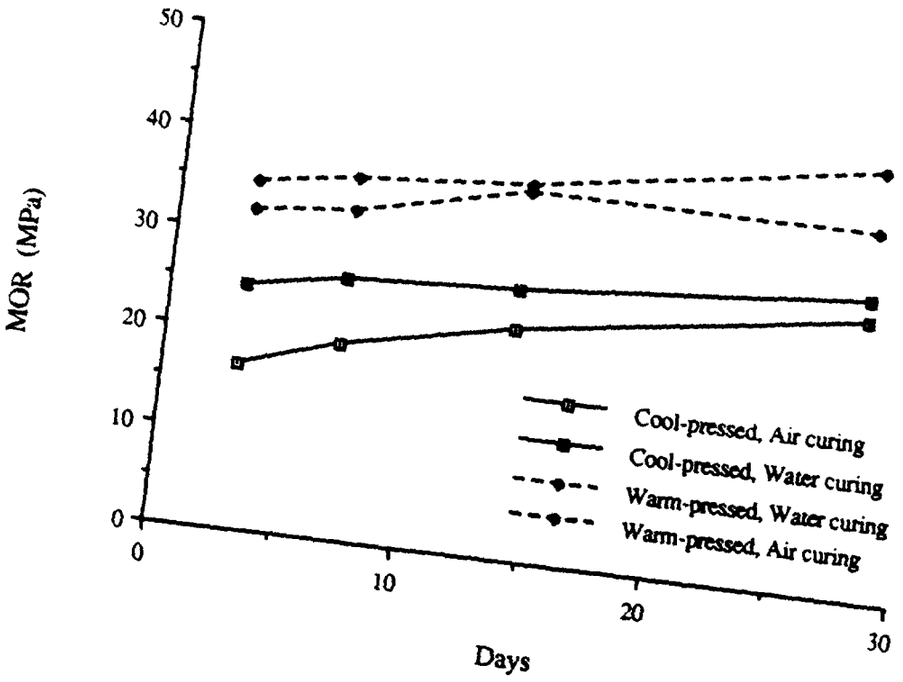

Figure 39. Comparison of flexural strength of No.11 and 12 by using different processing and curing conditions

pressing is not as effective as in air curing, and they have 50% higher strengths than the cool pressed ones.

3.2.1.4 Effects of W/C Ratio

Figure 40 shows the variation in flexural strength for the samples with W/C of 0.20 and 0.25. when cool-pressed, in contrast to the common view, samples with higher W/C have higher strengths. The reason may be that much unhydrated cement remains at the lower W/C due to a lack of sufficient water for hydration. Warm-pressed samples with lower W/C (0.20) exhibit a slightly higher strength than ones with higher W/C (0.25). Thus, warm pressing has more effect at the lower W/C compared to the higher W/C samples.

3.2.1.5 Water Sensitivity

Water sensitivity of the material is one of the properties which is concerned in this study. Table 19 shows the strengths of three groups of calcium phosphate-modified samples which have different W/S ratios and P/C ratios. The samples were cured in air and in water at room temperature, respectively. The samples with lower W/S ratios (equal to 0.182 and 0.176, respectively) have higher strengths when cured in water than in air (except for the strength of No.17 at 14 days). The reason is the same as has been mentioned before, that is, lack of sufficient water for hydration. For the samples with higher W/C (equal to 0.25), the strength is somewhat lower in water other than in air, but the values are very close. These data suggest that this material is not very sensitive to water.

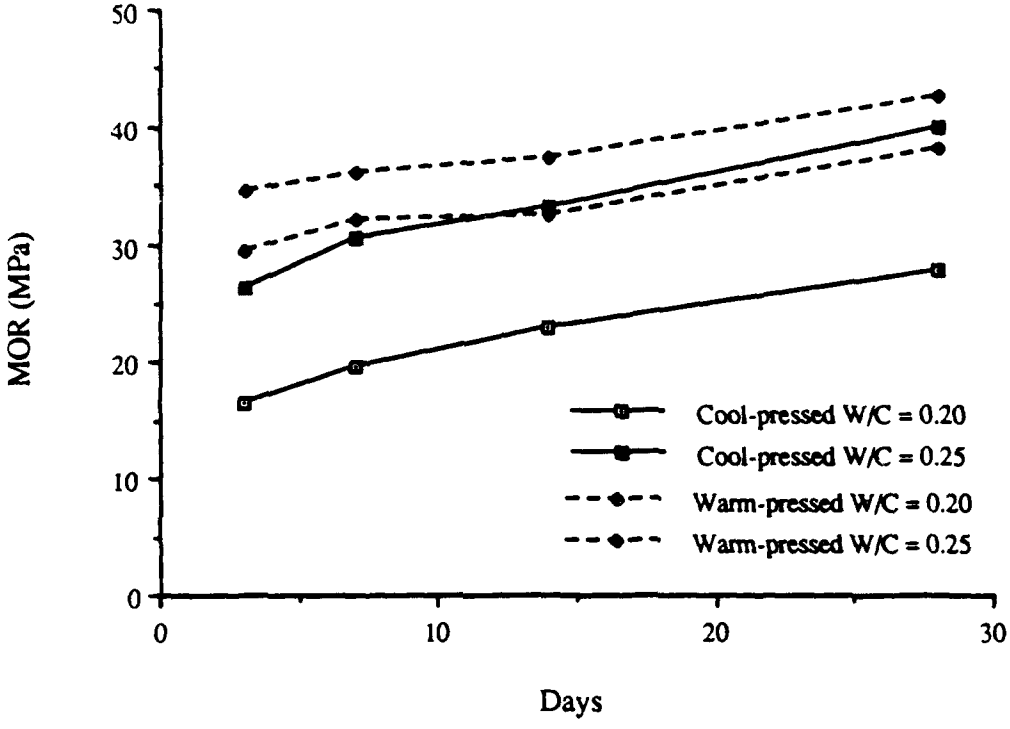

Figure 40. Variation of strength for the samples with different W/C, 0.20 and 0.25

Table 19. Water sensitivity of calcium phosphate-modified samples

No.	Curing Conditions	W/S Ratio	P/C Ratio	Flexural Strength (MPa) 3D	7D	14D	28D
11	In Air	0.182	0.10	16.6	19.6	20.1	28.0
11	In Water (25°C)	0.182	0.10	24.6	26.1	27.2	30.1
17	In Air	0.176	0.42	21.1	28.1	32.0	30.3
17	In Water (25°C)	0.176	0.42	29.3	31.0	28.8	37.6
20	In Air	0.25	0.42	26.0	34.3	38.1	40.1
20	In Water (25°C)	0.25	0.42	33.8	32.6	33.2	33.3

3.2.1.6 Effects of Curing Conditions

Samples were cured at different temperatures (25°C and 80°C) and the strength data are shown in Table 20. It is observed that the samples cured in higher temperature water have much higher strengths than those cured in low temperature water. Therefore, the temperature of curing water is an important factor in influencing strength.

3.2.2 Calorimetry Measurements Results

Figure 41 shows the calorimetric curves for pure OPC and $(NaPO_3)_n$ and $(NaPO_3)_n \cdot Na_2O$-modified samples during the first four hours of hydration. It was found from studying heat evolved during hydration that faster hydration rates occurred when OPC was modified by sodium phosphates, and both modified samples produced more heat than pure OPC at the beginning of hydration. Furthermore, the $(NaPO_3)_n \cdot Na_2O$ modified sample reacted more rapidly than $(NaPO_3)_n$ modified sample, and produced more heat. Longer time behavior, up to 48 hours, is shown in Figure 42. This figure indicates the colorimetric curves for pure OPC and $Na_5P_3O_{10}$ and $(NaPO_3)_3$ modified samples. It is difficult to observe the first peak, which usually occurs within the first few of hours, due to the scale. OPC exhibits the second peak between the fourth hour and twelfth hour. However, this main peak is less evident in the two modified samples. It is also been able to observe that modified samples produce higher total heat than pure one.

It has been seen from Table 16 that all of the sodium phosphate-modified samples except the one with $(NaPO_3)_n \cdot Na_2O$ have higher

Table 20. Comparison of flexural strength by curing at different temperature

No.	Materials	Amount (g)	Curing Conditions	Flexural Strength (MPa)			
				3D	7D	14D	28D
19	OPC DI Water	80 20	In Air	22.7	30.0	27.0	30.5
			In Water (25°C)	32.5	35.6	36.1	32.8
			In Water (80°C)	38.7	40.7	43.0	42.3
20	OPC $CaHPO_4$ DI Water	60 25.2 21.3	In Air	16.0	34.3	38.1	-
			In Water (25°C)	33.8	32.6	33.2	-
			In Water (80°C)	45.6	47.4	49.0	-
50	OPC $CaHPO_4$ DI Water	80 4 24	In Air	35.8	-	31.7	37.5
			In Water (25°C)	23.9	-	21	21.7
			In Water (80°C)	-	-	51.4	53.2
51	OPC $CaHPO_4$ DI Water	80 12 24	In Air	34.2	-	26.1	38.9
			In Water (25°C)	25.5	-	22.2	32.6
			In Water (80°C)	-	-	57.2	43.6
53	OPC $2CaO{\cdot}P_2O_5$ DI Water	80 26.7 24	In Air	23.5	-	37	39.5
			In Water (25°C)	19.2	-	27.2	32.8
			In Water (80°C)	-	-	64.7	59.1

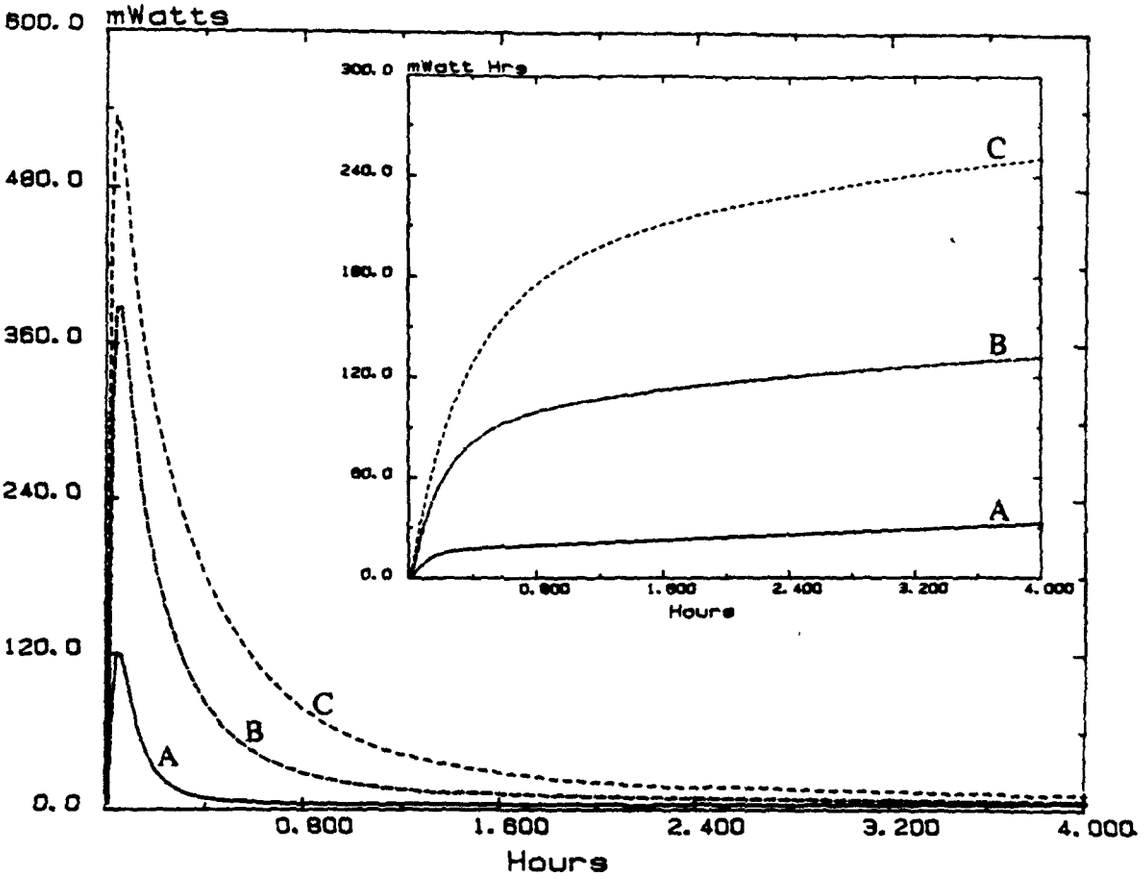

Figure 41. Calorimetric curves showing the rate of heat evolution and total heat as a function of time for pure OPC and modified samples by $(NaPO_3)_n$ and $(NaPO_3)_n \cdot Na_2O$ during the first 4 hours of hydration. A -- Pure OPC, B -- 10% $(NaPO_3)_n$ modified OPC, C -- 10% $(NaPO_3)_n \cdot Na_2O$ modified OPC

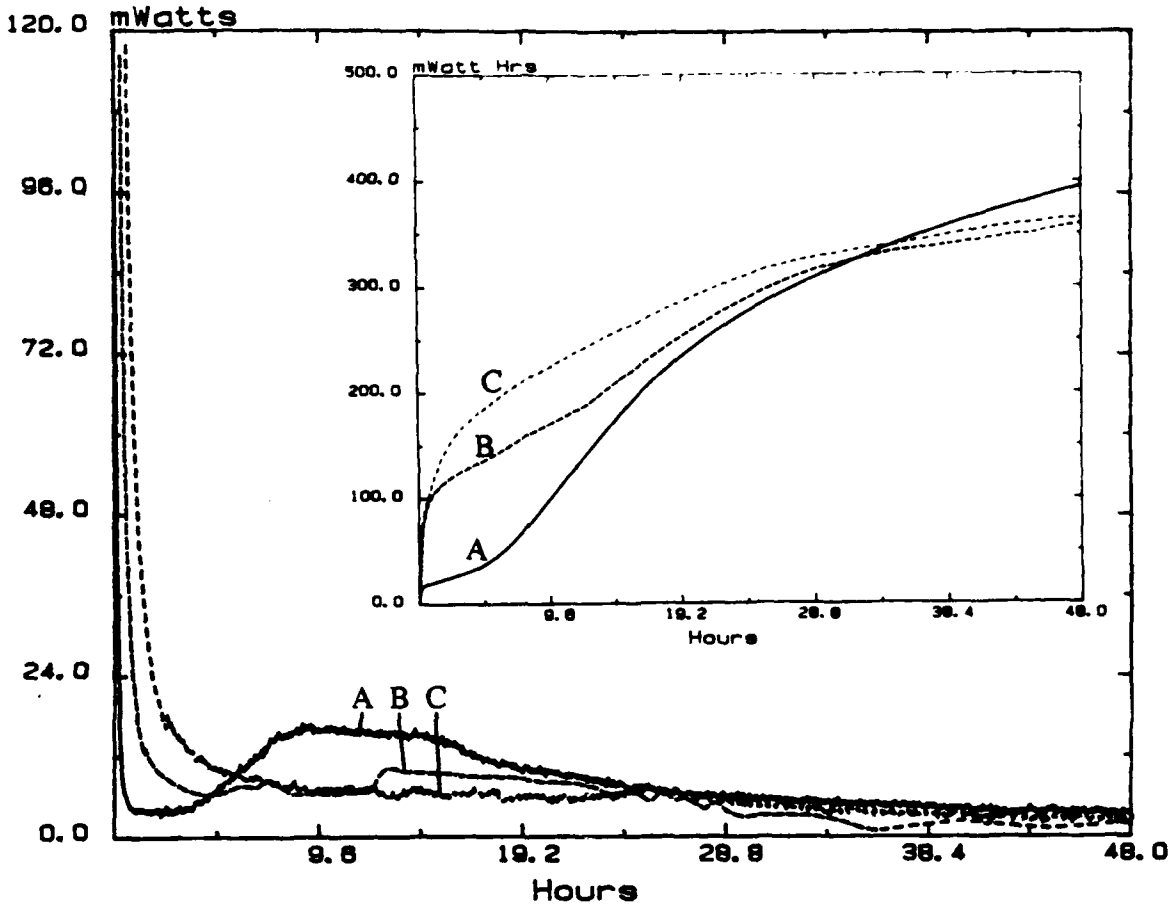

Figure 42. Calorimetric curves showing the rate of heat evolution and total heat as a function of time for pure OPC and modified samples by $Na_5P_3O_{10}$ and $(NaPO_3)_3$ during the first 48 hours of hydration. A -- Pure OPC, B -- 10% $Na_5P_3O_{10}$ modified OPC, C -- 10% $(NaPO_3)_3$ modified OPC

flexural strengths than does OPC. Therefore, the same conclusions may apply regarding the relationship between strength and the rate of hydration, as was discussed in the last chapter for modified HAC, the faster the reaction, the higher strength the sample exhibits. The reason that the sample with $(NaPO_3)n{\cdot}Na_2O$ exhibited relatively low strength was perhaps that this sample produced a large amount of heat at the beginning (see Figure 41). The low strength is believed to be the result of cracks caused by expansion from this heat.

The effects of calcium phosphate additions were also studied as shown in Figure 43 and 44. Figure 43 shows the heat evolved during the first 24 hours of hydration for both pure cement and $2CaO{\cdot}P_2O_5$ modified samples. The proportions of phosphate used are 10%, 25% and 40%. The figure indicates that no matter how much calcium phosphate was added the effect on the heat evolved at early ages is small. Moreover, the total heat evolved from each of the samples as shown in Figure 44 decreases with increasing proportion of $2CaO{\cdot}P_2O_5$.

3.2.3 X-ray Diffraction Analysis

Figure 45 shows x-ray diffraction pattens for pure OPC and for the four samples modified by different sodium phosphate, after curing in air for 28 days at room temperature. All samples were hydrated at a water/solid ratio of 0.182, and a phosphate/cement ratio of 0.1. Although there was a difference in the mechanical properties among these samples, as discussed previously, the difference in the x-ray diffraction pattens is minimal. Nearly, all the peaks remained in the same position. Only difference can be observed is that the $Ca(OH)_2$

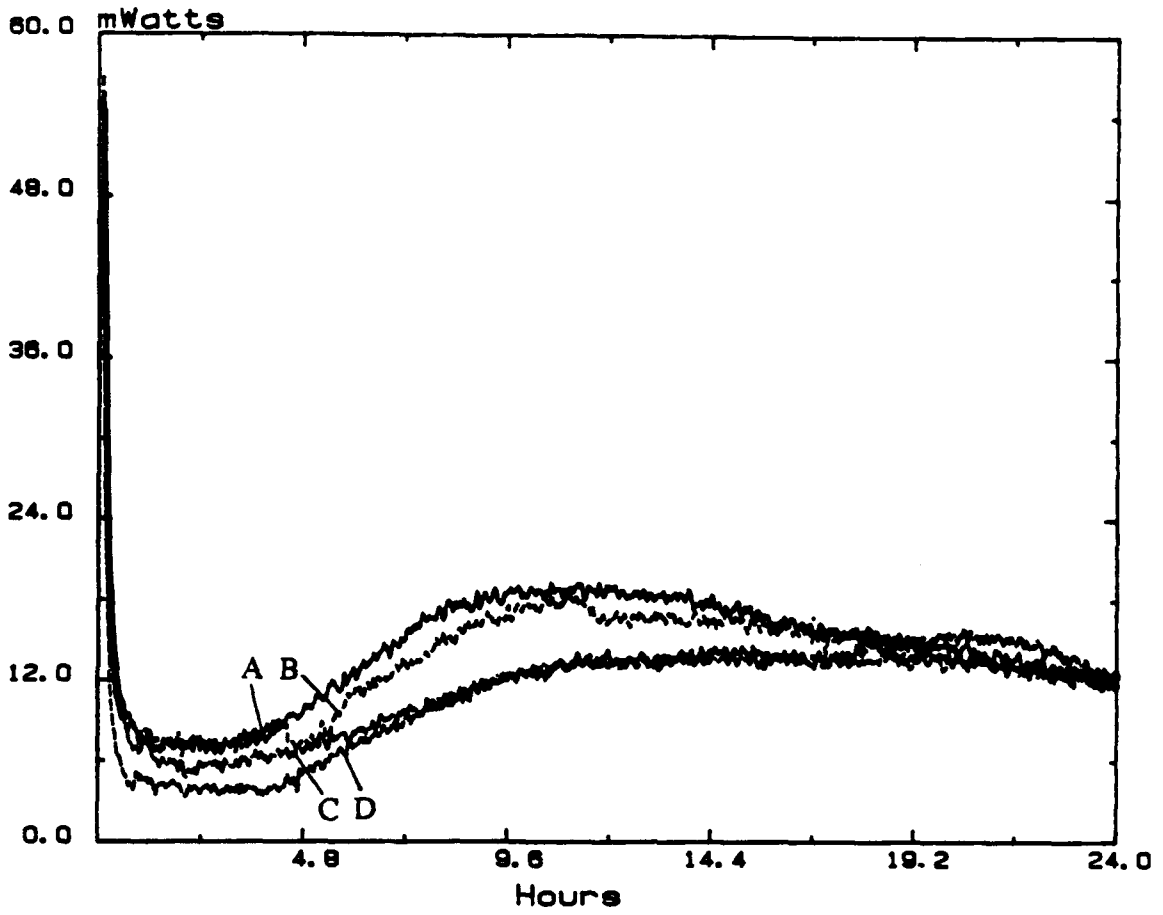

Figure 43. Heat evolved for both pure OPC and modified samples by $2CaO \cdot P_2O_5$ during the first 24 hours of hydration. A -- Pure OPC, B -- 10% $2CaO \cdot P_2O_5$ modified sample, C -- 25% $2CaO \cdot P_2O_5$ modified sample, D -- 40% $2CaO \cdot P_2O_5$ modified sample.

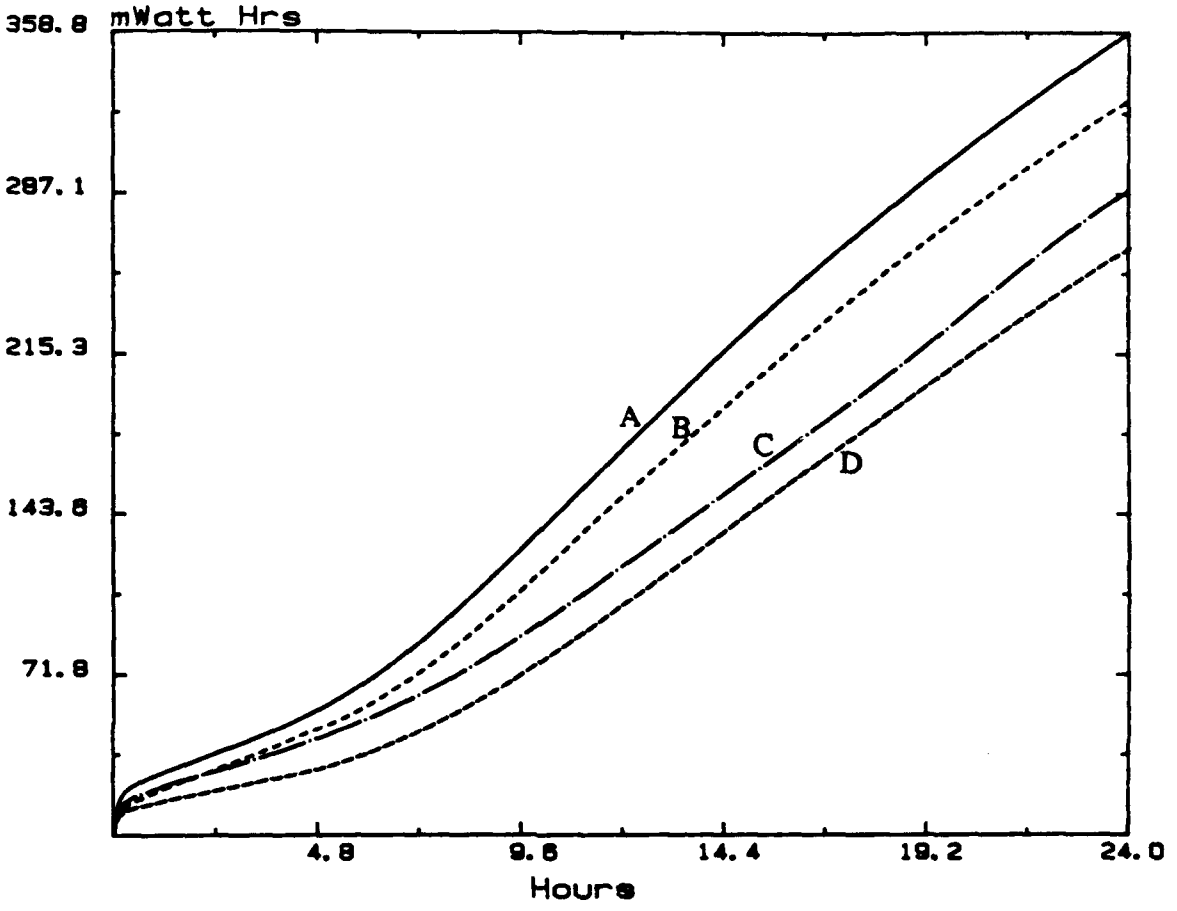

Figure 44. Total heat for both pure OPC and modified samples by $2CaO \cdot P_2O_5$ during the first 24 hours of hydration. A -- Pure OPC, B -- 10% $2CaO \cdot P_2O_5$ modified sample, C -- 25% $2CaO \cdot P_2O_5$ modified sample, D -- 40% $2CaO \cdot P_2O_5$ modified sample

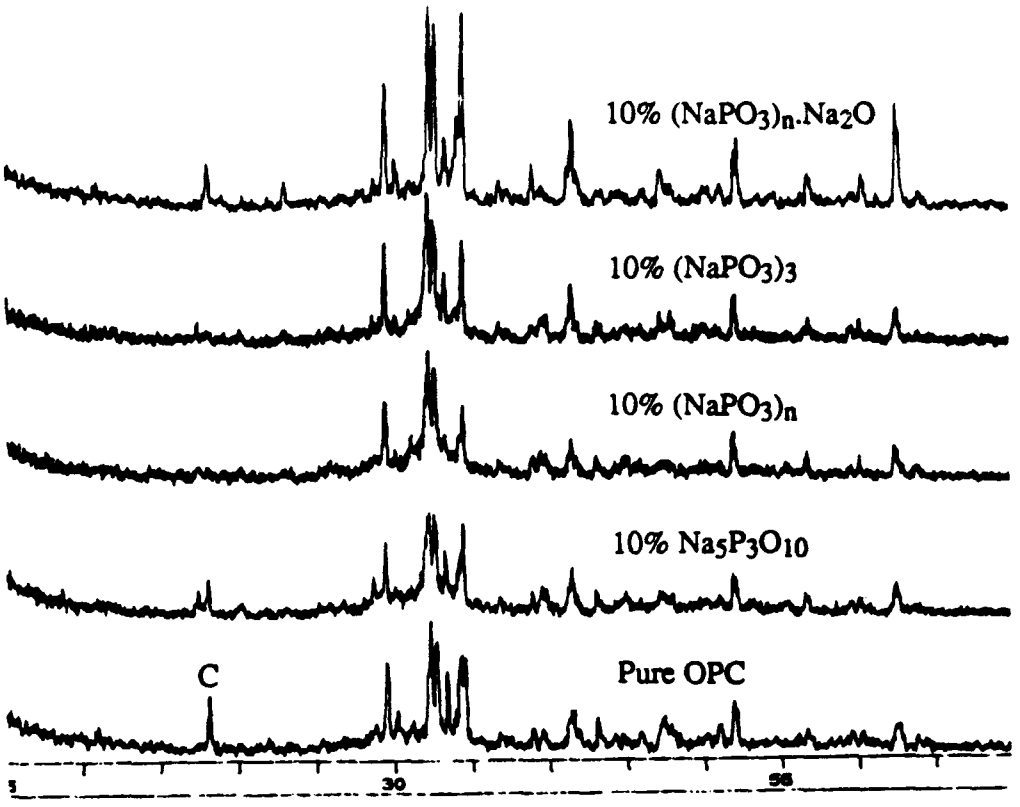

Figure 45. XRD of pure OPC and four samples modified by sodium phosphate curing in air for 28 days at room temperature. C -- $Ca(OH)_2$ (Blended samples contain 10 wt% phosphate)

peaks have lower intensities or have disappeared. All other positions of the peaks do not change.

Diffraction patterns of calcium phosphate modified samples are shown in Figure 46 and 47. Figure 46 presents XRD patterns of pure OPC, pure $2CaO \cdot P_2O_5$ and modified sample with a calcium phosphate addition of 33.4 Wt.% $2CaO \cdot P_2O_5$. The samples were cured in air for 28 days at room temperature. It is observed that the mixture is just a combination of two pure compounds, new crystalline reaction products cannot be observed. A similar result can also be seen in $CaHPO_4$ modified samples. Figure 47 shows XRD patterns of pure OPC, pure $CaHPO_4$ and two modified samples containing 10 Wt.% and 42 Wt.% $CaHPO_4$ additions, respectively. The samples were cured in air for 28 days at room temperature. Again no new peaks are observed. These data suggest the mechanism by which strength increases may be similar with that of HAC-Phosphate system; it may be related to formation of an amorphous phase which is stronger than the C-S-H gel produced by pure ordinary portland cement.

Figure 48 shows the XRD patterns of $CaHPO_4$ modified samples cured in water in the early stage at room temperature. It can be observed that $Ca(OH)_2$ appeared between 8 and 15 hours. The appearance of $Ca(OH)_2$ in XRD patterns occurred later in time than in pure OPC. This is perhaps due to the consumption of $Ca(OH)_2$ in the formation of a phosphate-containing product phase.

3.2.4 Scanning Electron Microscopy

Figure 49 to 52 show micrographs of cements modified by calcium phosphates. As in the HAC-phosphate system, the

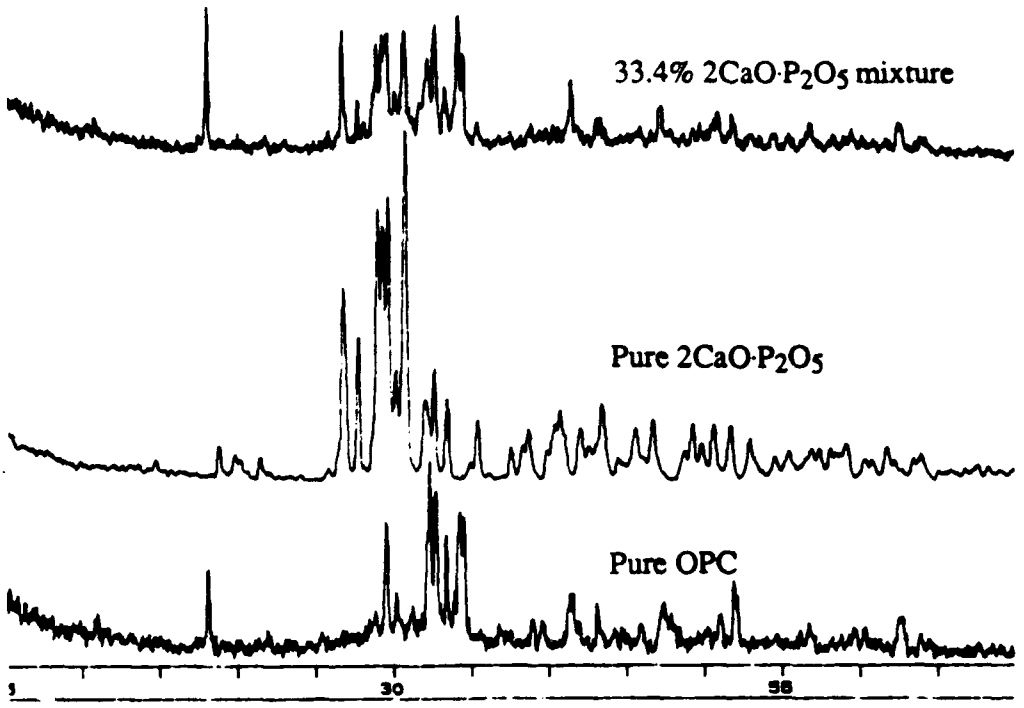

Figure 46. XRD of pure OPC, pure $2CaO \cdot P_2O_5$ and 33.4 Wt.% $2CaO \cdot P_2O_5$ modified sample curing in air for 28 days at room temperature

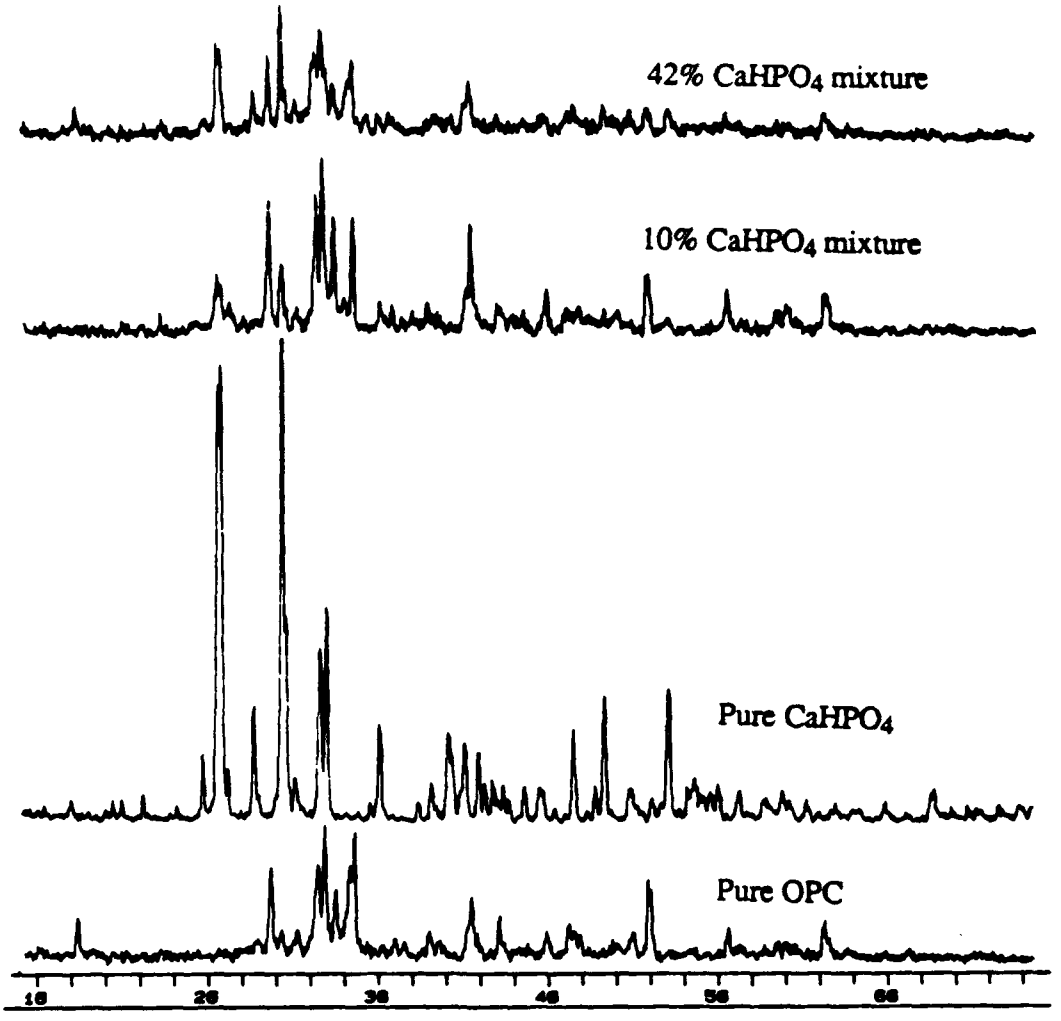

Figure 47. XRD of pure OPC, pure $CaHPO_4$ and two different amount of $CaHPO_4$ modified samples curing in air for 28 days at room temperature

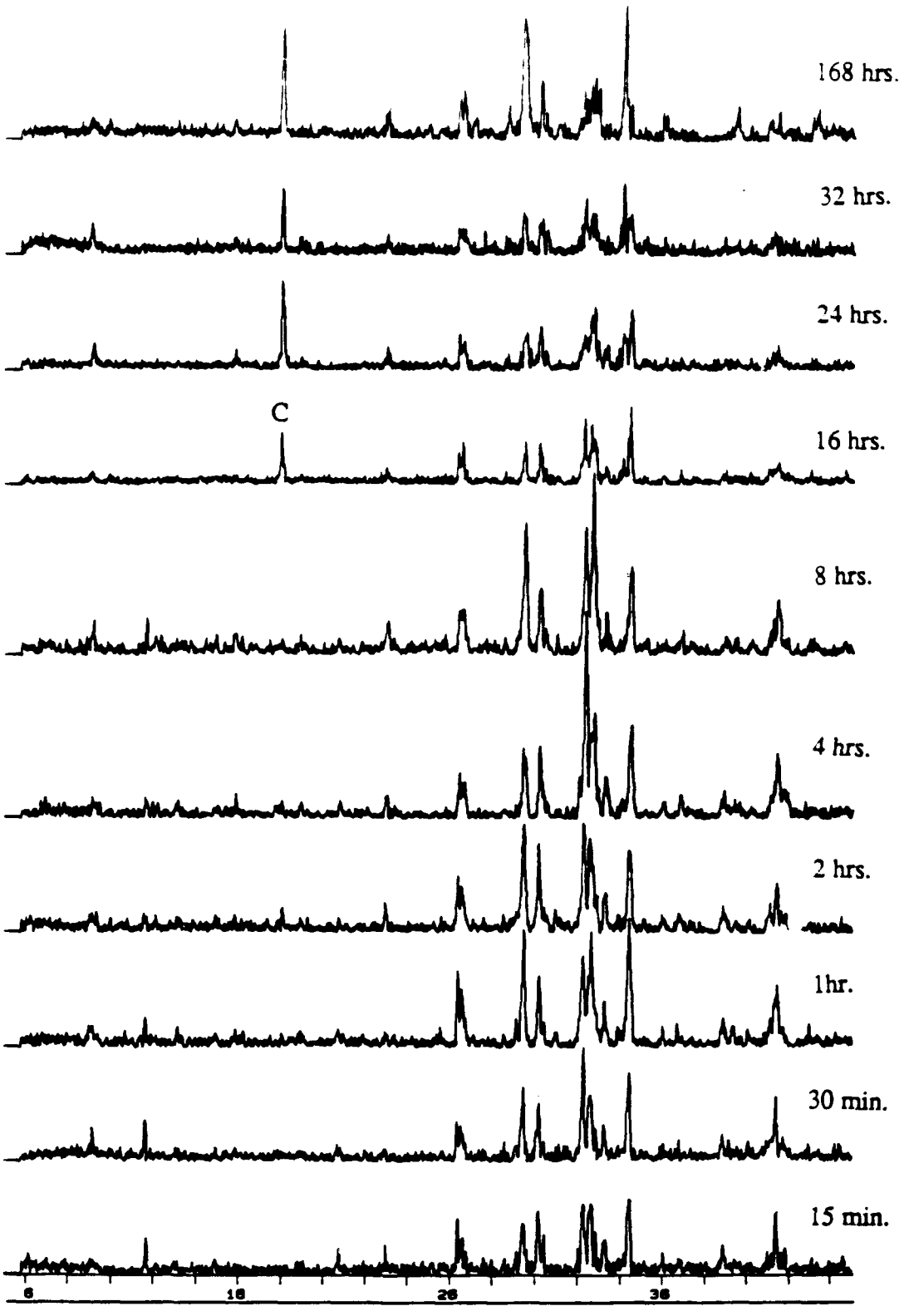

Figure 48. XRD of $CaHPO_4$ modified OPC cured in sufficient water in the early stage at room temperature. C -- $Ca(OH)_2$

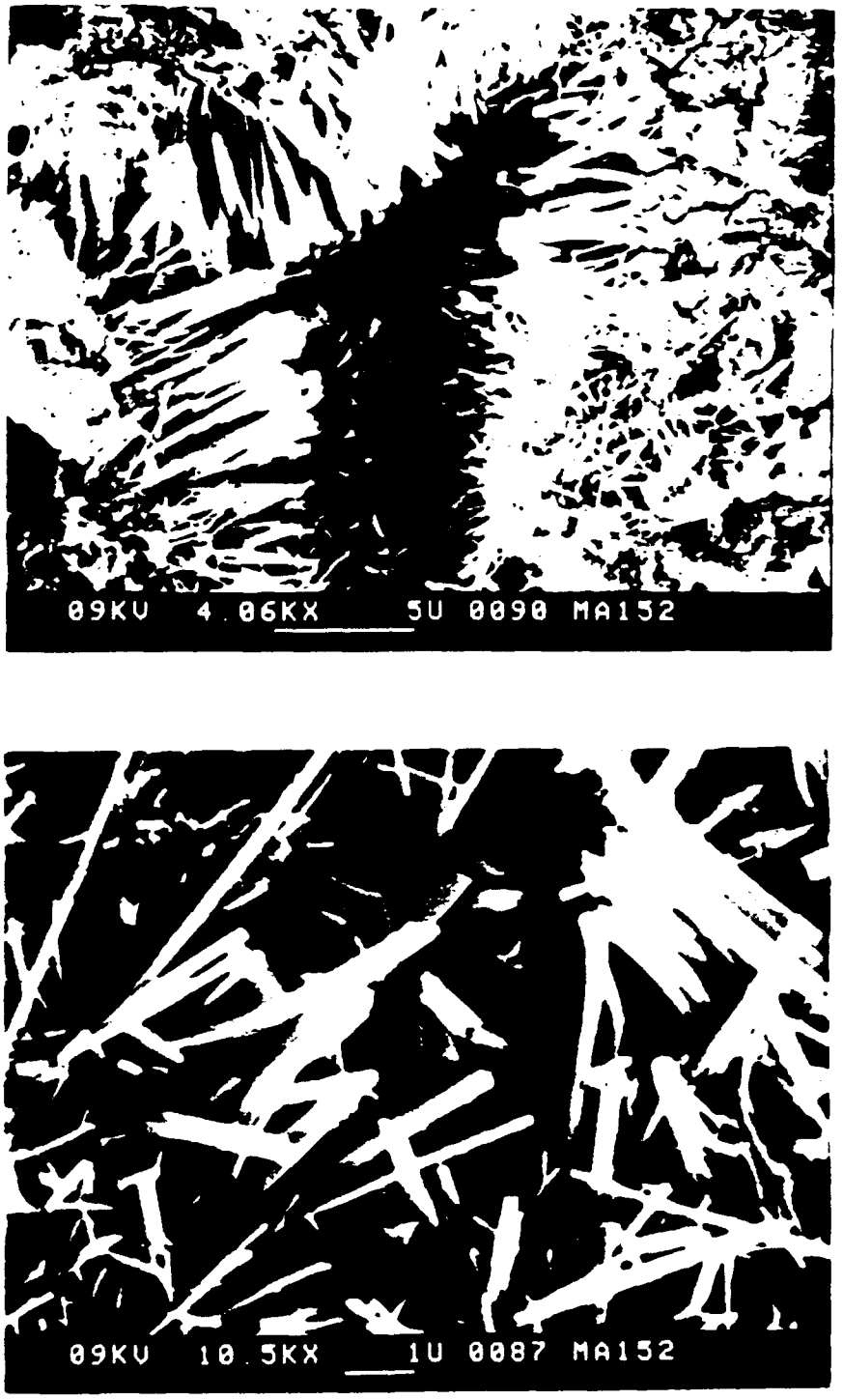

Figure 49. SEM images of calcium phosphate $CaHPO_4$ modified OPC

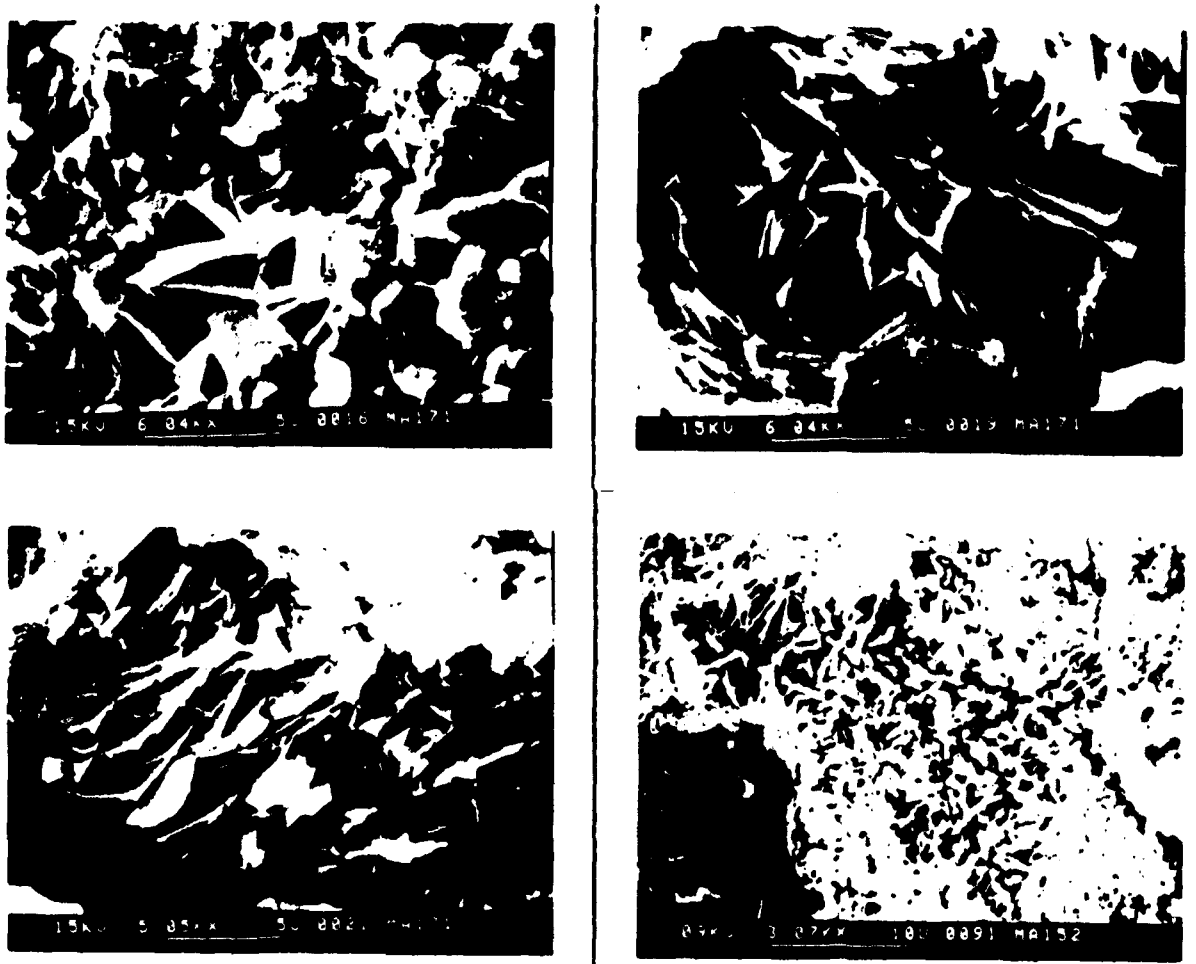

Figure 50. SEM images of calcium phosphate $CaHPO_4$ modified OPC

Figure 51. SEM images of calcium phosphate $CaHPO_4$ modified OPC by warm-pressed processing

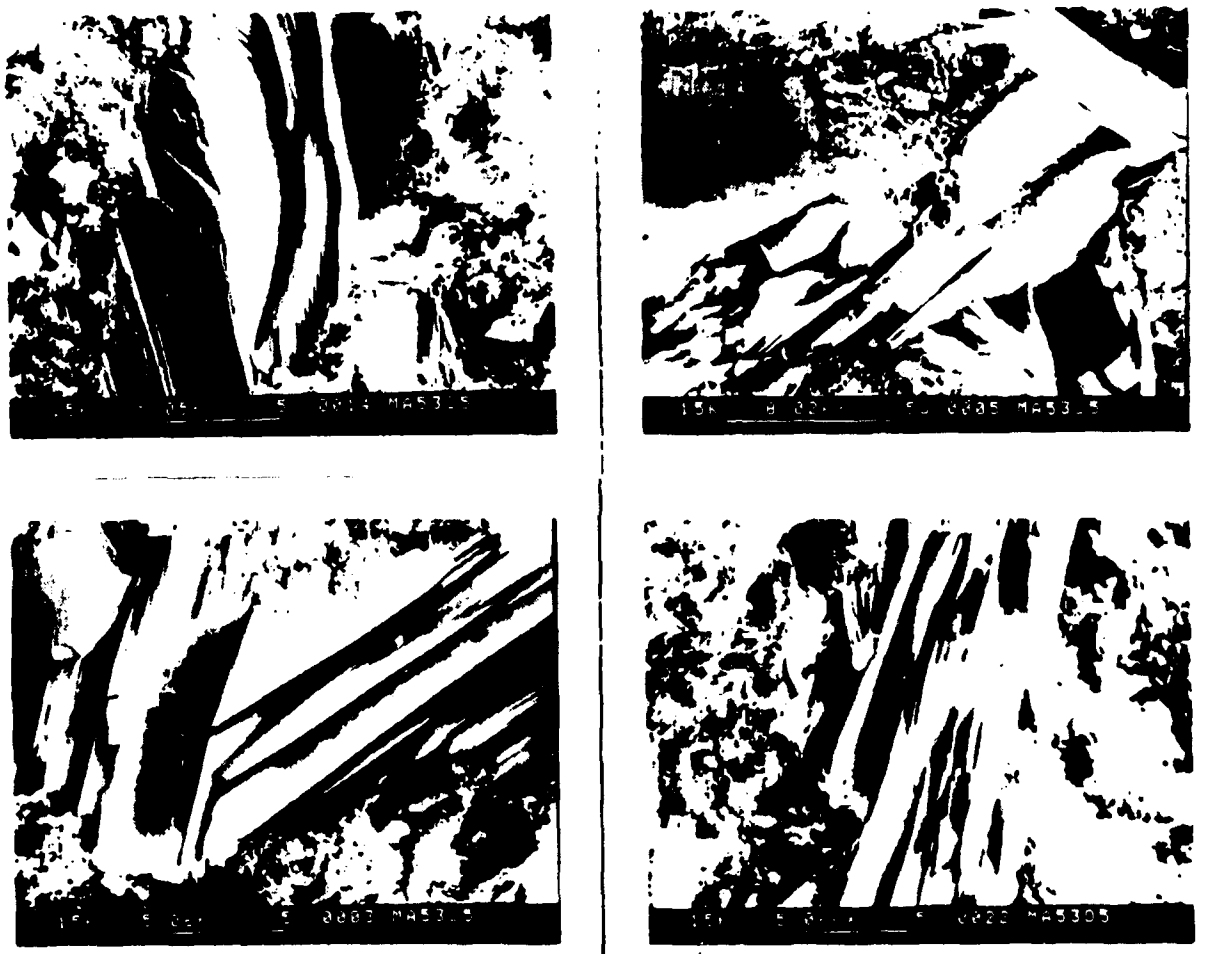

Figure 52. SEM images of calcium pyrophosphate $2CaO \cdot P_2O_5$ modified OPC

microstructures of these cements are not consistent with the diffraction data. Even though x-ray diffraction gave limited evidence for the growth of new crystalline phases in these materials, the micrographs indicated that there is some degree of order in the newly developed phases. Figure 49 to 50 show the morphology of calcium phosphate $CaHPO_4$ modified sample, and different types of crystals can be observed. The morphology is very similar to that of hydroxyapatite (Brown and Fulmer, 1991). XRD and micrographs suggest that poorly crystalline hydroxyapatite is formed in this system. The microstructure of $CaHPO_4$ modified samples by warm-pressed processing is shown in Figure 51. It is observed that some plate-like crystals are embedded in the round grains. The micrographs shown in Figure 52 indicate a lot of massive columnar-like growths in the binding matrix.

Chapter 4
SUMMARY AND CONCLUSIONS

4.1 Summary

This research has been concerned with mechanical behavior and microstructural development in cementitious materials modified by various phosphate-based inorganic polymers or compounds. Two systems were studied, the HAC-based system and the OPC-based system.

4.1.1 HAC-Phosphate System

It is found that all of the phosphate modified cements have higher strengths than pure HAC. The strengths increased very rapidly with age for about 3 to 7 days for both pure HAC and modified cements. The differences between pure HAC and the modified cement are significant. The maximum strength of pure HAC was 14 MPa at 7 days, while $(NaPO_3)_n \cdot Na_2O$, $(NaPO_3)_n$ and $(NaPO_3)_3$ modified samples attained maximum strengths of 35, 40, 29 MPa, respectively, at 3 days ($Na_5P_3O_{10}$ modified sample reached a maximum strength of 34 MPa at 7 days). The modified cements had strengths 2 to 3 times that of the pure cements. However, the modified cements followed

the same trend as pure cement in that their strengths began to decrease after reaching maxima. Between one month and three months of curing, the strengths for all the samples were lower than the strengths exhibited during the first thirty days. After ten months of hydration, $(NaPO_3)_n \cdot Na_2O$, $(NaPO_3)_n$, $Na_5P_3O_{10}$ and $(NaPO_3)_3$ modified cements attained strengths of 35, 27, 29 and 28 MPa, respectively, while pure cement only reached 12 MPa. While strength regression occurs in phosphate modified formulations, the strengths of the modified cements always exceed those of the unmodified cement. These data suggest that it may be possible to develop an HAC-based cementitious material exhibiting desirable chemical reactions and physical properties.

The reason for the loss in strength is probably due to same mechanism in all cases. The initial products of HAC hydration under room temperature are hexagonal calcium aluminate hydrates CAH_{10}, C_2AH_8, and alumina gel. These three products are all metastable. With time, both hexagonal CAH_{10} and C_2AH_8 crystals, which are unstable both at normal and higher temperatures, slowly convert to C_3AH_6 and alumina gel with a consequent increase in porosity and strength loss. This change is known as convertion.

The effects of calcium phosphate additions were also studied. No matter how much calcium phosphate is added, the effect on the flexural strength at early ages is small. However, the more calcium phosphate that is added initially, the higher the long-term strength. The splitting strengths showed the same trend. It was found that calcium phosphate was not as effective as sodium phosphate in achieving increases of strength of HAC. Samples cured in water had

significantly lower strengths. This indicates that the calcium phosphate modified HAC composite is sensitive to water.

When silica fume was used to replace the same amount of HAC. The resultant strength of the samples exhibited the same trend as the previous sample. The strength is very high at early ages, but it also decreases during the conversion reaction. The strength of the phosphate modified cement is higher than that of pure HAC. After ten months of curing, the strength of silica fume replaced sample was still twice as high as that of pure cement. Furthermore, strength loss in silica fume replaced samples is less than in samples without silica fume, although they have approximately the same strength at the end of ten months curing. Thus, adding silica fume retards the loss in strength.

It was found that fluidity increased by adding the sodium phosphate to HAC during sample processing. Therefore lower W/C can be used to obtain the same fluidity. It is found that samples with lower W/C exhibit lower strength than samples with higher W/C during the early stages. However, with time, the lower W/C samples develop higher strengths than samples with higher W/C. After about seven days of hydration, the strengths of samples with higher W/C decrease while those with lower W/C maintain their strengths and show minimal strength loss. This indicates that using a lower W/C is an effective way to minimize the conversion reaction and to retard the loss in strength.

The addition level of phosphate has an effect on strength. Strength increases with amount of added phosphate until 20%, and then decreases rapidly at higher addition levels. It can be concluded

that amount of phosphate strongly affects the mechanical properties of HAC.

Isothermal calorimetry was used to study the major effects on the hydration of HAC by phosphate additions. It was found that the phosphate modification accelerates the initial hydration rates regardless of phosphate composition. The hydration rate depends on the amount and type of phosphates addition. A relationship appears to exist between the strength and the rate of hydration reaction; the faster the reaction is, the higher strength the sample exhibits. It is found that the samples modified by sodium phosphate have faster reaction rates than samples with calcium phosphate. It is significant that higher strengths are achieved even though the extent of reaction maybe reduced in the presence of phosphates. It can be concluded that the phosphate modifiers have their greatest effect at the onset of hydration, and adding a phosphate-based additions strongly accelerates the hydration reaction.

The morphologies of hydration products of pure Secar 71 were identified by ESEM. The micrographs show that the hydration of HAC modified by different phosphates can result in morphologically distinct hydration products.

X-ray diffraction (XRD) patterns show the difference between pure HAC and modified samples is minimal although there are significant differences in the mechanical properties among these samples. The positions of the peaks do not change, only differ in intensity. XRD patterns further confirms that phosphate addition accelerates the hydration reaction. Thus the increase in strength may be related to formation of a amorphous, or phase which appears to be

an aluminate-phosphate gel. Such a gel may be stronger than the aluminate gel which produced by pure high alumina cement.

EDX was used to study the compositions of the hydration products. It shows the existence of aluminum, phosphorus and calcium in the amorphous phase. For all four classes of sodium phosphate modified HAC, the relative percentages of the constitutents in hydration products are very similar. These data indicate that an amorphous calcium aluminate phosphate hydrate (C-A-P-H) gel is produced during hydration reaction in these systems. The microstructure of this phase varies with different phosphate modifications. The CAPH appears to bond both the anhydrous HAC grains as well as to the calcium aluminate hydrates which form thus providing improved structural integrity to high alumina cement. Although there is still a regression in the strength as the hexagonal calcium aluminate hydrates undergo conversion to the hexagonal hydrate, the losses in strength appear to be mitigated by the presence of this phosphate-containing hydration product.

It is found that modified cements have lower total porosity and pore distribution consisting of smaller pores than the pure cement from the mercury intrusion porosimetry (MIP) measurement. These porosity results are in accord with mechanical properties observed.

The previous results and discussion are not entirely consistent with the analysis of the microstructure of the hardened pastes using the scanning electron microscope (SEM). While x-ray diffraction results do not indicate the growth of new crystalline phases in these mixture, the micrographs indicate that there is some degree of order in the newly developed phases.

4.1.2 OPC-Phosphate System

In this system, all of the sodium phosphate modified samples except the one with $(NaPO_3)_n \cdot Na_2O$ exhibits higher flexural strength than that of the pure one for almost all curing times. The strengths for modified cements show large variability after 14 days. However, after this, the strengths continue to increase for three months. The strengths at one year for pure OPC was 26 MPa, while $Na_5P_3O_{10}$, $(NaPO_3)_n$, $(NaPO_3)_3$ and $(NaPO_3)_n.Na_2O$ modified samples reached 32, 38, 33, and 23 MPa, respectively. The reason for the slow strength increase during the first three months is probably related to low W/C ratio. Because a very low W/C was used, the samples continue to hydrate in the air for a longer period. The effects of calcium phosphate additions indicated that for samples with lower W/S, the strengths did not increase significantly during the early time, but had relatively high long-term values.

The cool-pressed and warm-pressed processing exhibits different influence on strength. It is found that all the warm-pressed samples have higher strengths than cool-pressed ones. In the air curing, samples with warm pressure exhibit much higher strength than that with cool pressure. The strengths of warm-pressed samples can reach about double that of cool-pressed ones. On the other hand, water curing has a much larger effect on the strength gain in cool-pressed samples. Samples with higher W/C have higher strengths in the cool-pressed condition.

Water sensitivity of the material is one of the properties of concern in this study. Samples with lower W/S have higher strengths

when cured in water other than in air. For the samples with a higher W/C, the strength is a little lower in water other than in air, but the values are very close. This indicates that this material is not very sensitive to water.

Curing at different temperature shows that samples cured at higher temperature have much higher strength than those cured in low temperature water. Therefore, the temperature of the curing water is an important factor influencing the strength of the material.

The calorimetric curves for OPC-modified samples show that faster hydration rates occur when OPC is modified by sodium phosphates, and the modified samples produced more heat than pure OPC at the beginning of hydration. However, the main peak, which occurs in OPC between 4 and 20 hours, is not observed in the modified samples. Although there was a difference in the mechanical properties among these samples, the difference in the x-ray diffraction patterns is minimal. Nearly, all the peaks remained in the same position. The only difference that can be observed is that the peaks represented $Ca(OH)_2$ have lower intensity or even disappeared. All other positions of the peaks do not change. The mechanism by which strength increased from x-ray diffraction may be similar with that of HAC-Phosphate system, it may be related to formation of poorly crystalline hydroxyapatite and a amorphous gel which is stronger than the C-S-H gel produced by pure ordinary portland cement. The reason for the appearance of $Ca(OH)_2$ on XRD occurred later or even missing in time is perhaps due to the consumption of $Ca(OH)_2$ in the formation of the amorphous gel and hydroxyapatite.

The microstructures of these cements are not very much in agreement with the analysis of the previous experiments. Even though x-ray diffraction gave limited evidence for the growth of new crystalline phases in these materials, the micrographs indicated that there is some degree of order in the newly developed phases.

4.2 Conclusions

1. High strength can be achieved by high alumina cement and ordinary portland cement with phosphate-based additions. Sodium phosphate is more effective than calcium phosphate on mechanical properties. The mechanical properties varied depending on the phosphate addition level.

2. Calcium phosphate modified OPC composite is not sensitive to water, while calcium phosphate modified HAC composite is water sensitive.

3. Silica fume replacement offers advantages for retarding the loss in strength.

4. A low water:cement ratio is required for HAC-phosphate system to achieve high strength in the long term. A modest W/C is needed for OPC-phosphate system in order to develop the strength.

5. The samples with warm pressed have higher strength than ones with cool pressed in OPC-phosphate system. Temperature of curing is an important factor for influence on the strength.

6. Phosphate modification of cement accelerates hydration. However, the total heat evolved in the hydration of unmodified cements is actually greater except calcium phosphate modified OPC. A relationship exists (except calcium phosphate modified OPC) between

the strength and the rate of hydration reaction; the faster the reaction is, the higher the strength the sample exhibits.

7. The phosphate-containing products formed in this system are x-ray amorphous. Although compositionally quite similar, ESEM shows that the hydration of HAC modified by different phosphates can result in morphologically distinct hydration products.

8. The amorphous C-A-P-H gel formed by reaction between HAC and the sodium phosphates serves as the bond interlinking the other constituents which are present. The presence of the phosphate-containing hydrates appear to reduce the strength losses associated with the conversion to cubic hydrates.

9. The amorphous gel and the poorly crystalline hydroxyapatite provide greater structural integrity to the cement. The increase in flexural strength is also related to the decrease in pore size and in porosity.

REFERENCES

Alford, N. McN., and J. D. Birchall. "The Properties and Potential Applications of Macro-Defect-Free Cement" Very High Strength Cement-Based Materials, Ed. J. F. Young, Mat. Res. Soc. Symp. Proc. Vol. **42** (1985)

Alford, N. McN., J. D. Birchall, A. J. Howard, and K. Kendall. "Macro-Defect Free Cement - Strong Solids Made Easy" Proc. First Conf. Mater. Engr., July 1984 (Inst. Metallurgists, U. K., 1984)

Alford, N. McN., G. W. Groves, and D. D. Double. "Physical Properties of High Strength Cement Pastes" Cem. Concr. Res., **12** 349-358 (1982)

Bache, H. H. "The New Strong Cements: Their Use in Structure" Phys. in Tech., **19** (1988)

Birchall, J. D. "Cement in the Context of New Materials for an Energy-Expensive Future" Technology in the 1990s: Developments in the Science and Technology of Hydraulic Cement, Ed. P. Hirsch, et al. (1983)

Birchall, J. D., A. J. Howard, and K. Kendall. "Flexural Strength and Porosity of Cements" Nature, **289** 388-389 (1981)

Bothe, J. V. Low Temperature Formation of Aluminum Phosphates, M. S. Thesis, The Pennsylvania State University, 1991

Brackenbury, W. R. E., R. Grzeskowiak, N. L. Reid, and M. E. Lynn. "Flexural Strength of Polymer Modified Cement Pastes Prepared by a Novel Curing Process" Cem. Concr. Res., **18** 971-979 (1988)

Brown, P. W. "Phase Equilibria and Cement Hydration" Materials Science of Concrete, Ed. J. Skalny, Am. Ceram. Soc., 73-94 (1989)

Brown, P. W. "Phase Relationships in the Ternary System CaO-P_2O_5-H_2O at 25°C" J. Am. Ceram. Soc., **75** 17-22 (1992)

Brown, P. W., and M. Fulmer. "Kinetics of Hydroxyapatite Formation at Low Temperature" J. Am. Ceram. Soc., **74** 934-40 (1991)

Brown, P. W., and P. LaCroix. "The Kinetics of Ettringite Formation" Cem. Concr. Res., **19** 879-884 (1989)

Buil, M., A. M. Paillere, and B. Roussel. "High Strength Mortars Containing Condensed Silica Fume" Cem. Concr. Res., **14** 693-704 (1984)

Bushnell-Watson, S. M., and J. H. Sharp. "The Effect of Temperature upon the Setting Behaviour of Refractory Calcium Aluminate Cements" Cem. Concr. Res., **16** 875-884 (1986)

Cassidy, J. E. "Phosphate Bonding Then and Now" Ceram. Bull., **56** 640-643 (1977)

Chandra, S., and P. Flodin. "Interactions of Polymers and Organic Admixtures on Portland Cement Hydration" Cem. Concr. Res., **17** 875-890 (1987)

Czernin, W. Cement Chemistry and Physics for Civil Engineers. Bauverlag, Wiesbaden und aberlin (1980)

Doehne, E., and D. C. Stulik. "Applications of the Environmental Scanning Electron Microscope to Conservation Science" Scanning Microscopy, **4** 285-286 (1990)

Eden, N. B., and J. E. Bailey. "On the Factors Affecting Strength of Portland Cement" J. Mat. Sci., **19** 150-158 (1984)

Edmonds, R. N., and A. J. Majumdar. "The Hydration of Monocalcium Aluminate at Different Temperatures" Cem. Concr. Res., **18** 311-320 (1988)

Edmonds, R. N., and A. J. Majumder. "The Hydration of Secar 71 Aluminous Cement at Different Temperatures" Cem. Concr. Res., **19** 289-294 (1989)

Eglinton, M. S. Concrete and Its Chemical Behaviour. Thomas Telford Ltd., Telford House (1987)

Fang, Y., D. K. Agrawal, D. M. Roy, R. Roy and P. W. Brown. "Ultrasonically Accelerated Synthesis of Hydroxyapatite" J. Mater. Res., **7** 2294-98 (1992)

Gimblett, F. G. R. Inorganic Polymer Chemistry. Butterworth and Co. (1963)

Hu, J., D. K. Agrawal, and R. Roy. "Investigation of Hydration Phases in the System CaO-SiO_2-P_2O_5-H_2O" J. Mater. Res., **3** 772-780 (1988)

Hu, J., D. K. Agrawal, and R. Roy. "Studies of Strength Mechanism in Newly Developed Chemically Bonded Ceramics in the System $CaO-SiO_2-P_2O_5-H_2O$" Cem. Concr. Res., **18** 103-108 (1988)

Kanazawa, T., Ed. Inorganic Phosphate Materials, Kodansha LTD., Tokyo (1989)

Kataoka, N., and H. Igarashi. "Expansion Property of Macrodefect-free Cement in Water" CCBC Meeting, Materials Research Lab., The Pennsylvania State University, 1987

Kendall, K., and J. D. Birchall. "Porosity and Its Relationship to the Strength of Hydraulic Cement Pastes" Very High Strength Cement-Based Materials, Ed. J. F. Young, Mat. Res. Soc. Symp. Proc. Vol. **42** 143-150 (1985)

Kingery, W. D. "Fundamental Study of Phosphate Bonding in Refractories: I - III" J. Am. Ceram. Soc., **33** 239-250 (1950)

Kistler, P. D. Optimization of Physical Properties of Chemically Bonded Ceramics: Silicates and phosphates, Ph. D. Thesis, The Pennsylvania State University, 1988

Li, H., M. R. Silsbee, and D. M. Roy. "Effect of Particle Size Distribution on Properties of High Strength Cementitious Composites" Presented to the American Ceramic Society Spring Meeting, 1990

Ma, W., and P. W. Brown. "Cement-Inorganic Polymer Composites, Microstructure and Strength Development" Proc., 9th Intl. Congress on the Chemistry of Cement 1992 (accepted)

Ma, W., and P. W. Brown. "Hydration of Sodium Phosphate-Modified High Alumina Cement" Submitted to J. Mater. Res.

Ma, W., and P. W. Brown. "Mechanical Behaviour and Microstructural Development in Phosphate modified High Alumina Cement" Cem. Concr. Res. (accepted)

Ma, W., P. W. Brown, and D. Shi. "Solubility of $Ca(OH)_2$ and $CaSO_4 \cdot 2H_2O$ in the Liquid Phase from Hardened Cement Paste" Cem. Concr. Res., **22** 531-540 (1992)

Ma, W., and P. W. Brown. "The Effect of Phosphate Addtions upon Behaviour of Portland Cement" (in preparation)

Mindess, S. "Relationships between Strength and Microstructure for Cement-Based Materials: an Overview" Very High Strength Cement-Based Materials, Ed. J. F. Young, Mat. Res. Soc. Symp. Proc. Vol. **42** (1985)

Neville, A. M. Properties of Concrete. Pitman Publishing Inc. 92-99 (1981)

Piasta, J., Z. Sawicz, and W. C. Piasta. "Durability of High Alumina Cement Pastes with Mineral Additions in Water Sulfate Environment" Cem. Concr. Res., **19** 103-113 (1989)

Robson, T. D. High-Alumina Cements and Concretes. John Wiley & Sons, Inc., 263 (1962)

Poon, C. S., and G. W. Groves. "The Microstructure of Macrodefect-free Cement with Different Polymer Contents and the Effect on Water Stability" J. Mat. Sci., **23** 657-660 (1988)

Rodger, S. A., S. A. Brooks, W. Sinclair, G. W. Groves, and D. D. Double. "High Strength Cement Pastes Part 2 Reactions during Setting" J. Mat. Sci., **20** 2853-60 (1985)

Roy, D. M. "New Strong Cement Materials: Chemically Bonded Ceramics" Science, **235** 651-658 (1987)

Roy, D. M. "Recent Advances in Phosphate Chemically Bonded Ceramics" MRS Int'l. Mtg. on Adv. Mats. Vol. **13** 213-227 (1989)

Roy, R. "Workshop on Chemically Bonded Ceramics" Held at the Materials Research Laboratory at The Pennsylvania State University, July 9-10 (1984)

Sarkar, A. K. "Phosphate Cement-Based Fast-Setting Binders" Ceram. Bull., **69** 234-238 (1990)

Shi, D., P. W. Brown, and W. Ma. "Lognormal Simulation of Pore Size Distributions in Cementitious Materials" J. Am. Ceram. Soc., **74** 1861-67 (1991)

Shi, D., W. Ma, and P. W. Brown. "Lognormal Simulation of Pore Evolution during Size Cement and Mortar Hardened" Scientific Basis for Nuclear Waste Management XIII, Materials Research Society, 143-48 (1990)

Silsbee, M. R. Synthesis of Ceramics at Low Temperatures. Ph. D. Thesis, The Pennsylvania State University, 1988

Sinclair, W., and G. W. Groves. "High Strength Cement Pastes Part 1 Microstructure" J. Mat. Sci., **20** 2846-52 (1985)

Sliva, P. The Development of Processing of Calcium Aluminate Cement as a Low Relative Dielectric Permittivity Material. Ph. D. Thesis, The Pennsylvania State University, 1988

Steinke, R. A. Sol-Gel Derived Chemically Bonded Ceramics in the System Calcium Oxide-Silicon Dioxide-Phosphorous Pentoxide-Water. M. S. Thesis, The Pennsylvania State University, 1989

Steinke, R. A., M. R. Silsbee, D. K. Agrawal, R. Roy, and D. M. Roy. "Development of Chemically Bonded Ceramics in the CaO-SiO_2-P_2O_5-H_2O System" Cem. Concr. Res., **21** 66-72 (1991)

Sugama, T., and L. E. Kukacka. "Magnesium Monophosphate Cement Derived from Diammonium Phosphate Solutions" Cem. Concr. Res., **13** 407-416 (1983)

Sugama, T., and N. R. Carciello. "Strength Development in Phosphate-Bonded Calcium Aluminate Cement" J. Am. Ceram. Soc., **74** 1023-30 (1991)

Taylor, H. F. M. Cement Chemistry. Academic Press Inc. 316-330 (1990)

Taylor, H. F. M., Ed. The Chemistry of Cements. Vil. 2, Academic Press Inc. (1964)

Thilo, E. "Condensed Phosphates and Arsenates" Adv. Inorg. Chem. and Radiochem., **4** (1962)

Timoshenko, S. P., and J. N. Goodier. Theory of Elasticity. McGraw-Hill, (1982)

Young, J. F. "Macro-Defect-Free Cement: A Review" Specialty Cements with Advanced Properties, Ed. B. E. Scheetz, et al., Mat. Res. Soc. Symp. Proc. Vol. **179** 101-121 (1991)

Uchiyama, M. Assessment of and Modeling the Mechanical Behavior of Macro-Defect-Free Cementitious Materials. M. S. Thesis, The Pennsylvania State University, 1989